INFLUENCE OF SURFACE ROUGHNESS AND SLIDING SPEED ON THE FRICTION AND WEAR OF LOW DENSITY POLYETHYLENE

by

MEHMET MERVAN BAYRAKTAROĞLU

Thesis submitted to the Graduate Faculty of the
Virginia Polytechnic Institute and State University
in partial fulfillment of the requirements for the degree of

MASTER OF SCIENCE
in
Mechanical Engineering

APPROVED:

N. S. Eiss, Jr., Chairman

H. H. Mabie

L. D. Mitchell

August 1978
Blacksburg, Virginia

ACKNOWLEDGEMENTS

The author would like to express his sincere gratitude and thanks to Dr. N. S. Eiss, Jr. for his fruitful guidance, advice, and assistance and to Dr. H. H. Mabie and Dr. L. D. Mitchell for their suggestions.

Special thanks are also extended to his parents for their invaluable support and encouragement during his studies.

The author wishes to express his deepest thanks to his fiance, Türkân Erden, for her continued moral support throughout his college career.

This research was sponsored by the U. S. Army Research Office.

TABLE OF CONTENTS

TABLE OF CONTENTS (Continued)

LIST OF FIGURES

LIST OF TABLES

DEFINITIONS

Lay:	For non-random processes - the predominant orientation of surface features.
Leading edge of groove:	The edge of groove that encounters the polymer pin first.
Leading edge of asperity:	The edge of asperity that encounters the polymer pin first.
Parallel sliding:	Sliding of the polymer pin parallel to the lay of the disk.
Pass:	One revolution of the disk.
Perpendicular sliding:	Sliding of the polymer pin perpendicular to the lay of the disk.
Roll:	Debris particle with a layered structure that has been rolled [Fig. 30].
Thick film:	A surface film whose thickness can be seen in scanning electron microscope pictures [Fig. 7].
Thin film:	A surface film whose thickness can not be seen in scanning electron microscope pictures [Fig. 3].
Tongue:	A plastic extension on polymer films which resembles the human tongue.

INTRODUCTION

Wear of polymers is a complex phenomenon which results in the loss of material from one or both of the sliding surfaces. It is affected by the properties of the polymer, roughness of the surfaces, and the external conditions. Different wear mechanisms, such as adhesion and abrasion have been identified, but both mechanisms are significant in polymer wear.

In studies of wear, experiments are usually designed to favor one mechanism. Abrasive wear is favored by sliding polymers on rough surfaces. Two techniques for modeling rough surfaces have been used in previous works: a simple description of real surfaces (i.e. centre-line average, CLA), or a simplified model of the surface geometry of the asperities (e.g. cones or hemispheres of same shape and size).

In the last 5 years, wear of polymers by rough surfaces has been studied in the Mechanical Engineering Department at Virginia Polytechnic Institute and State University (VPI & SU). The major thrust of this work has been the characterization of real surfaces by several parameters and the prediction of wear using these parameters. Comparison of predicted wear with measured wear was facilitated by the development of a high sensitivity wear measuring technique using Neutron Activation Analysis.

In the VPI & SU work, low sliding speed, single pass experiments have been performed to keep the temperatures of the sliding surfaces low and to prevent the deposited material from changing the surface

topography. Wear models for these conditions have been developed and used to predict wear by the topography of the harder surface and polymer properties.

However, polymer application in machine parts usually require a high number of passes at high speeds of sliding. Under these conditions the above models are not applicable.

The purpose of this research is to obtain wear and friction data on high speed sliding by multipass experiments. The influence of surface roughness and sliding speed on the wear mode of low density polyethylene (LDPE) will be studied.

LITERATURE SEARCH

A. Introduction

Wear is the removal of material from surfaces in relative motion. It is a complex process involving one or more wear mechanisms. One of such mechanisms is adhesive wear, which arises primarily from adhesion between the sliding surfaces. Another one is abrasive wear, which is the removal of material by shearing or cutting caused by the penetrating asperities of the harder surface. In many wear processes both of these mechanisms cause loss of material. However, operating variables of experiments usually tend to favor one or the other of the mechanisms. Therefore, the two mechanisms will be considered separately in the following two sections of this review.

The third section will cover the effect of temperature on the wear rate of polymers. When two surfaces are in sliding contact energy is dissipated as heat, and this results in an increase in the temperature of the contact zone. Even at the low speeds of sliding, the temperature over the contact area rises appreciably and affects the wear rate of the polymer.

As the sliding speed is increased, the temperature increases and thermal effects dominate the wear process. Further increase in speed and the accompanying rise in temperature leads to very high wear rates due to gross melting at the interface.

B. Adhesive Wear Mechanisms

Adhesive wear is caused by the strong adhesive bonds at the junction between sliding surfaces.

The equation for the volume of wear, V, produced by sliding a distance, x, was shown by Archard (1)* in 1953 to be

$$V = \frac{k\ L\ x}{3\ H} \qquad [1]$$

where L is the normal load, H is the hardness of the material being worn, and k is a non-dimensional constant, namely the wear coefficient. In his paper, Archard showed that this equation was consistent with the available experimental data.

Bowden and Tabor (2) proposed the adhesion theory of friction, using the fact that when surfaces are loaded against each other, they make contact only at the tips of their asperities. Since the contact area formed this way is small, the pressure over the contacting asperities is high enough to cause them to deform plastically. This plastic deformation causes an increase in the area of contact until it is large enough to support the load. Thus, regions of intimate metal-to-metal contact are formed, and strong adhesive forces "cold weld" the junctions.

In 1955, Green (3) studied the forces involved during the shearing of an individual junction, by carrying out experiments in large scale metal models. He showed that plastic deformations in ductile

*Numbers in parenthesis refer to references at the end of the thesis.

metals cause the junction to tear in two separate places in opposite directions and form a whorl of loose debris. This model could be used to explain the formation of loose debris during adhesive processes.

In 1965, Rabinowicz (4) used the residual elastic energy of adherent fragments to explain the formation of loose wear particles. According to his theory, the elastic energy stored in the potential particle prior to detachment must be equal to or greater than the energy of formation of the new surfaces. Rabinowicz, also assumed that the potential wear particles have a hemispherical shape and calculated the stored energy in one particle. By equating the stored energy to the surface energy of the particle he found a minimum diameter required for a loose particle to be formed. He then assumed this minimum diameter to be the average diameter of loose particles.

In 1971, Bahadur and Ludema (5) stated that for polymers the sliding force or frictional resistance to motion is caused by making and breaking of adhesional bonds between the sliding bodies. They also showed that the sliding force is proportional to the shear strength of adhesional bonds and to the area of contact between touching bodies.

In 1972, Pooley and Tabor (6, 7) analyzed the wear mechanisms of a variety of polymers and observed a lumpy transfer on both smooth and rough surfaces. Two years later, Briscoe, Pooley, and Tabor (8) showed that the transfer of a polymer to hard smooth surfaces occurred in two modes: a thin-film transfer and the previously observed lumpy

transfer. The thin film transfer was explained by adhesive forces drawing out polymer molecules, which could easily slide by each other because of their smooth molecular profile. Whereas, the lumpy transfer occurred in polymers with bulky side chains sliding on smooth or rough surfaces and in polymers with smooth profiles sliding on rough surfaces.

Tabor (9) explained the mechanism of polymer friction in terms of adhesion and deformation processes. He described the mechanism of adhesion in terms of electric surface changes and Van der Waal's forces and suggested that a simple monistic view was not valid. He added that the adhesion component of friction depended on speed, temperature, and contact pressure, in a manner implying a close correlation with bulk viscoelastic properties.

Tanaka and Uchiyama (10) studied the effects of sliding speed on the friction and wear of several polymers with spherulitic structure sliding on smooth surfaces. For polymers on glass, they found critical speeds above which the wear rates rapidly increased, because of the melting of the surface layers. They also observed that these critical speeds do not appear for polymers on steel, with the exception of low density polyethylene. They stated that for this polymer shearing occurs at some depth from the frictional surface and a film was formed on a large scale over the apparent area of contact.

Bahadur (11) studied the sliding friction of bulk polymers under varying conditions of normal load, contact pressure, and sliding velocity. He found that the coefficient of friction depended upon the

velocity and pressure and that the variation could be explained by the adhesion theory of friction.

Briscoe, Parry, and Tabor (12) studied the effect of hydrostatic gas pressure on the coefficient of sliding friction of several polymers and proposed models in an attempt to explain the data. In 1975, Briscoe and Tabor (13) described the effect of normal pressure on the shear properties of very thin polymeric films and found that the shear yield strength increased in proportion to the applied pressure. The also used polymethylmethacrylate films to show that the shear strength fell markedly at a critical temperature, which corresponded to the glass transition temperature of the polymer. This critical temperature was affected by the sliding speed and by the contact pressure.

In 1977, Amuzu, Briscoe, and Tabor (14) described experiments where thin films of polymers were deposited on smooth substrates and rigid smooth sliders were slid over the organic films. They also covered the influence of bulk temperature on the interfacial shear properties of a range of poly n-alkyl methacrylates. The same authors (15) measured the shear strength and friction of a number of polymers, using thin films of polymers deposited on hard, smooth substrates. They concluded that in the sliding of bulk polymers energy was dissipated within a thin region close to the sliding interface, and that it was the pressure in the contact area which largely governed the magnitude of the interfacial shear strength.

In the opening speech of the International Symposium of Wear in 1977, Tabor (16) discussed critically some of the major processes that

were likely to be involved in wear. He reviewed the general theories of wear and concluded that it was still impossible to predict the wear behavior of any given sliding system. In the same symposium, Rabinowicz (17) stressed the role of surface energy in the release of transferred fragments and suggested that the wear coefficient was proportional to the second power of the ration of the interfacial surface energy of adhesion to the sum of the surface energies of the contacting materials and to the fifth power of the friction coefficient.

Rhee and Ludema (18) discussed the role of the transfer film in reducing wear of polymers. They also showed that the transfer film formed more readily on roughened surfaces and that the transfer film could exist in a solid state or in a low viscosity state. They concluded that each state controls friction and wear of the polymer in a different way.

Belyi, et al. (19) also worked on the adhesion theory of friction. They found that in local regions of the real contact an intensive molecular (adhesive) interaction occurred under rubbing conditions and that adhesive forces were stronger than the bonds between individual elements in the supermolecular formations. They added that wear products could escape from the contact region as gases or solids, or they could form a "third body," i.e. a transferred layer of one material deposited on the surface of the other.

The adhesion theory of friction was rejected by Bikerman (20), who said that the adhesion theory contradicted the modern science of adhesive joints and, hence, was erroneous. He added that the belief,

that the roughness theory of friction could not explain frictional heat, could be shown to be incorrect by a thermodynamic reasoning. This assertion was highly criticized by competent scientists, however he wrote another paper (21) on the nature of polymer friction to support his initial view through experimental evidence. He proposed that contact of a solid polymer with another solid in a gas did not give rise to adhesion and that the work of sliding friction between a solid polymer and another solid depended on the rate of sliding and temperature in the same manner as did the work of mechanical deformation of slider and support. He thus concluded that the adhesion theory of friction was incorrect and that the deformation theory of polymer friction was the most probable.

C. Abrasive Wear Mechanisms

In 1960, Ratner and Farberova (22) stated that the wear resistance of any material was determined not only by its properties and the effect of external parameters, such as load and speed, but also by the surface roughness, which determined the mechanism of wear. They added that abrasive wear produced lines parallel to the direction of sliding on the worn surface when deformations were plastic, and lines perpendicular to the direction of sliding when deformations were elastic. They found an equation, which related abrasive wear, V, to pressure P,

$$V = K\ (P/H)^{\alpha} \qquad [2]$$

where H was the hardness of the plastic and K and α ($\alpha > 1$) were material constants.

In 1963, Ratner, et al. (23) defined wear as "the breakdown of a material on the friction surface", and related wear, V, to mechanical properties by the following qualitative relationship:

$$V \sim \frac{M}{H \sigma E}, \qquad [3]$$

where M was friction coefficient, H was hardness, σ was strength and E was breaking elongation.

Rabinowicz (24) derived a quantitative equation for abrasive wear, by assuming that the asperities on the rough surface were conical. His equation for the volume of wear, V, was

$$V = \frac{\overline{\tan \theta}\ L\ x}{\pi \qquad H} \qquad [4]$$

where $\overline{\tan \theta}$ was a weighted average of tan θ values of all the individual cones having θ as the half apex angle, L was the load, x was the sliding distance, and H was the hardness. This equation closely resembled equation 1, which was for adhesive wear.

In 1967, Ratner (25) analyzed the mechanism of abrasion as the whole combination of phenomena leading to the removal of the surface layer. He then discussed, separately, the type of interaction of the contacting surfaces, changes in the surface layer during friction, the failure of this layer, and, finally, the method of separation of the failed material.

In 1969, Lancaster (26) outlined the main features of abrasion of polymers and discussed the relative roles of plastic and elastic deformation in the wear process. He stated that variations in the mechanical properties as well as changes in the abrading surface during repeated sliding affected the wear rates.

Giltrow (27) showed that the rate of abrasive wear of a thermoplastic polymer was inversely proportional to the square root of its cohesive energy, provided that plastic deformation predominated during the wear process. He attributed the non-linearity of this relationship to the complex structure of polymers and to the high strain rates occurring during the abrasion process.

In 1970, Rhee (28) proposed an empirical wear equation for predicting material losses of asbestos reinforced polymers caused by sliding against metal surfaces. His equations for weight loss, ΔW, was

$$\Delta W = K F^a V^b t^c \qquad [5]$$

where K was the wear factor, F was the load, V was the speed, t was the time and a, b, and c were system parameters.

Recently in 1977, Eiss and Warren (29) used the depth of penetration as a predictor of the wear of polymers on abrasive surfaces. Using loads high enough to cause full penetration, they have found that different polymers are sheared off at different angles and correlated this to the energy-to-rupture of the polymers. They also found that for polymers sliding under partial penetration, wear of

different polymers could be discriminated by the depth of penetration parameter, and added that surface profile statistics must be based on the amount of profile in contact with the polymer.

D. Effect of Temperature on the Wear Rate of Polymers

One of the earliest attempts to characterize the effects of temperature on rubbing surfaces was in 1958 by Archard (30), who pointed out that very high temperatures occurred close to the areas of true contact, at which the energy was dissipated. He called these short duration temperatures the flash temperatures and stated that they had a considerable influence on the friction and wear of polymers. He added that direct measurements of these temperatures were difficult because they occurred only over small regions for a short duration. Archard also stressed the influence of surface films, such as oxides of low thermal conductivity, on the surface temperatures. He assumed that the film thickness was small compared to the dimensions of the contact and that there was no change in the experimental conditions apart from changes in thermal conduction. He concluded that the surface film acted as a protective layer at low speeds and that the temperature of the substrate was unaffected, although the film temperature rose. At high speeds of sliding nearly all the generated heat penetrated to the substrate and its temperature rose to the values obtained without a film.

In 1963, Ratner, et al. (23) stated that equation 3 is of particular interest in studies of the temperature effects on the wear

rate, because careful examinations of the variations of the mechanical properties with temperature gave the variation of wear rate with temperature.

In 1966, Steijn (31) conducted experiments on PTFE and found that there was a linear relationship between sliding speed and temperature, in low humidity environments. He showed that the relationship was linear from 70°C to the crystalline transition temperature, 19°C, and that below this temperature there was an abrupt change in behaviour.

Ratner and Lure (32) stated that abrasion depends on hardness, strength, and elasticity. Since these properties behave differently with temperature, the curve of wear rate versus temperature should have a minima or maxima. They concluded that there was an increase in abrasion above the glass transition temperature, when the material was fairly elastic, and in the premelting zone, where the hardness decreased and the coefficient of friction increased.

In 1969, Lancaster (33) determined the influence of hardness, elastic modulus, and breaking strength on the wear rate of polymers sliding against a metal surface. He demonstrated that the minimum wear rate occurred at the glass transition temperature, as he had predicted (27). He also showed that the ratio of hardness to elastic modulus was almost independent of temperature, until near the softening point, and concluded that this ratio could not be used to predict changes in wear rate. Lancaster added that the other important parameter, the product of breaking strength, S, and the elongation to

break, E, was dependent on temperature, and that it could be used to predict changes in wear rate. He demonstrated for many polymers that in single traversal abrasive wear, wear rates were linearly correlated to 1/SE, and that in many traversals this relation deviated from linearity because of film transfer and change in type of wear.

Vinogradov, et al. (34) studied the friction of isotactic polypropylene and high "pressure" polyethylene in contact with steel over a wide range of temperatures. They bonded polyethylene to the steel surface and determined the friction force to break the adhesive bonds. They have also established a qualitative correlation between friction and the dynamic characteristics of the polymers.

In 1971, Lancaster (35) calculated the critical speeds at which the flash temperatures reached the melting or softening points of several thermoplastics and showed that these values were in agreement with experimental measurements of the speed at which the wear rate began to increase rapidly. He extended his analysis to predict the limiting PV relationships (the product of nominal pressure and the linear velocity) for polymer bearings of different sizes, by incorporating an estimate for the mean temperature rise of the surfaces.

In 1973, Lancaster (36) associated energy losses with the shearing of adherent junctions and with the deformation of asperities, and added that thermal properties played an important role especially when the thermal conductivity was low. He stated that for adhesive wear processes the coefficient of friction, M, was given by the

formula $M = S/P_m$, where S was the shear strength of the junctions and P_m was the flow pressure. He then showed that both shear strength and flow pressure decreased with increasing temperature, but since the variations were not to the same extent the coefficient of friction could increase or decrease depending upon the particular polymer involved. Lancaster also made the following observations, which showed that the coefficient of friction could not be used to predict the wear rate. For low loads there was a rise in friction due to frictional heating and thermal softening, which led to an increase in the real area of contact. For high loads there was a decrease in friction due to the lubrication caused by the molten material. On the other hand the decrease in wear rate with increasing temperature was due to the decrease in elastic modulus, which resulted in a change in the mode of deformation, which in turn changed the type of wear. For low speeds, that is, when the temperatures were low, the wear rates and the coefficients of friction were low. When the speed was increased up to about 1.0 m/sec, thermal softening resulted in deeper penetration and high wear rates and high coefficients of friction were observed. If the speeds were increased further, melting started and the coefficient of friction decreased but an increase was observed in the wear rate.

In 1974, Price and Burks (37) constructed an apparatus to measure simultaneously the coefficient of sliding friction and the friction generated temperature. They measured the coefficient of

sliding friction up to surface velocities of 2.0 m/sec and the coefficient of thermal expansion from 300° to 500°K, using polyimide and "pyrrone" polymers. Their results showed that the coefficient of friction was almost independent of surface velocity for speeds higher than 0.4 m/sec.

Tanaka and Uchiyama (10) pointed out the difference in the wear rate and in friction between sliding on glass and sliding on steel. They assumed that the lower thermal conductivity of glass compared to the steel resulted in higher surface temperatures. These higher temperatures were then assumed to cause an increase in the wear rate of polymers sliding on glass. They also stated that for high speeds of sliding, polymer friction originated from the viscous resistance of the molten layer. The friction force could then be approximated as $F = n V A_{\alpha}/H$, where n was the effective viscosity of the molten polymer, V was the sliding speed, H was the mean depth of melting over the apparent area of contact, A_{α}. The term effective viscosity was used to compensate for the variation of viscosity with depth, which resulted in the variation of shear rate with depth.

E. Summary

This literature search covers the modes of wear that are likely to occur when a polymer slides over a metal surface. It also points out the parameters that are likely to influence the wear mechanisms. These mechanisms are so complex in nature that they

have to be isolated to get a better understanding of the nature of the wear phenomena.

The two major types of wear are the adhesive and abrasive modes, which are primarily determined by the surface roughness. When energy dissipation is lower than the generated energy the temperature of the system rises and the properties of the polymer change. The temperature changes could be obtained by changing the speed of sliding, if the dissipation of heat is limited.

The following research will try to clarify the influence of the major parameters on the friction and wear of the LDPE.

EXPERIMENTAL

A. Description of the Apparatus

The pin-on-disk type wear testing apparatus, shown in Fig. 1, was used to wear low density polyethylene pins on steel disks. The pins were fastened to the pivot arm with their axis perpendicular to the surface of the disks.

The arm was pivoted vertically and horizontally, and it was balanced vertically with an adjustable counter weight. The normal load on the pins was added by placing a mass on the platform. The pivot arm was allowed to rotate vertically to keep the load constant as the pin wore. The horizontal motion was stopped by clamping the arm during the wear experiments. It was restrained by a spring during friction measurements. This spring was a thin cantilever beam with strain gages mounted on each side. The output signal from these strain gages was amplified by a carrier amplifier and was recorded on an X-Y plotter to obtain the friction coefficients. The amplified signal was also fed to the Fast Fourier Transformer (FFT) processor through the data memory system to obtain the frequency analysis.

The radius of the circular track of the polymer deposited on the disks was adjusted by the movement of the pivot support. Rotational speed of the disk was controlled by a variable speed transmission with power supplied by a synchronous motor [Appendix A].

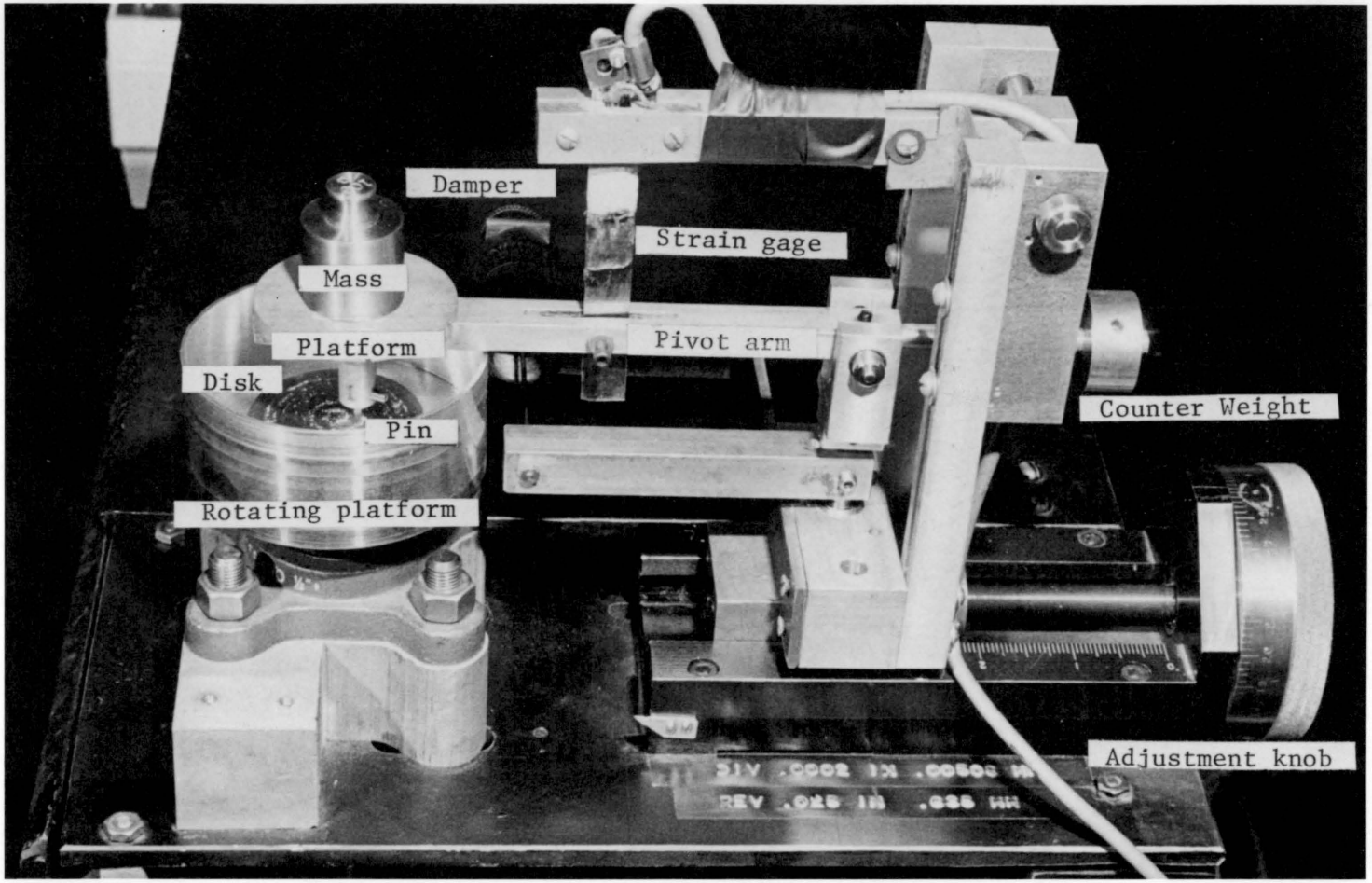

Figure 1. The pin-on-disk wear machine

B. Test Specimens

Cylindrical pins were machined from an extruded rod of LDPE of diameter 6.35 mm (0.25 in.) to a diameter of 1.5875 mm (0.0625 in.) and length of 7.9375 mm (0.3125 in.). The pins were then placed into marked vials and were kept in the vials to minimize the effect of the moisture absorption.

Steel disks were machined from a 1018 cold rolled steel bar of diameter 50.8 mm (2.0 in.) to dimensions of 6.35 mm (0.25 in.) thickness and 44.45 mm (1.75 in.) diameter. These disks were then ground by an unidirectional grinder to obtain the desired surface roughness. The surface roughness statistics for the smooth, medium roughness, and rough disks are listed in Table 1. The disks were cleaned separately by the procedures listed in Appendix B and were kept in a dessicator with calcium chloride, $CaCl_2$, to decrease the humidity.

C. Test Conditions

All tests were run with a normal load of 0.981 N and a rotational speed of 600 RPM at room temperature and relative humidity [ca. $28^{o}C$ and 65%], which varied over the time the experiments were run. The friction measurements were made in an air conditioned room [ca. $22^{o}C$ and 51%].

A low speed of 0.32 m/sec and a high speed of 1.28 m/sec was obtained by running on tracks of radii 5.08 mm and 20.32 mm,

TABLE 1

SURFACE ROUGHNESS STATISTICS*

	SMOOTH	MEDIUM ROUGHNESS	ROUGH
CLA Roughness (μm)	$6.52\ (10)^{-2}$	$6.45\ (10)^{-1}$	1.16
RMS (μm)	$8.57\ (10)^{-2}$	$8.60\ (10)^{-1}$	1.38
Skewness	$-9.12\ (10)^{-1}$	-1.18	$-2.32\ (10)^{-1}$
Kurtosis	6.03	5.25	2.45

*Based on two measurements from each of the two randomly chosen disks from each group.

respectively. Wear experiments were run on the three surfaces at the two speeds for 2400, 4800, 9600, 19200, 38400, 57600, 76800 and 115200 passes. These numbers of passes were chosen after some initial experiments, which showed that this range would cover the time to reach a steady state and would also show variations in the process throughout the initial stages.

D. Experimental Procedures

a. Wear Experiments

The pins, which were marked and weighed [Appendix D] were placed in a teflon sleeve, which was slid into a cylindrical cavity in the pivot arm. The sleeve was then squeezed by a screw so that the pin would be secured. The disks were mounted on the platform by the use of two alignment pins. The motor was turned on and the transmission was adjusted to obtain the required speed. The pin was carefully loaded onto the rotating disk to avoid any impact load. The experiment was run for the required time to complete the necessary number of passes and the pivot arm was lifted off. The pin was re-weighed to determine the weight loss and was then taken to the scanning electron microscope (SEM) with the disks. The disks with excessive wear debris and the pins were coated by 200 Å film of gold-palladium alloy to avoid charging in the microscope. Then they were examined under the microscope and representative pictures were taken.

b. Friction Measurements

The pivot arm was balanced horizontally with the pin mounted on it and the zero adjustment of the X-Y plotter was made [Appendix C]. Then the normal load was applied and the disk was rotated for 115200 passes. The arm was viscously damped for the first 19200 passes and continuous friction measurements were taken. The output was also analyzed by the FFT processor to obtain the frequency response. Then the arm was restrained from motion in the horizontal direction as it was in the wear experiments, and the frequency response was determined. The arm was released for short durations at 38400, 57600, 76800 and 115200 passes to obtain the friction measurements. These experiments were carried for smooth and rough surfaces at the low and high speeds.

RESULTS

A. Observations of Transferred Films, Loose Debris, and Wear Scars

Surface roughness is the major parameter in determining the wear mode of the polymer. Hence, the three different surface roughnesses will be handled separately in the following sections.

Since the disks have a unidirectional lay the direction of sliding with respect to lay changes from parallel to perpendicular to parallel twice each revolution of the disk. This factor has the second major influence in the wear mechanisms. Therefore, parallel sliding and perpendicular sliding will be dealt in different subsections.

The effect of speed is the increase in temperature, which results in the softening and even melting of the polymer. This phenomenon increases the wear rate of the polymer, but does not change the wear mechanisms. Therefore, low speed and high speed will be discussed in each of the previously defined subsections.

The observations in the following sections are presented as SEM photo micrographs of the surfaces and pins. The terminology used to describe these figures is given in the definitions listed on page xii.

a. Smooth Surfaces

Sliding of the polymer pin on the smooth surface results in an adhesive wear mechanism, where thin layers of the polymer are sheared off from the pin and adhere to the steel surface. This mechanism is favored by parallel sliding and the deposits on the steel surface are tightly bonded thick films, as opposed to loosely bonded and

thinner films formed in perpendicular sliding. Very small amounts of loose debris are generated during this process and only small amounts of the frictional energy is removed by the formation of loose particles. This results in an increase in the temperature of the contact zone and causes softening and even melting of the polymer at the high speed.

Parallel Sliding

At the low speed of sliding initial deposits are thin, non-uniform films [Fig. 2, 3], which later become more uniform [Fig. 4] and thicker [Fig. 5]. Small debris particles, which have a layered structure, are generated from films that are removed from the surface [Fig. 6].

At the high speed of sliding, initial deposits are in the form of thick, non-uniform films, the smoothness of which indicates softening of the polymer [Fig. 7]. Loose debris generation is initiated at the early stages of sliding [Fig. 8]. As the number of passes increases the deposited films become more uniform [Fig. 9]. Later, when a certain thickness is reached the load is carried by the polymer film, and the top layers are sheared by adhesive forces and form tongues [Fig. 10]. These plastic deformations tend to make the deposited film more uniform in the direction of sliding [Fig. 11, 12]. As the film reaches a uniform thickness plastic deformations decrease and the whole film starts deforming elastically. The transfer from the pin to the film on the surface continues until the elastic

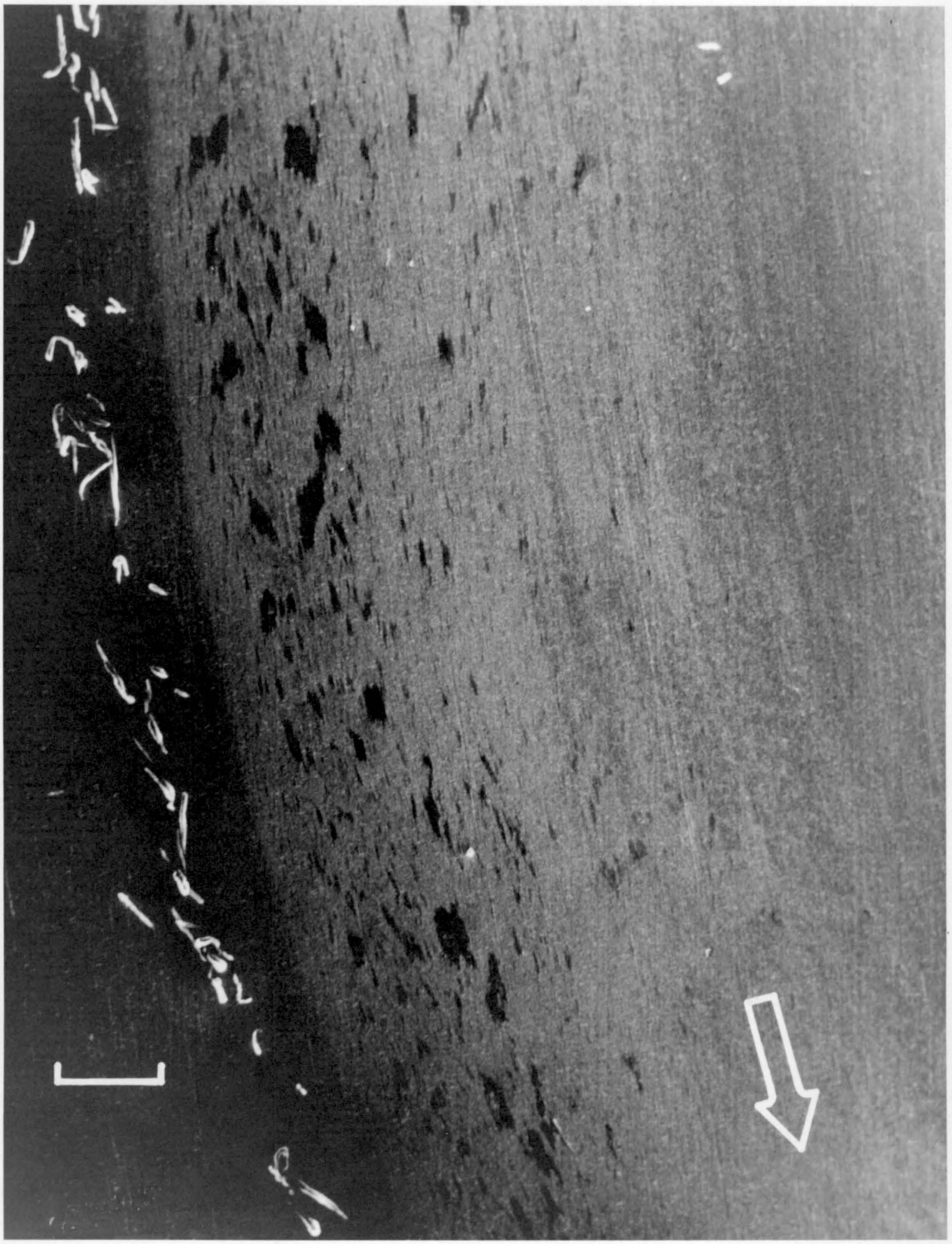

Figure 2. Scanning electron microscope picture of a smooth disk after 2400 passes at 32 cm/sec. Index mark is 200 μm. Arrow shows the direction of sliding of the pin.

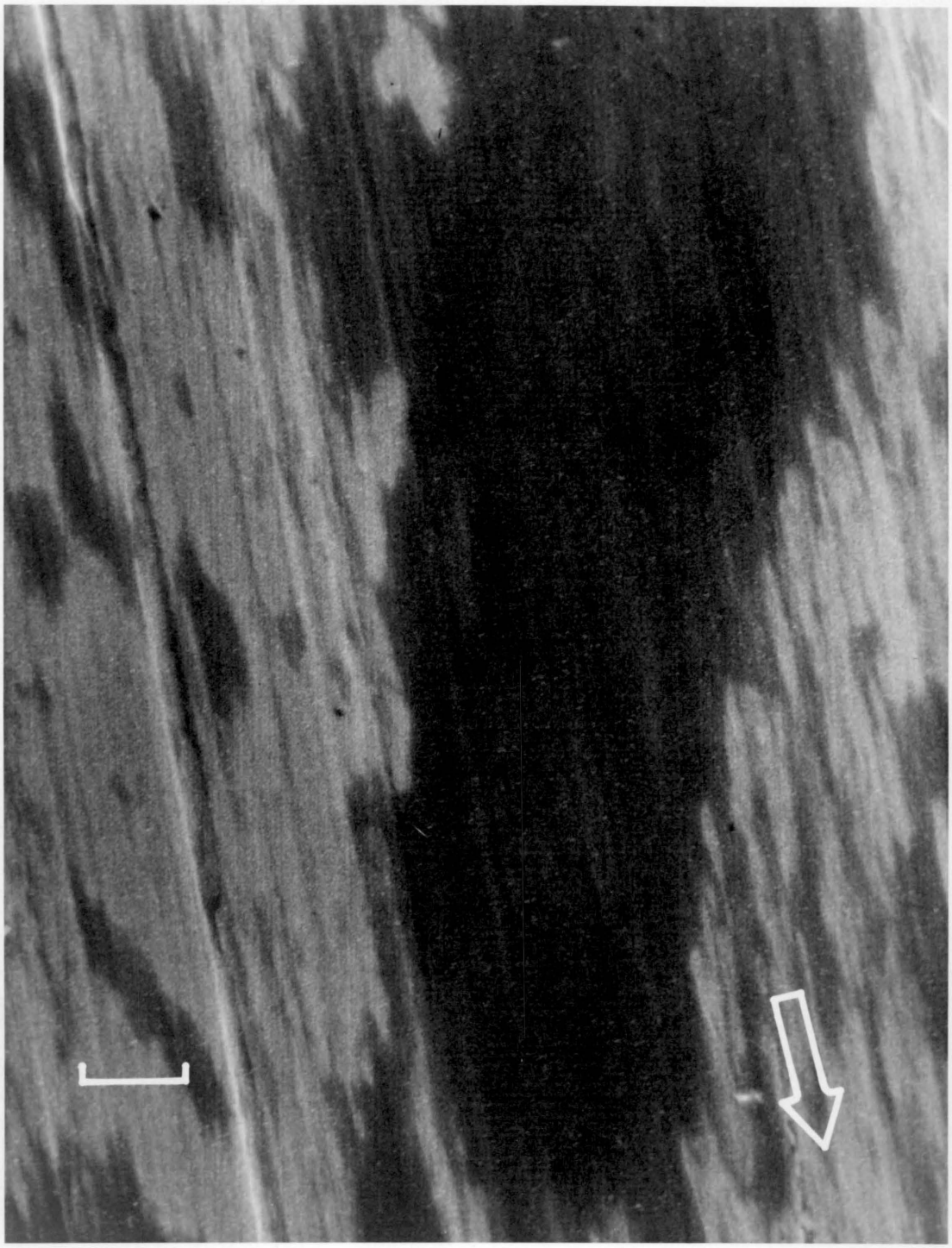

Figure 3. Scanning electron microscope picture of a smooth disk after 2400 passes at 32 cm/sec. Index mark is 10 μm. Arrow shows the direction of sliding of the pin.

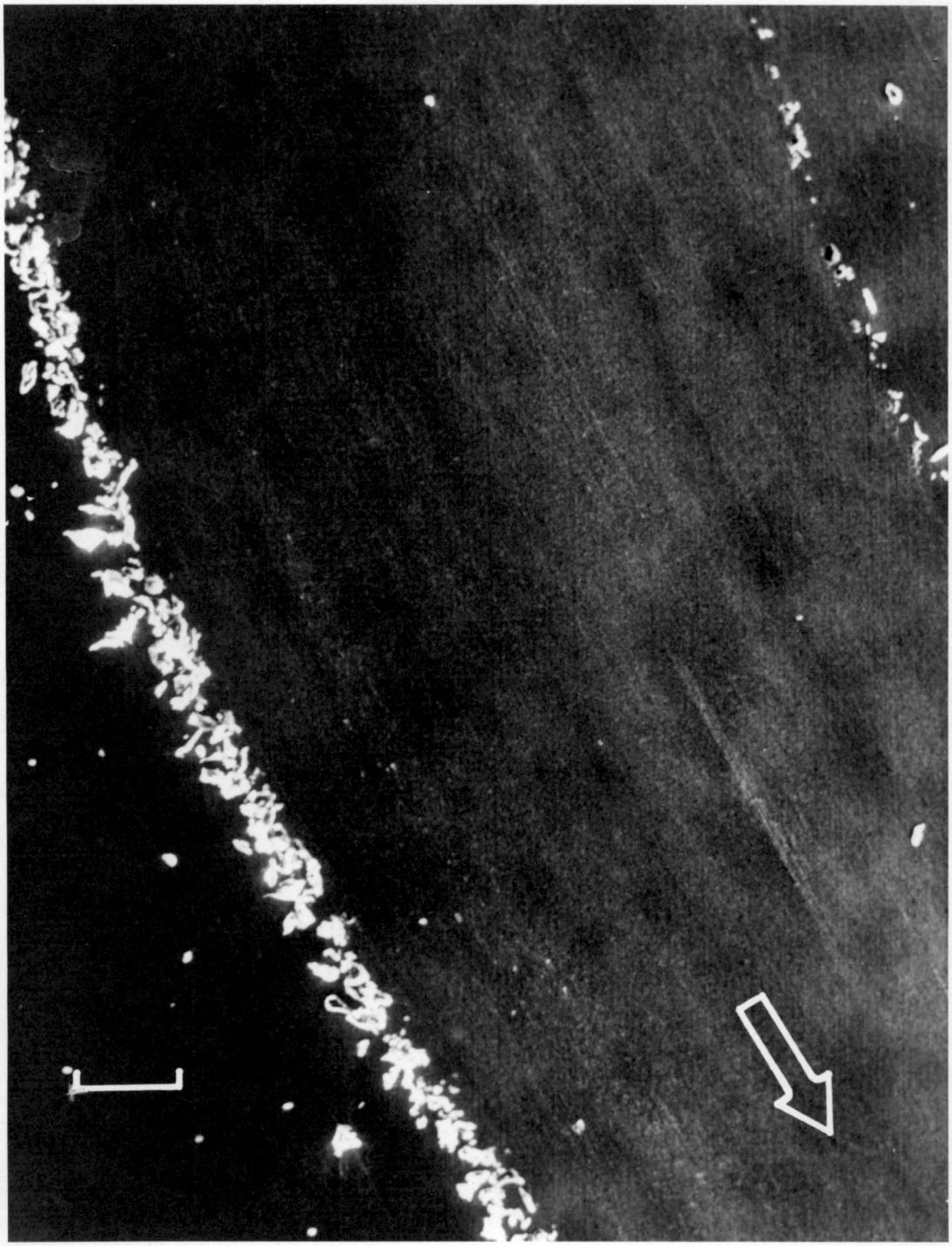

Figure 4. Scanning electron microscope picture of a smooth disk after 38400 passes at 32 cm/sec. Index mark is 200 μm. Arrow shows the direction of sliding of the pin.

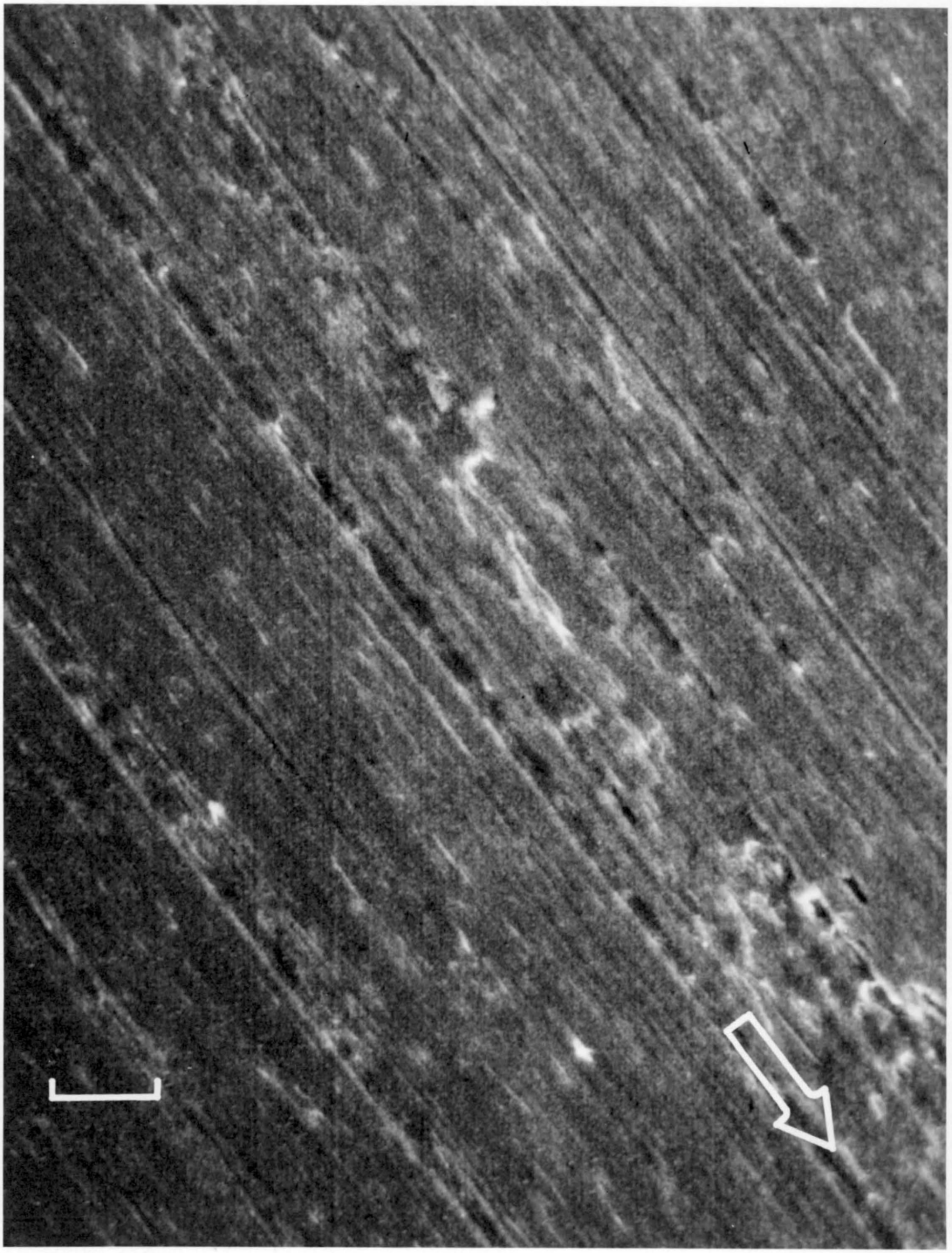

Figure 5. Scanning electron microscope picture of a smooth disk after 76800 passes at 32 cm/sec. Index mark is 10 μm. Arrow shows the direction of sliding of the pin.

Figure 6. Scanning electron microscope picture of a smooth disk after 76800 passes at 32 cm/sec. Index mark is 10 μm. Arrow shows the direction of sliding of the pin.

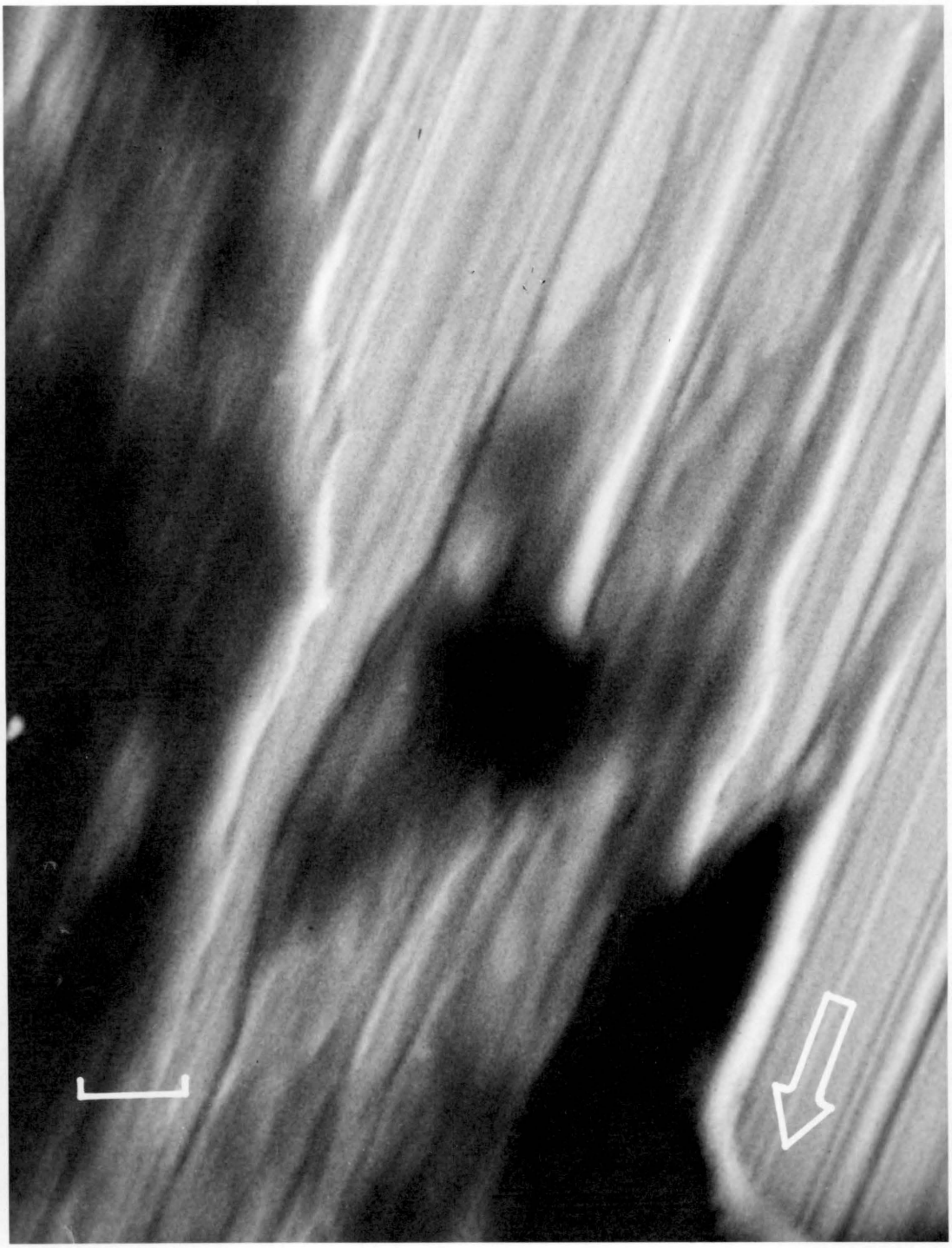

Figure 7. Scanning electron microscope picture of a smooth disk after 2400 passes at 128 cm/sec. Index mark is 10 μm. Arrow shows the direction of sliding of the pin.

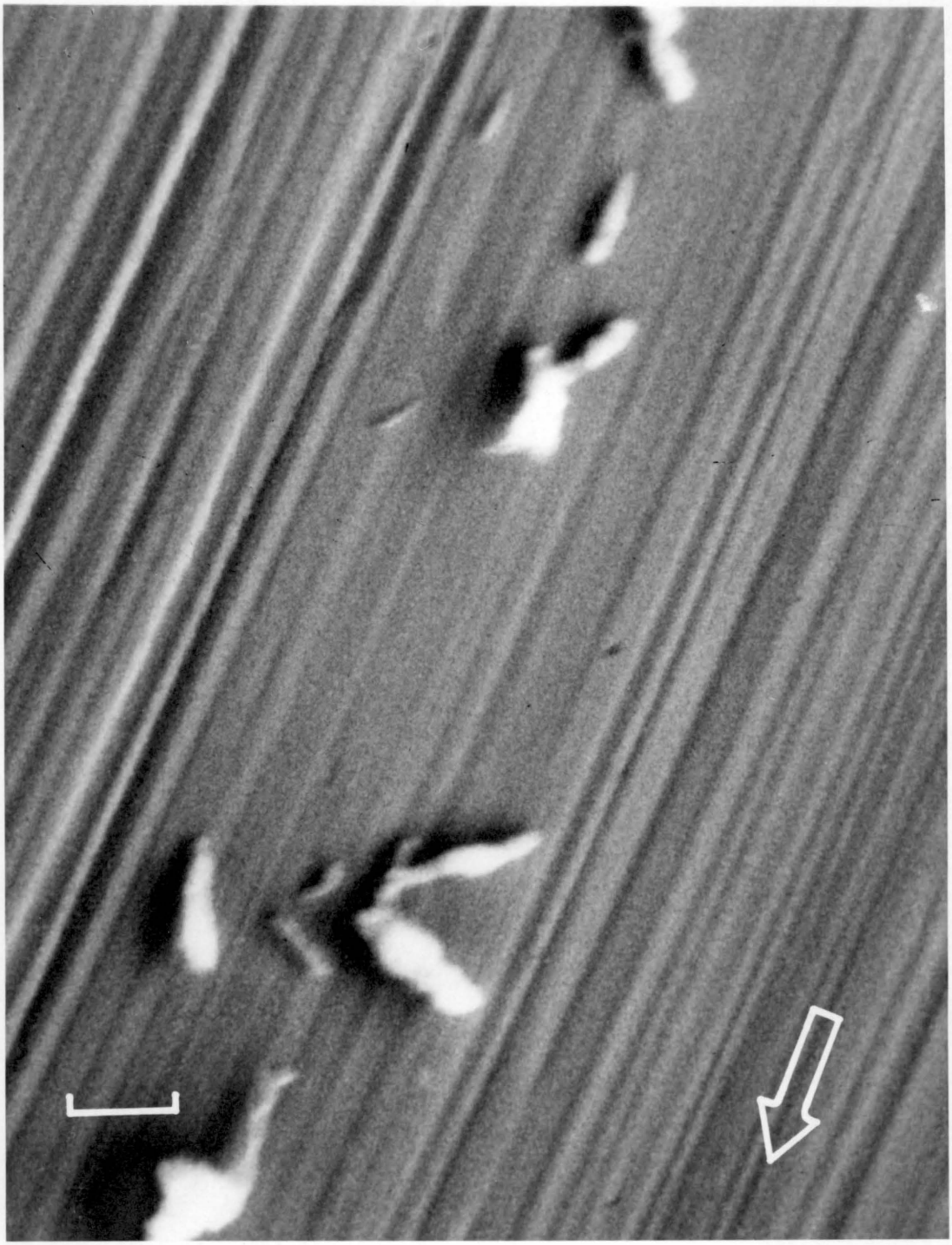

Figure 8. Scanning electron microscope picture of a smooth disk after 2400 passes at 128 cm/sec. Index mark is 10 μm. Arrow shows the direction of sliding of the pin.

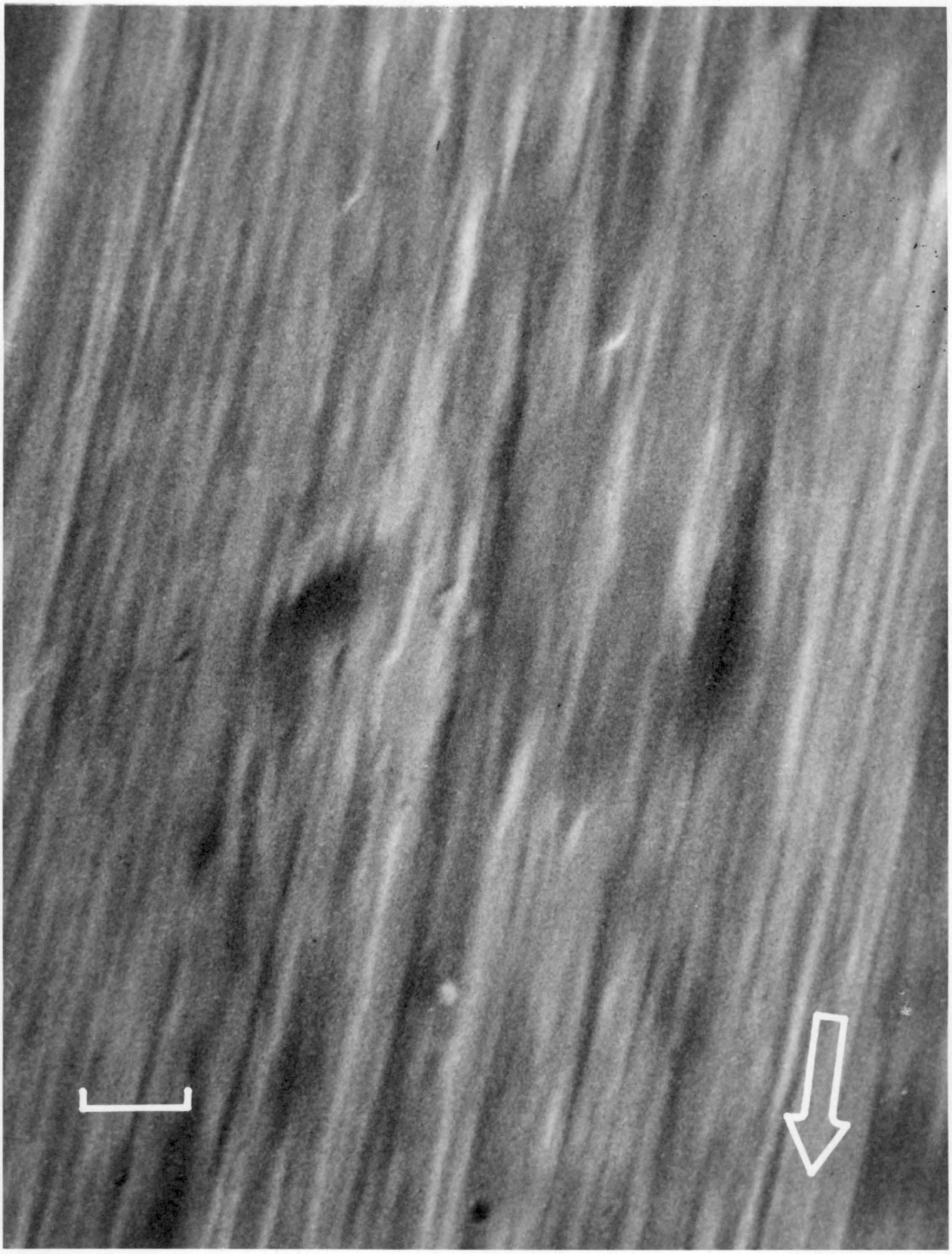

Figure 9. Scanning electron microscope picture of a smooth disk after 4800 passes at 128 cm/sec. Index mark is 10 μm. Arrow shows the direction of sliding of the pin.

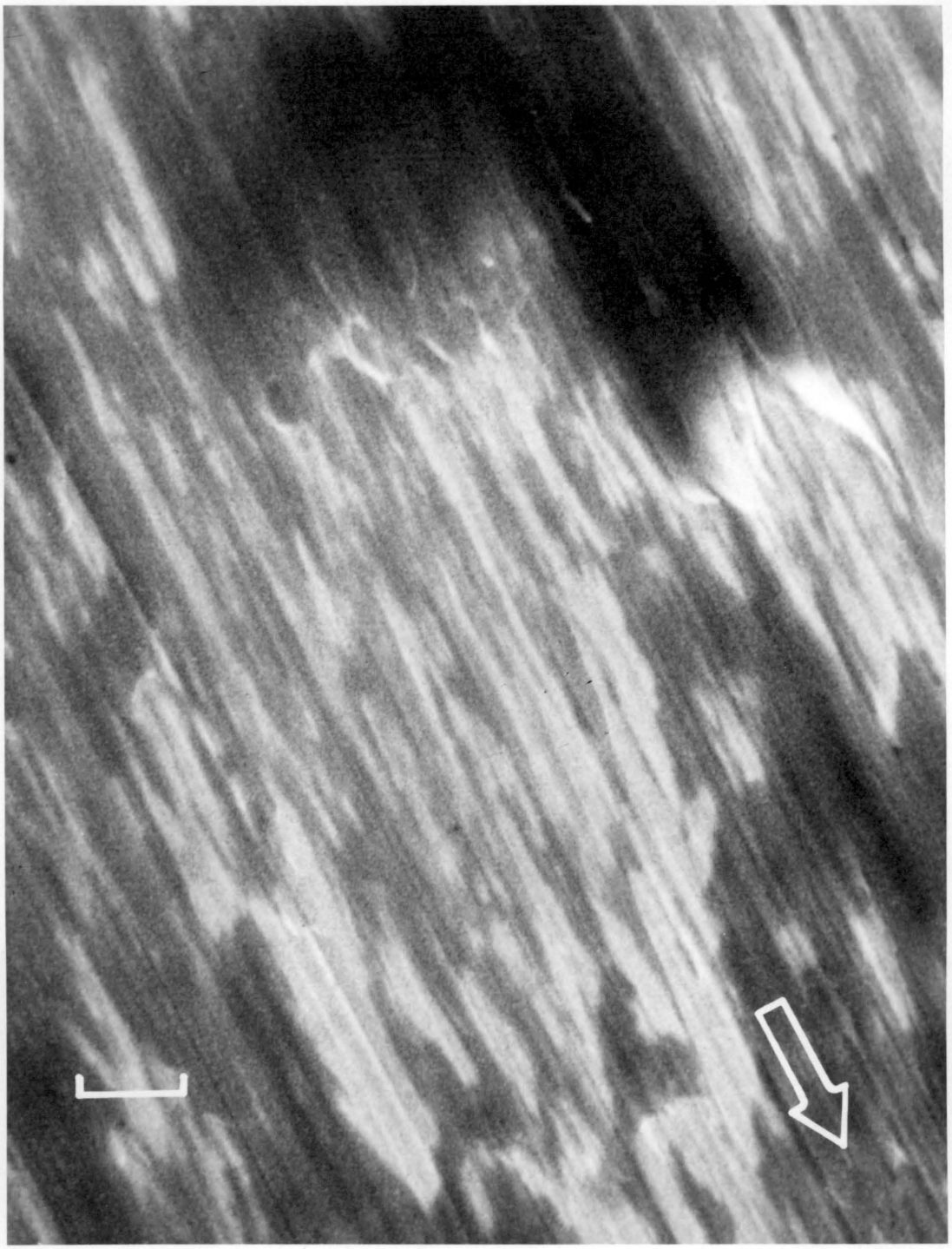

Figure 10. Scanning electron microscope picture of a smooth disk after 9600 passes at 128 cm/sec. Index mark is 10 μm. Arrow shows the direction of sliding of the pin.

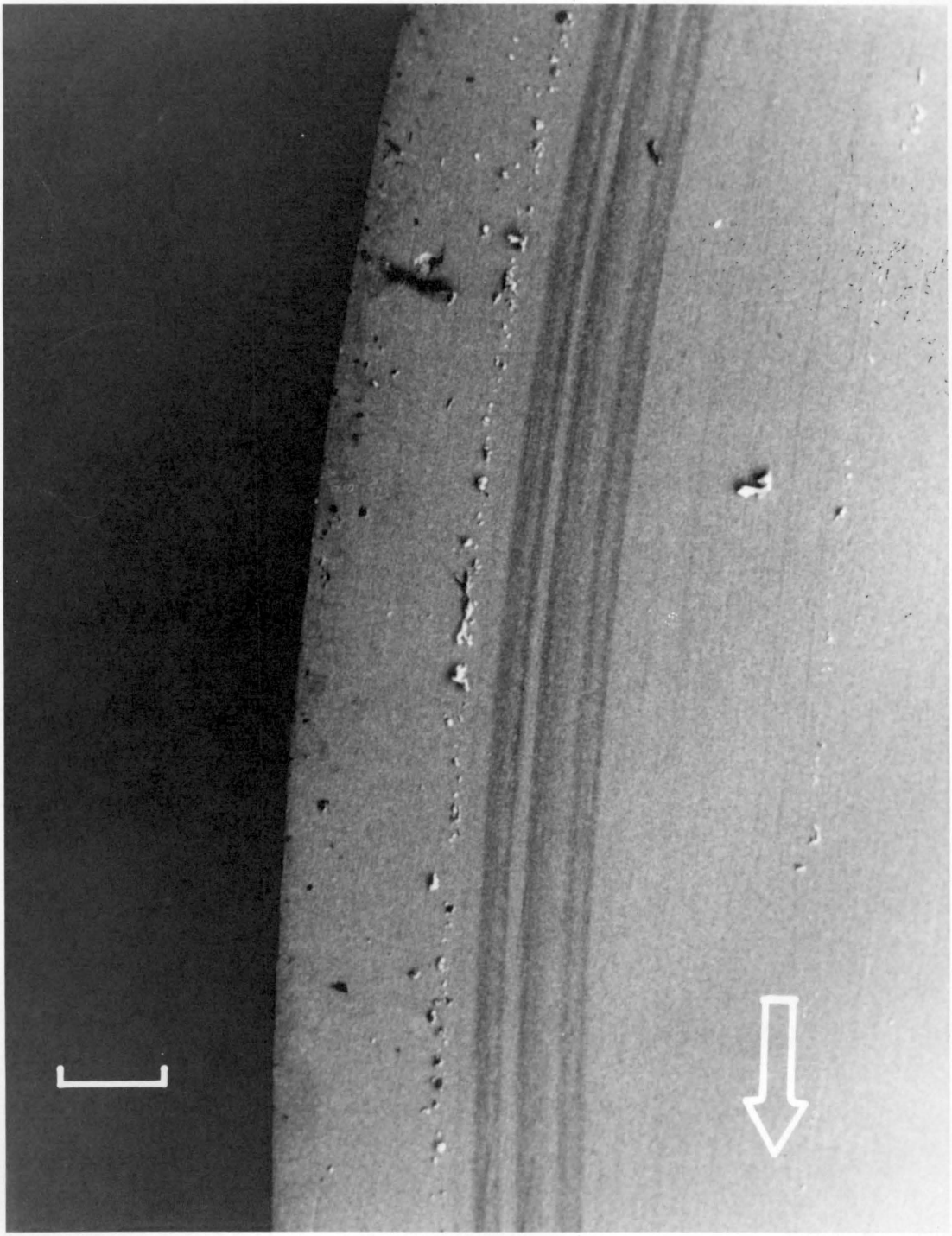

Figure 11. Scanning electron microscope picture of a smooth disk after 57600 passes at 128 cm/sec. Index mark is 500 μm. Arrow shows the direction of sliding of the pin.

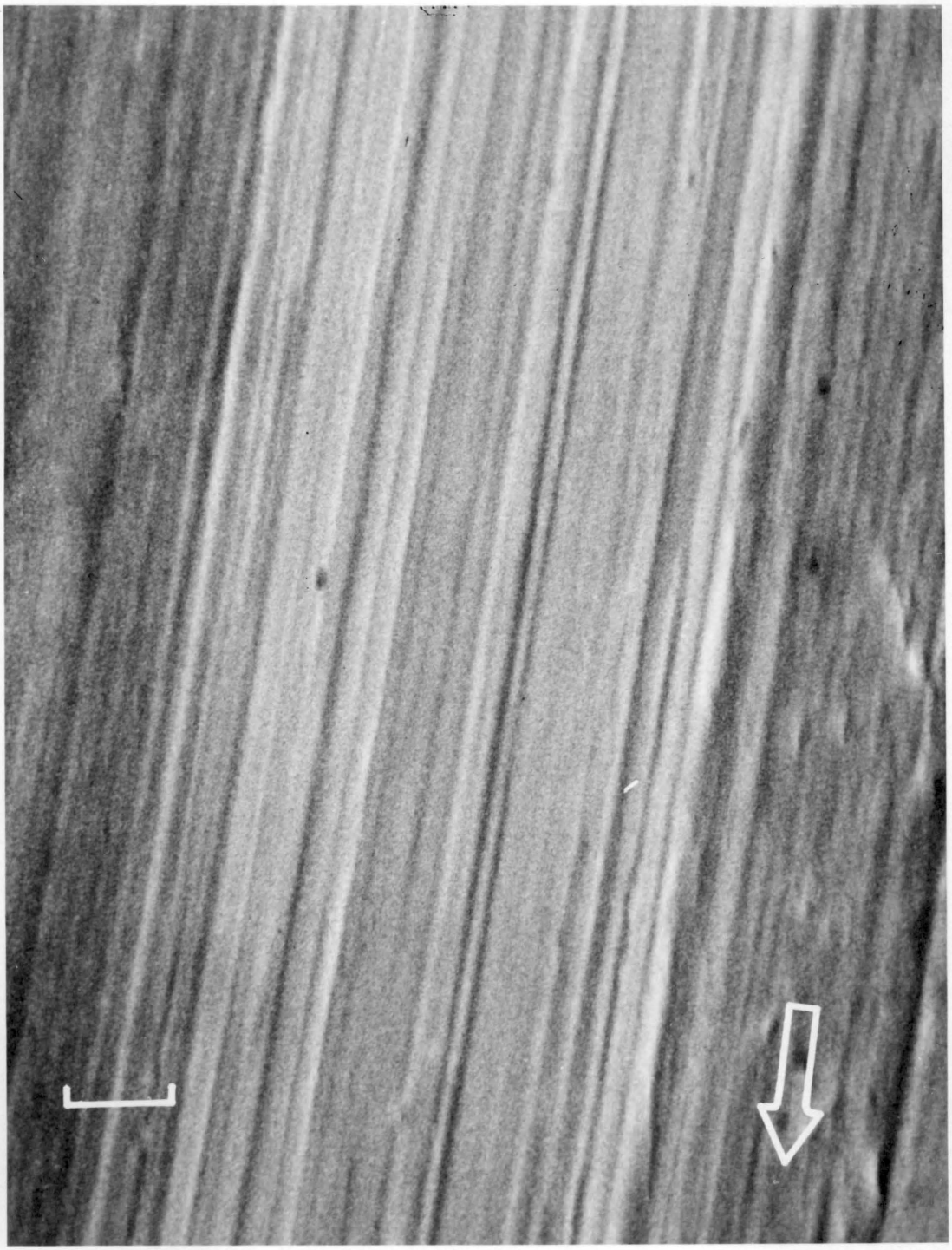

Figure 12. Scanning electron microscope picture of a smooth disk after 57600 passes at 128 cm/sec. Index mark is 10 μm. Arrow shows the direction of sliding of the pin.

energy that can be stored in the film exceeds the energy of adhesion between the film and the steel surface. At this point, parts of the film break off leaving sharp edged holes in the surface [Fig. 13]. Removal of the film from the surface continues [Fig. 14] until all of the film breaks off and forms large debris particles made up of layers [Fig. 15]. Then a new film starts forming [Fig. 16] and the process repeats.

Perpendicular Sliding

The adhesive mechanism governs the wear process in perpendicular sliding and no abrasive cutting is observed. The deposits on the steel surface are in the form of thin films, which are not affected by the irregularities of the surface.

At the low speed of sliding non-uniform films adhere to the surface [Fig. 17] and become thicker [Fig. 18] and more uniform [Fig. 19] as the number of passes increase. At the high speed non-uniform films are also formed [Fig. 20], and they get thicker [Fig. 21]. However, at the high speed the thick films form in fewer passes than is observed in the low speed. Softening of the polymer results in a higher wear rate and loose debris particles are formed. As the process continues, some of those loose debris particles are pushed into the grooves, which later become favorable places for the initiation of film formation [Fig. 22].

This phenomenon can readily be observed in deeper grooves, which are partially filled by layers of polymer film [Fig. 23, 24]. The

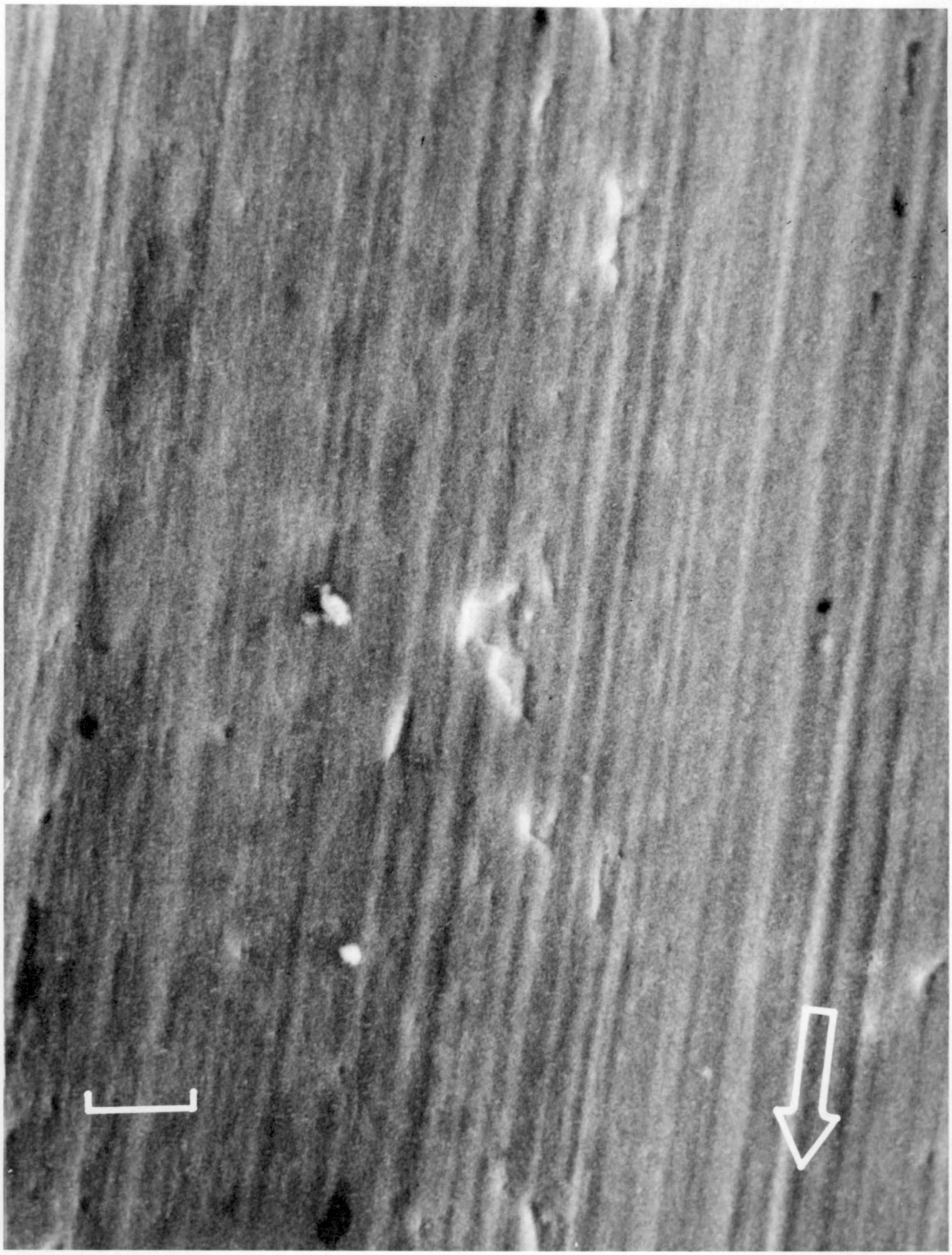

Figure 13. Scanning electron microscope picture of a smooth disk after 57600 passes at 128 cm/sec. Index mark is 10 μm. Arrow shows the direction of sliding of the pin.

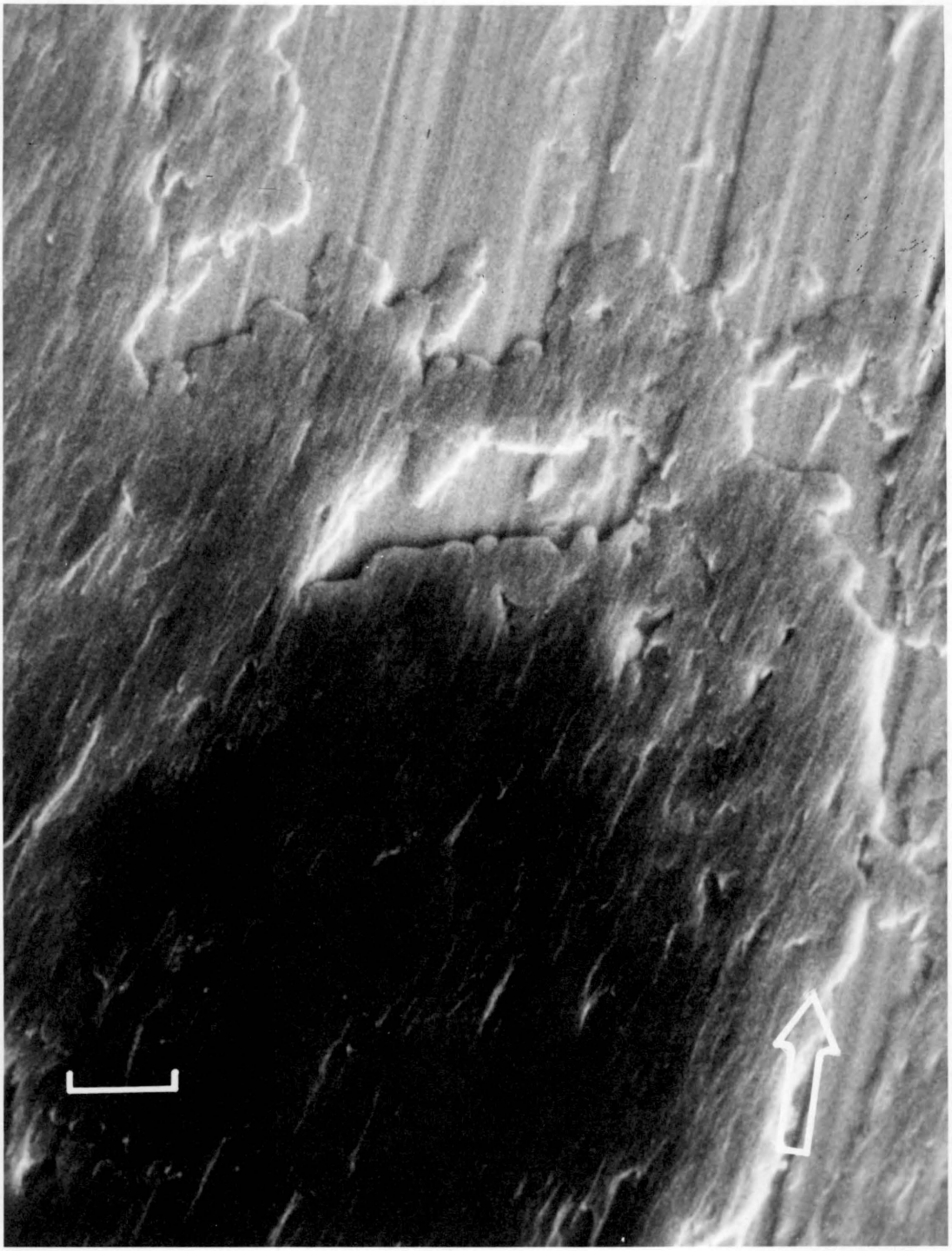

Figure 14. Scanning electron microscope picture of a smooth disk after 76800 passes at 128 cm/sec. Index mark is 10 μm. Arrow shows the direction of sliding of the pin.

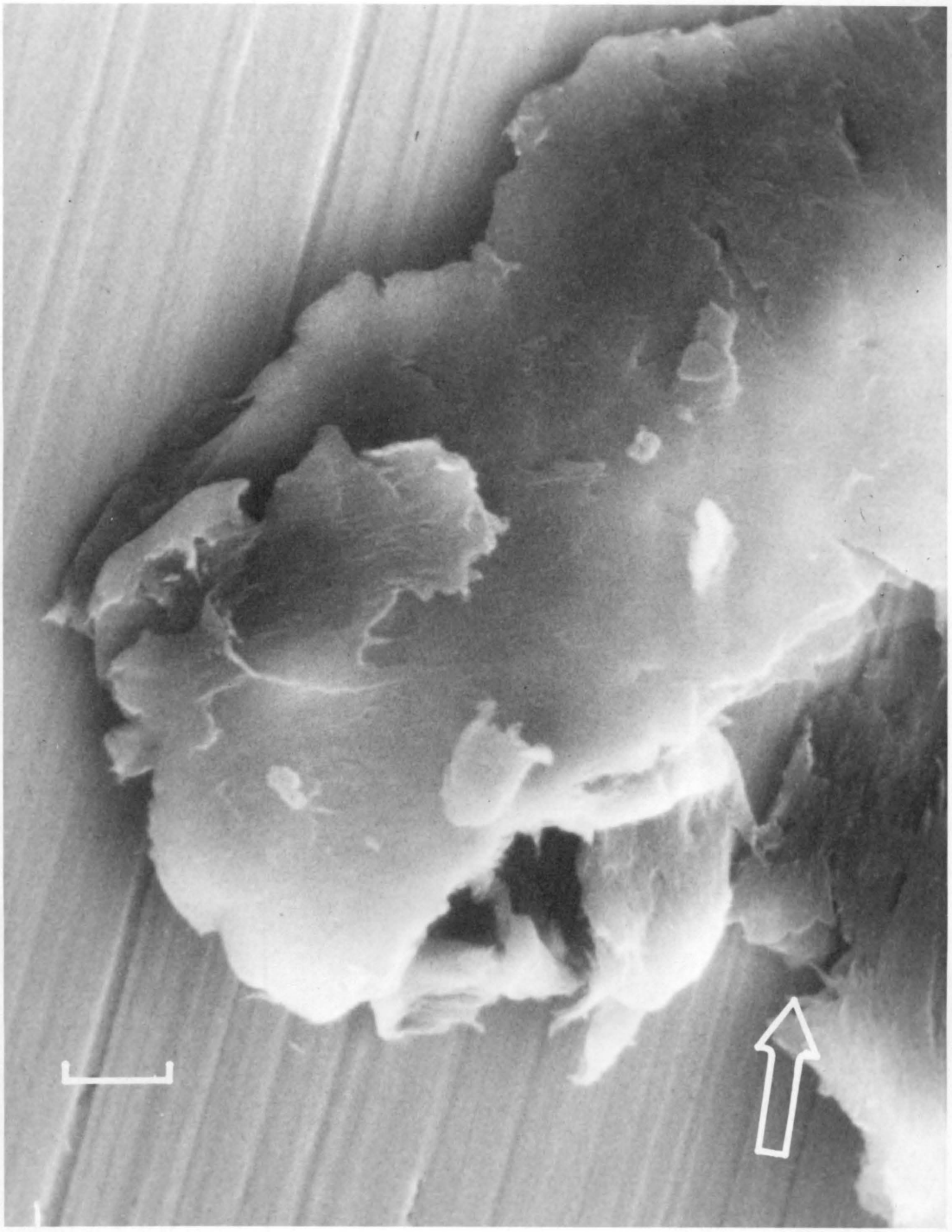

Figure 15. Scanning electron microscope picture of a smooth disk after 76800 passes at 128 cm/sec. Index mark is 10 μm. Arrow shows the direction of sliding of the pin.

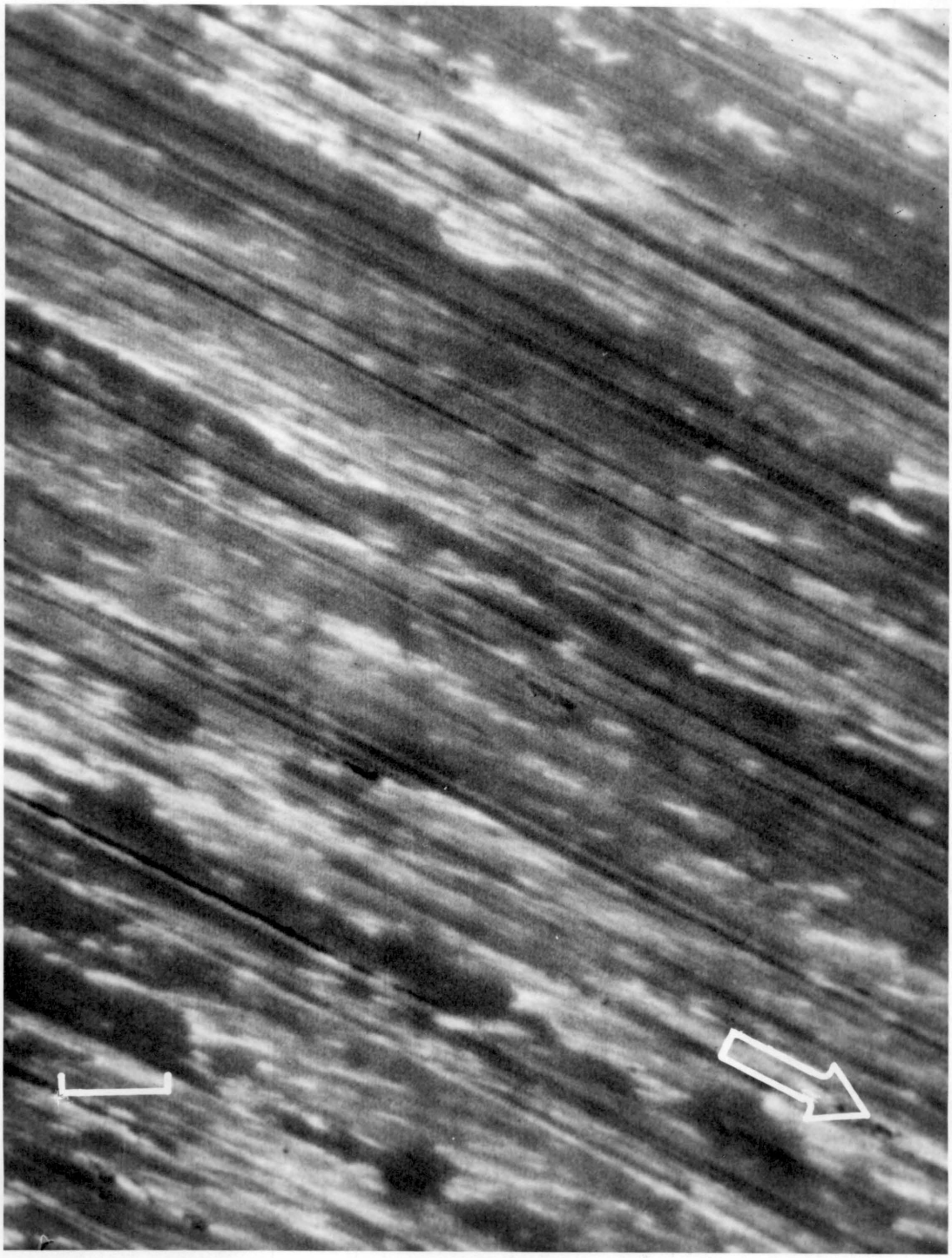

Figure 16. Scanning electron microscope picture of a smooth disk after 115200 passes at 128 cm/sec. Index mark is 10 μm. Arrow shows the direction of sliding of the pin.

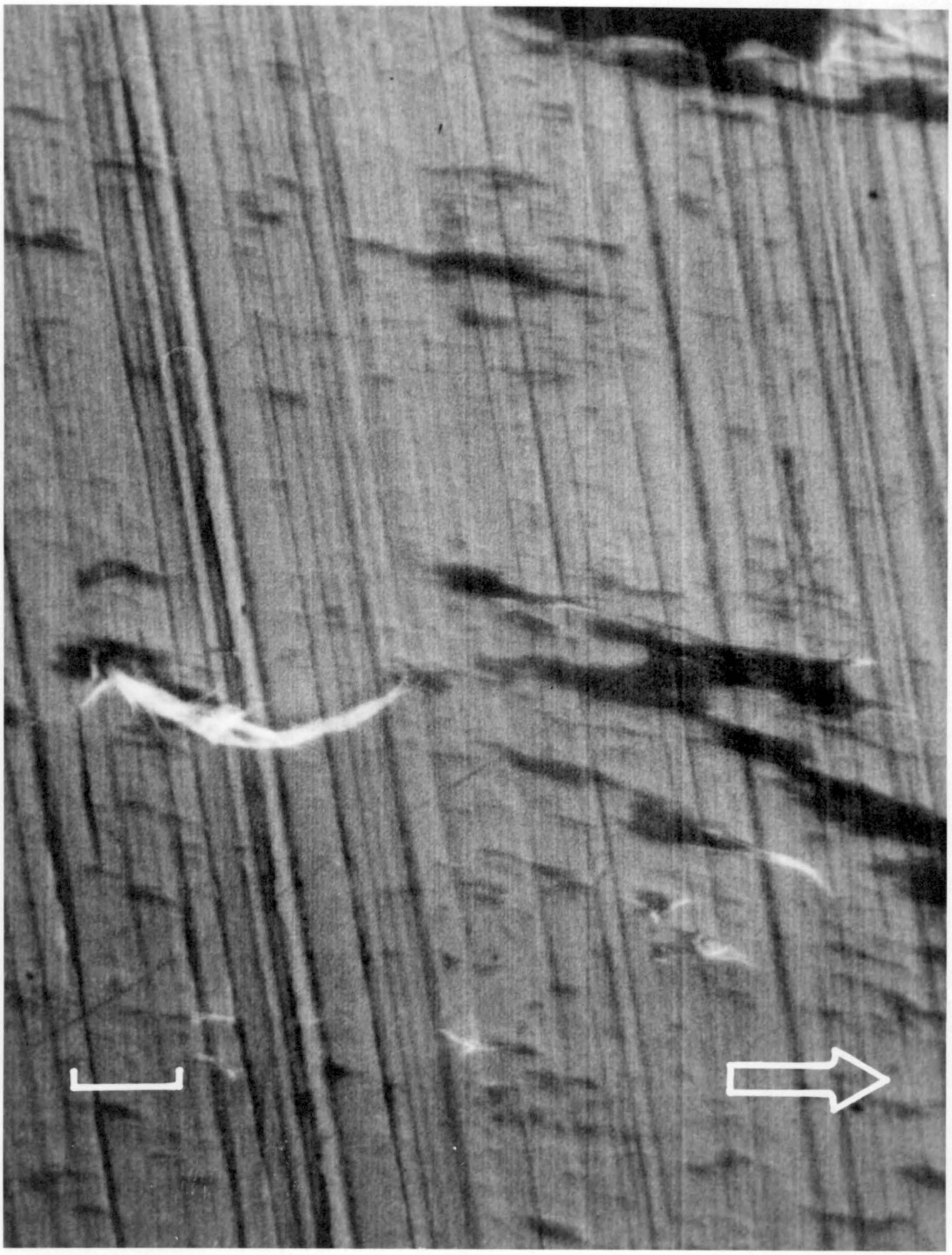

Figure 17. Scanning electron microscope picture of a smooth disk after 2400 passes at 32 cm/sec. Index mark is 10 μm. Arrow shows the direction of sliding of the pin.

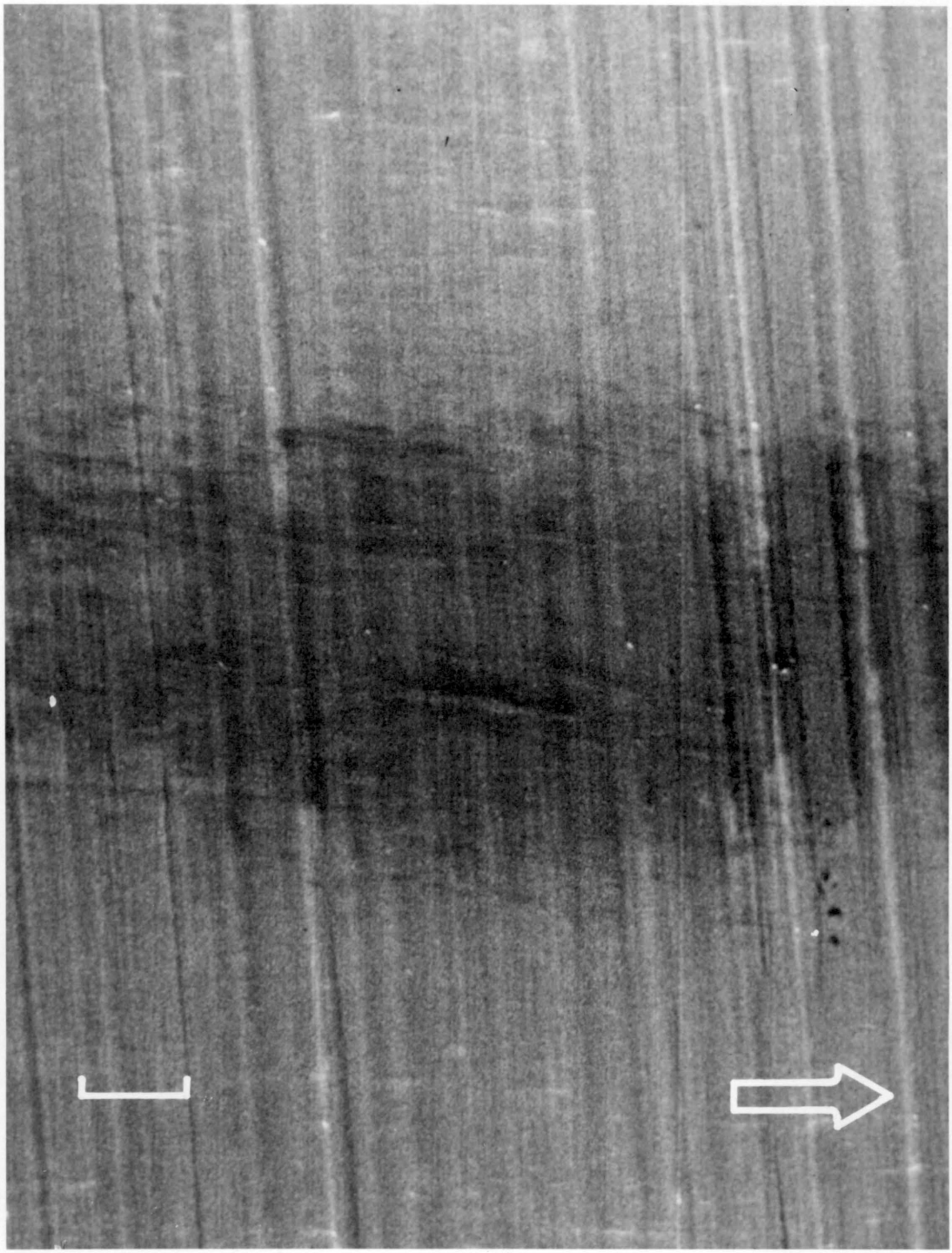

Figure 18. Scanning electron microscope picture of a smooth disk after 9600 passes at 32 cm/sec. Index mark is 10 μm. Arrow shows the direction of sliding of the pin.

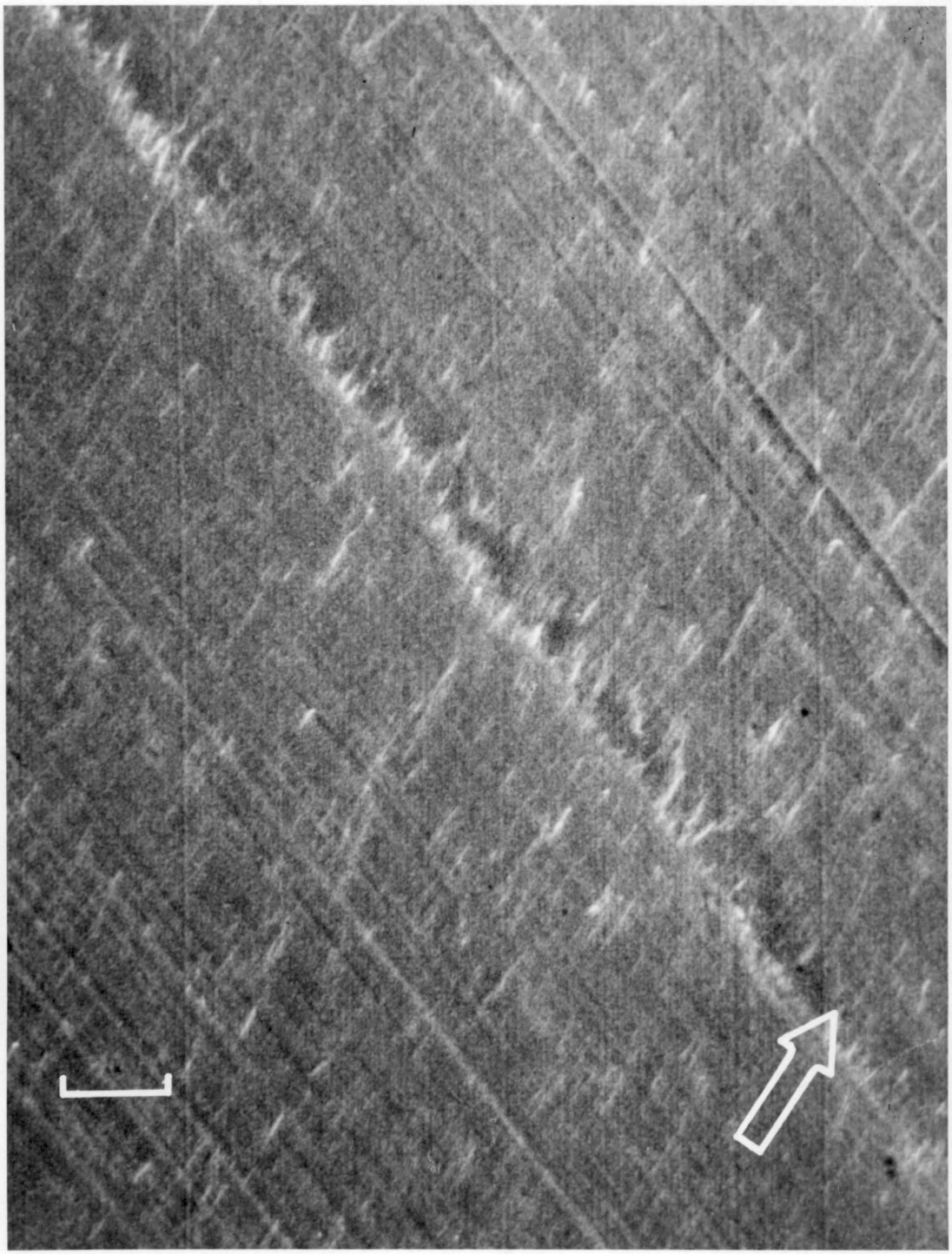

Figure 19. Scanning electron microscope picture of a smooth disk after 76800 passes at 32 cm/sec. Index mark is 10 μm. Arrow shows the direction of sliding of the pin.

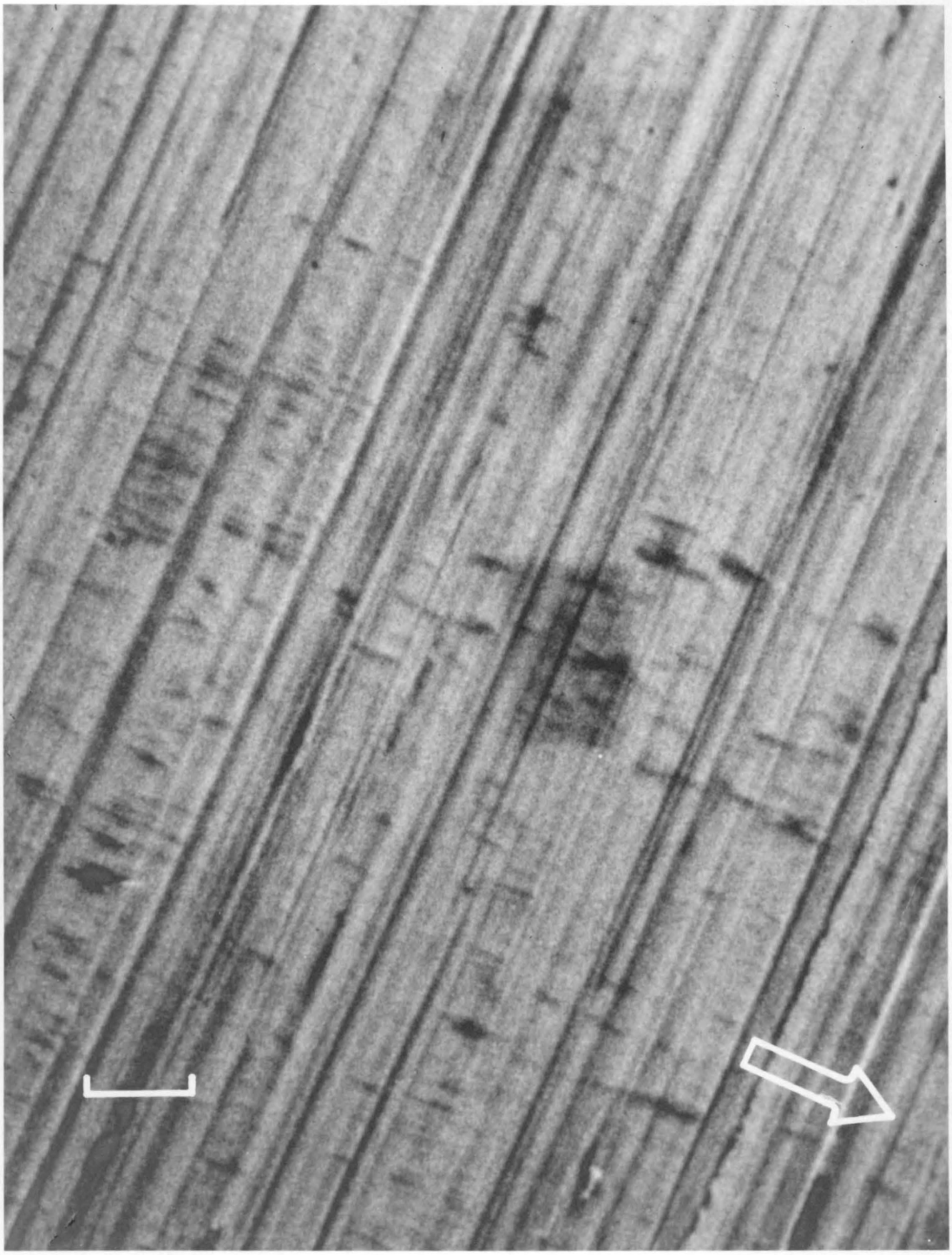

Figure 20. Scanning electron microscope picture of a smooth disk after 2400 passes at 128 cm/sec. Index mark is 10 μm. Arrow shows the direction of sliding of the pin.

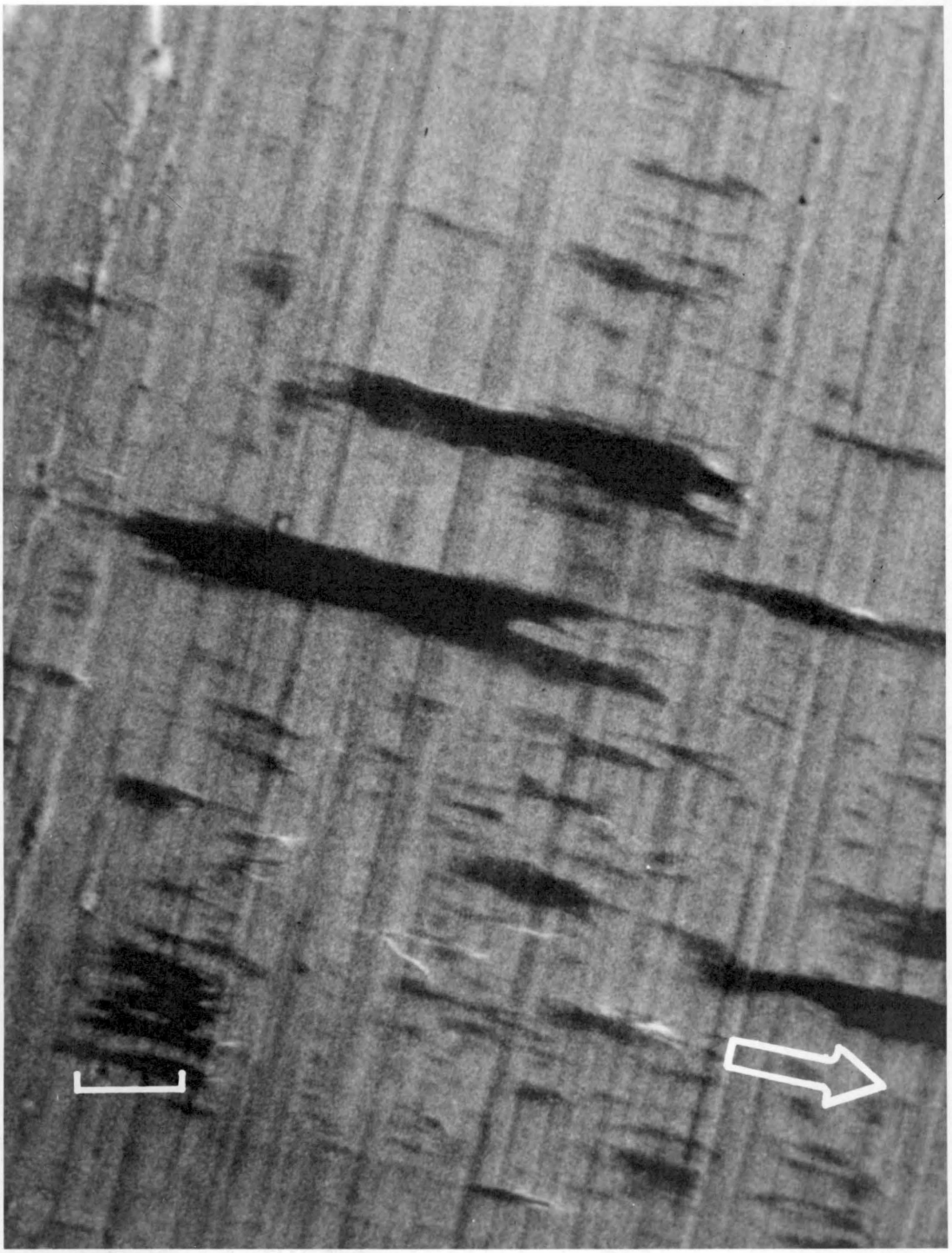

Figure 21. Scanning electron microscope picture of a smooth disk after 4800 passes at 128 cm/sec. Index mark is 10 μm. Arrow shows the direction of sliding of the pin.

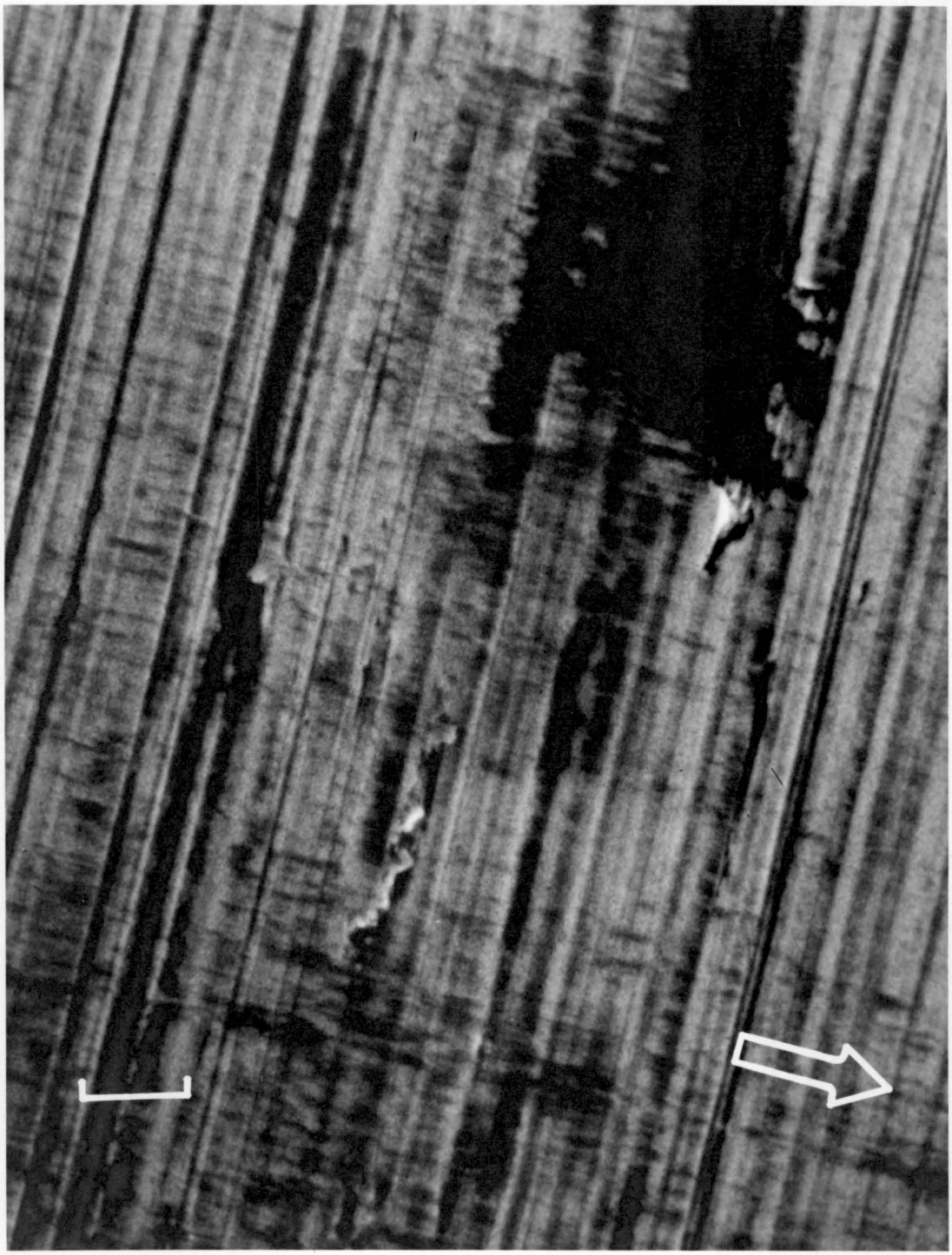

Figure 22. Scanning electron microscope picture of a smooth disk after 38400 passes at 128 cm/sec. Index mark is 10 μm. Arrow shows the direction of sliding of the pin.

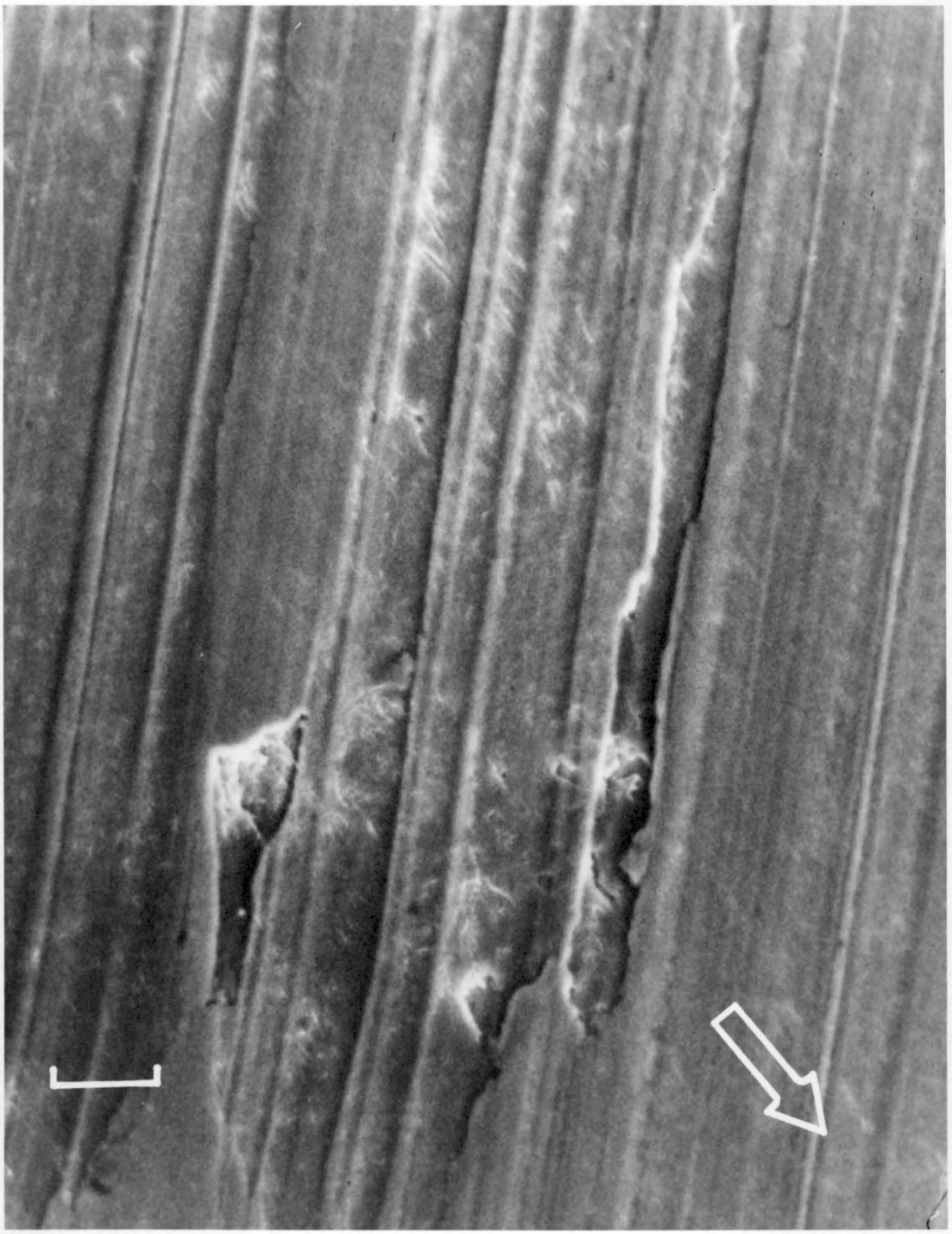

Figure 23. Scanning electron microscope picture of a smooth disk after 57600 passes at 128 cm/sec. Index mark is 10 μm. Arrow shows the direction of sliding of the pin.

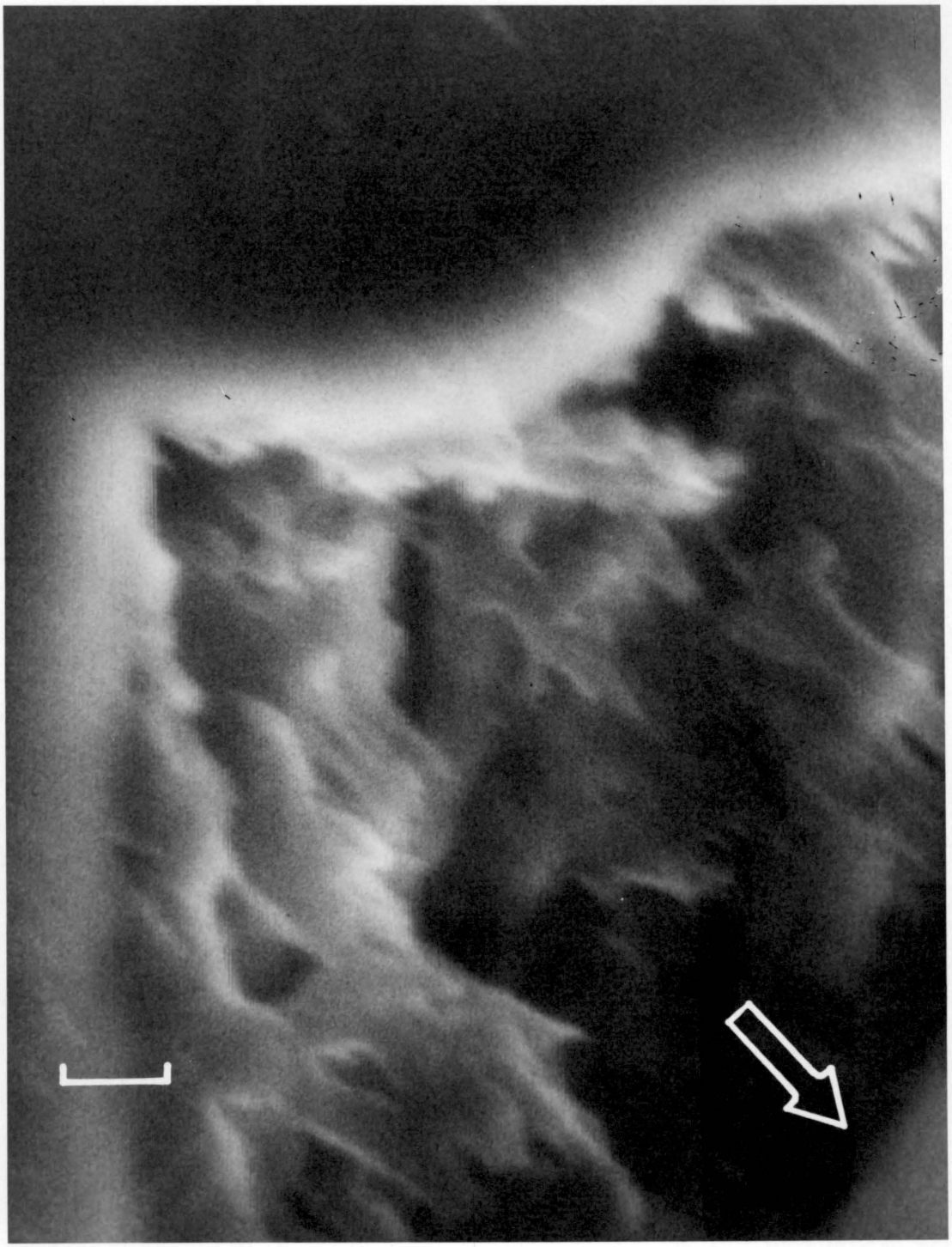

Figure 24. Scanning electron microscope picture of a smooth disk after 57600 passes at 128 cm/sec. Index mark is 1 μm. Arrow shows the direction of sliding of the pin.

fact that filling starts from the leading edge of the groove shows that the mechanism is an adhesive mechanism, because abrasive cutting would occur at the trailing edge of the groove and the deposits would be gathered in front of the leading edge of the asperity.

Wear Surfaces of the Pins

Pins that are worn at the low speed show that adhesive forces play a dominant role in the shearing of the surface films. These adhesive forces cause plastic deformations forming tongues [Fig. 25], and also remove thick layers, [Fig. 26], which become loose debris particles [Fig. 27]. Although melting is not expected at this speed of sliding [Ref. 10], flow can be observed at higher number of passes [Fig. 28].

The wear rate is higher at the high speed, but initial wear results in the shearing of thinner layers, and in the production of smoother surfaces [Fig. 29]. This is due to the temperature effects, which cause the softening and flow of the top layers over lower layers [Fig. 30]. As the number of passes increase excessive heating and probably gross melting takes place. As a result of this softening, sheared films adhere to each other and are removed in thicker films made up of many layers [Fig. 31].

b. Rough Surfaces

Rubbing of the polymer film on the rough surface causes an abrasive wear mechanism to control the wear process, and chunks of

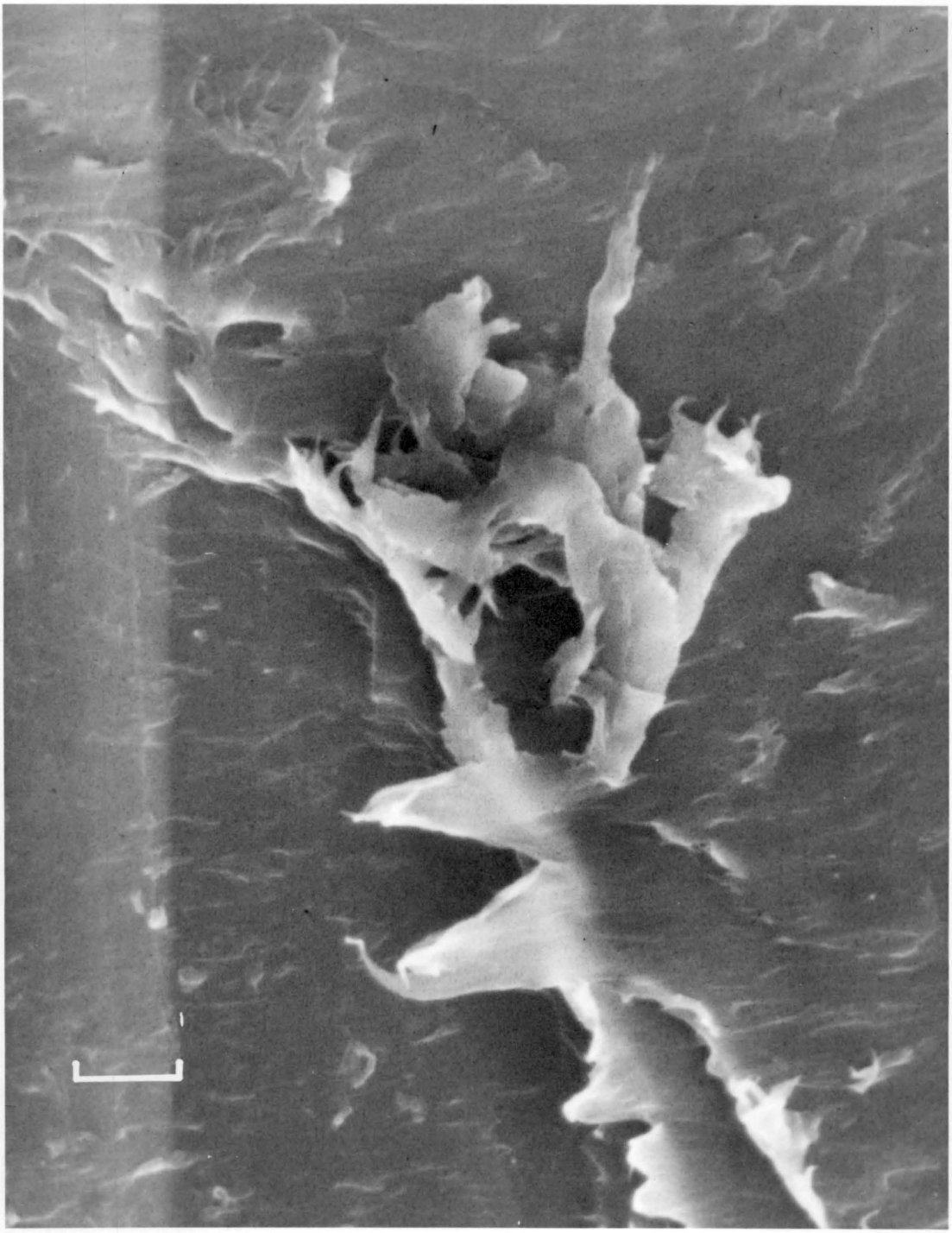

Figure 25. Scanning electron microscope picture of a pin after 9600 passes on a smooth disk at 32 cm/sec. Index mark is 10 μm.

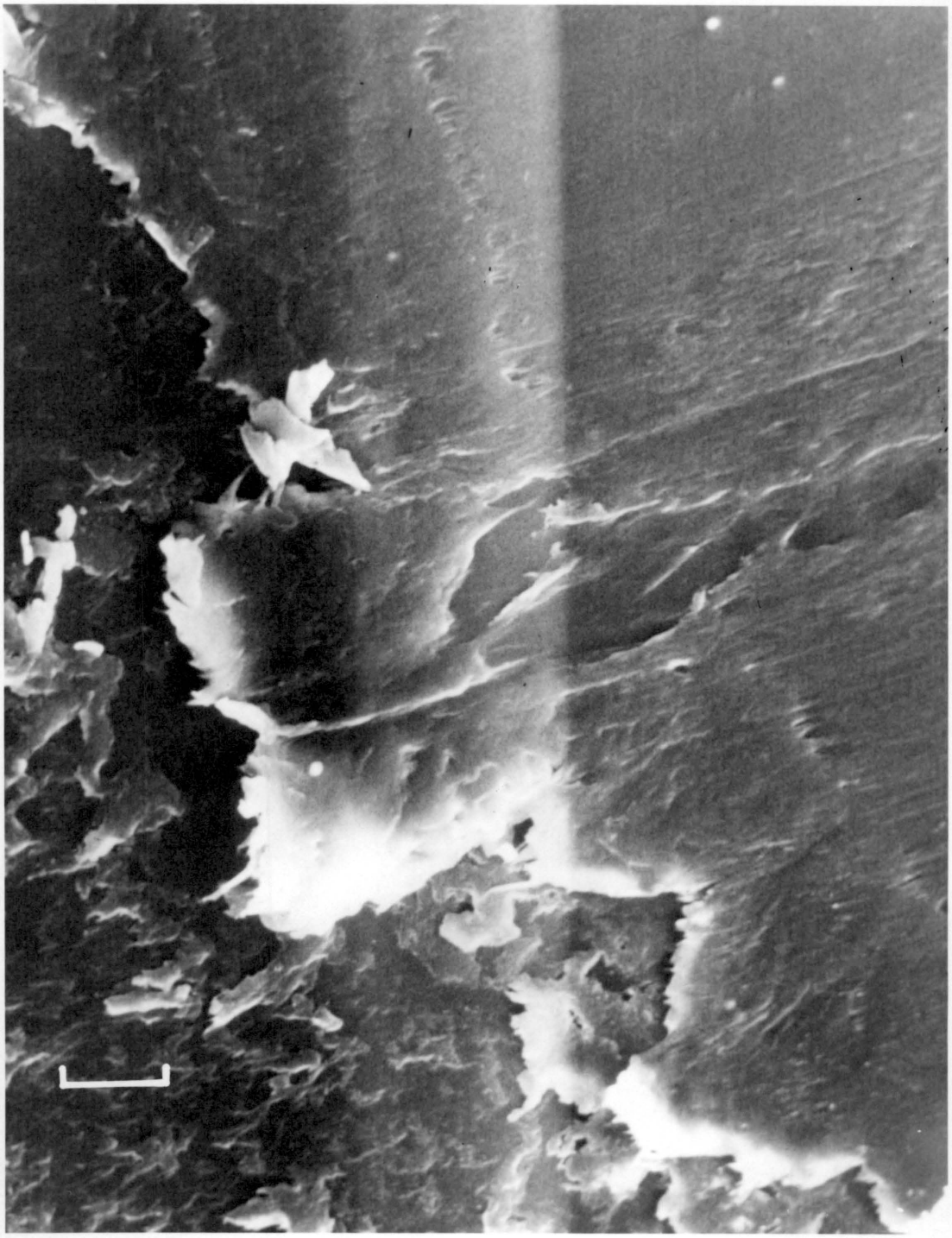

Figure 26. Scanning electron microscope picture of a pin after 9600 passes on a smooth disk at 32 cm/sec. Index mark is 20 μm.

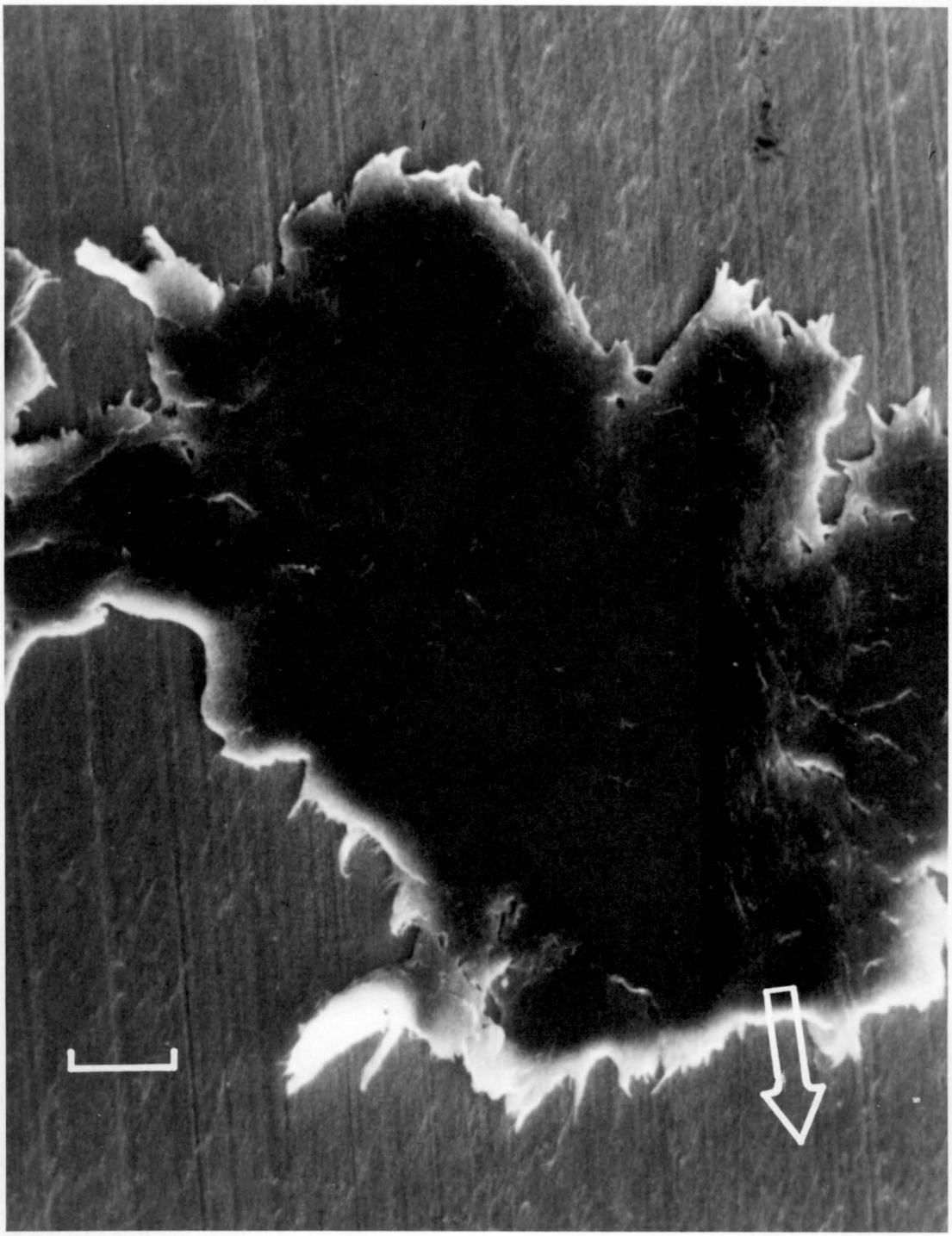

Figure 27. Scanning electron microscope picture of a smooth disk after 9600 passes at 32 cm/sec. Index mark is 20 μm. Arrow shows the direction of sliding of the pin.

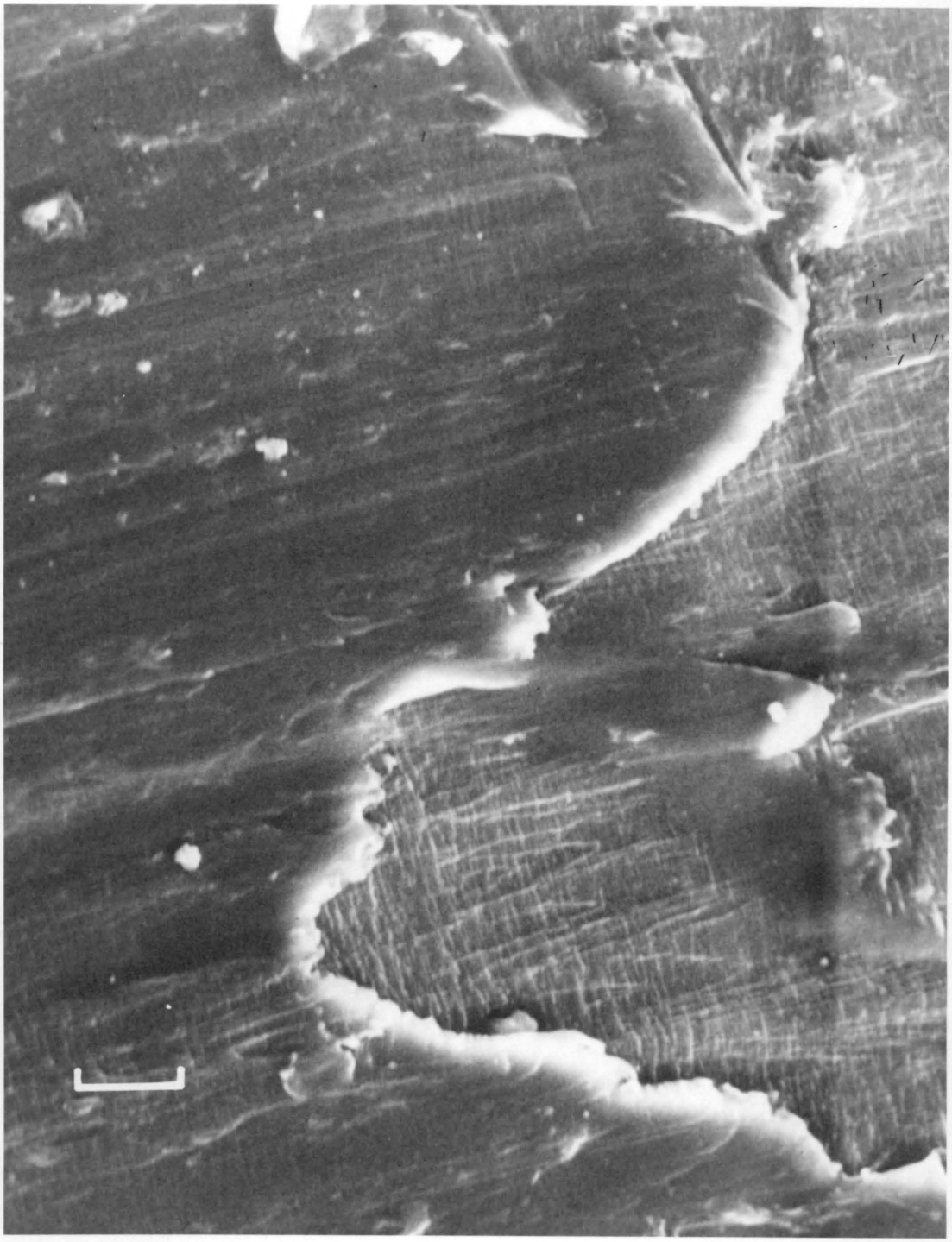

Figure 28. Scanning electron microscope picture of a pin after 76800 passes on a smooth disk at 32 cm/sec. Index mark is 20 μm.

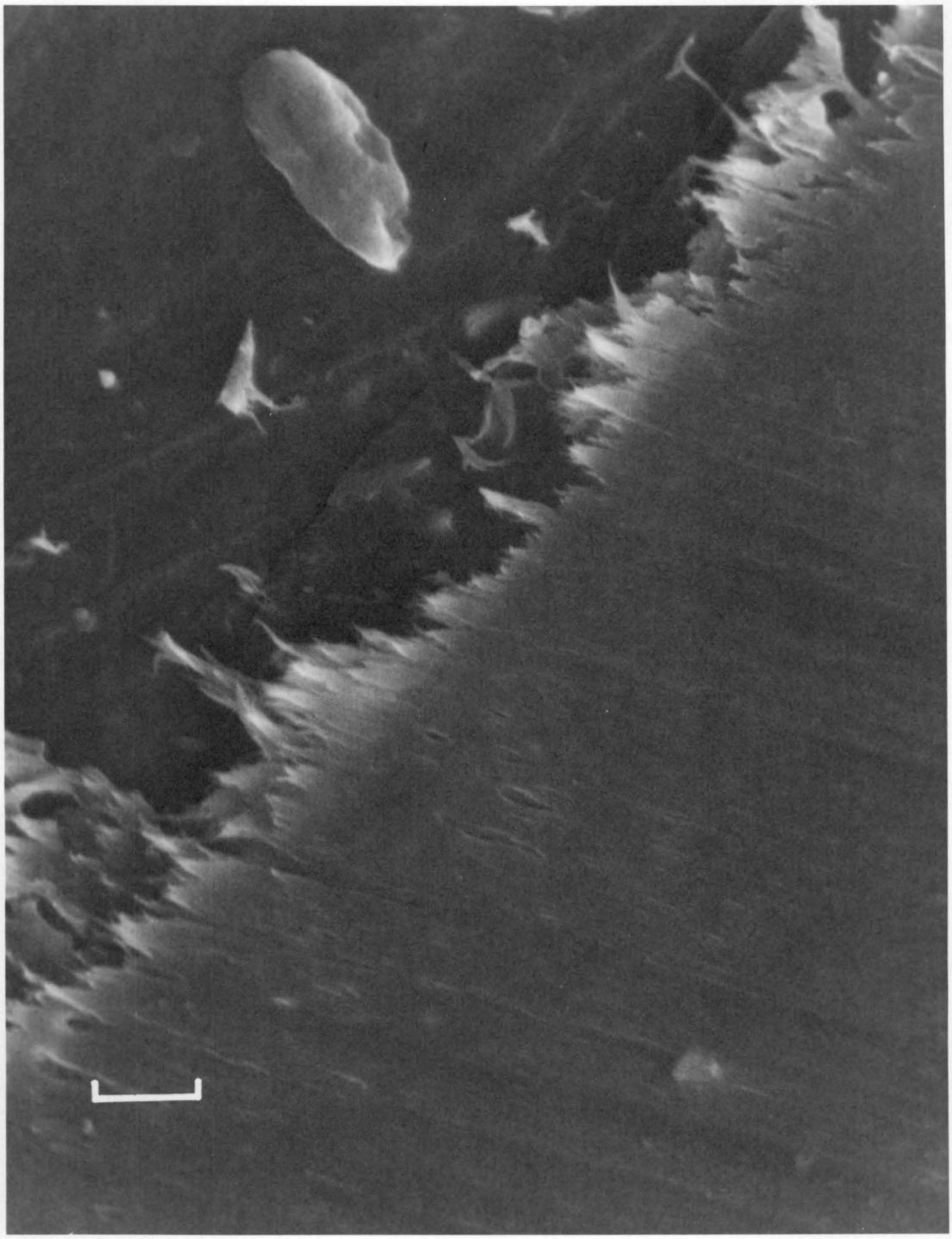

Figure 29. Scanning electron microscope picture of a pin after 2400 passes on a smooth disk at 128 cm/sec. Index mark is 10 μm.

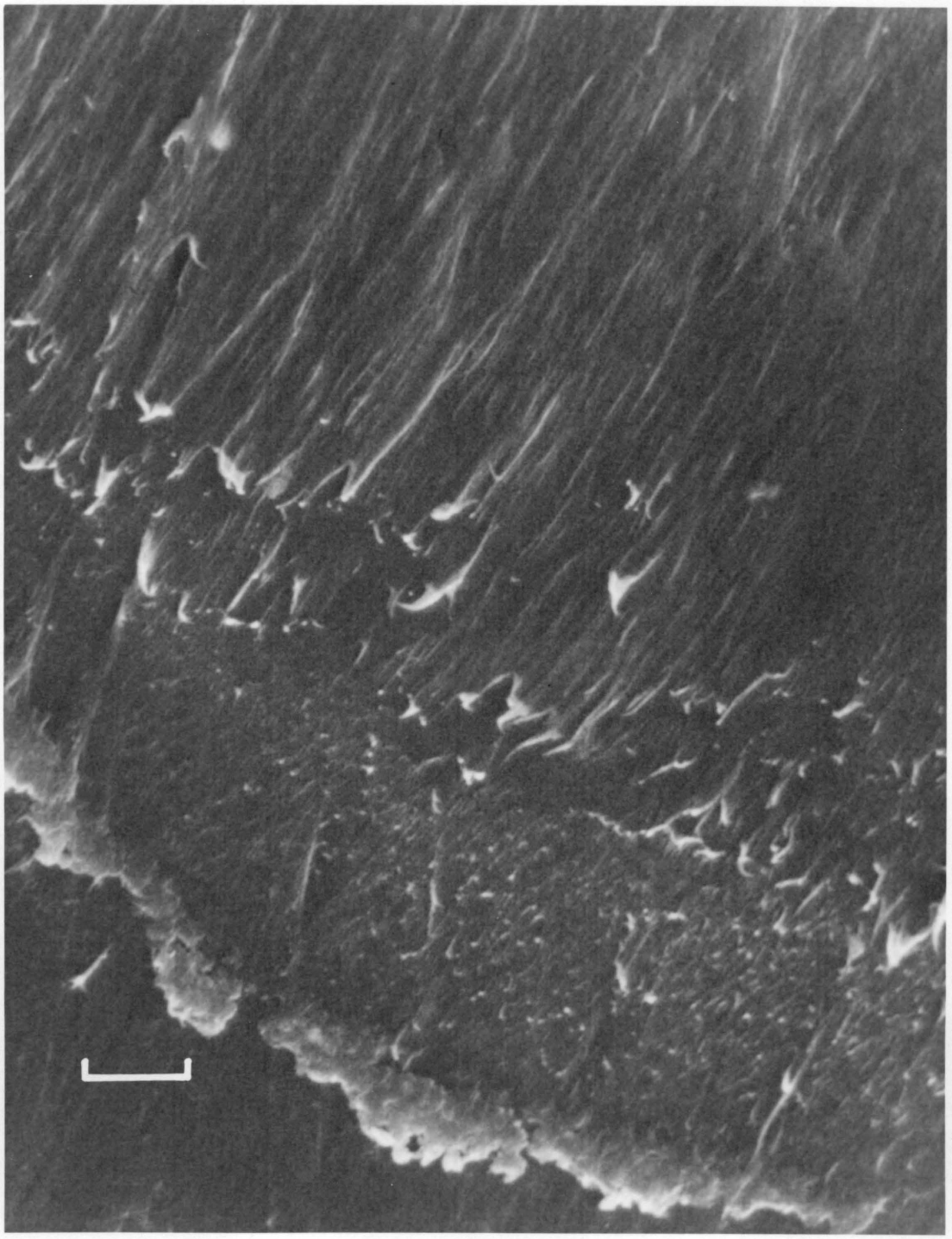

Figure 30. Scanning electron microscope picture of a pin after 4800 passes on a smooth disk at 128 cm/sec. Index mark is 10 μm.

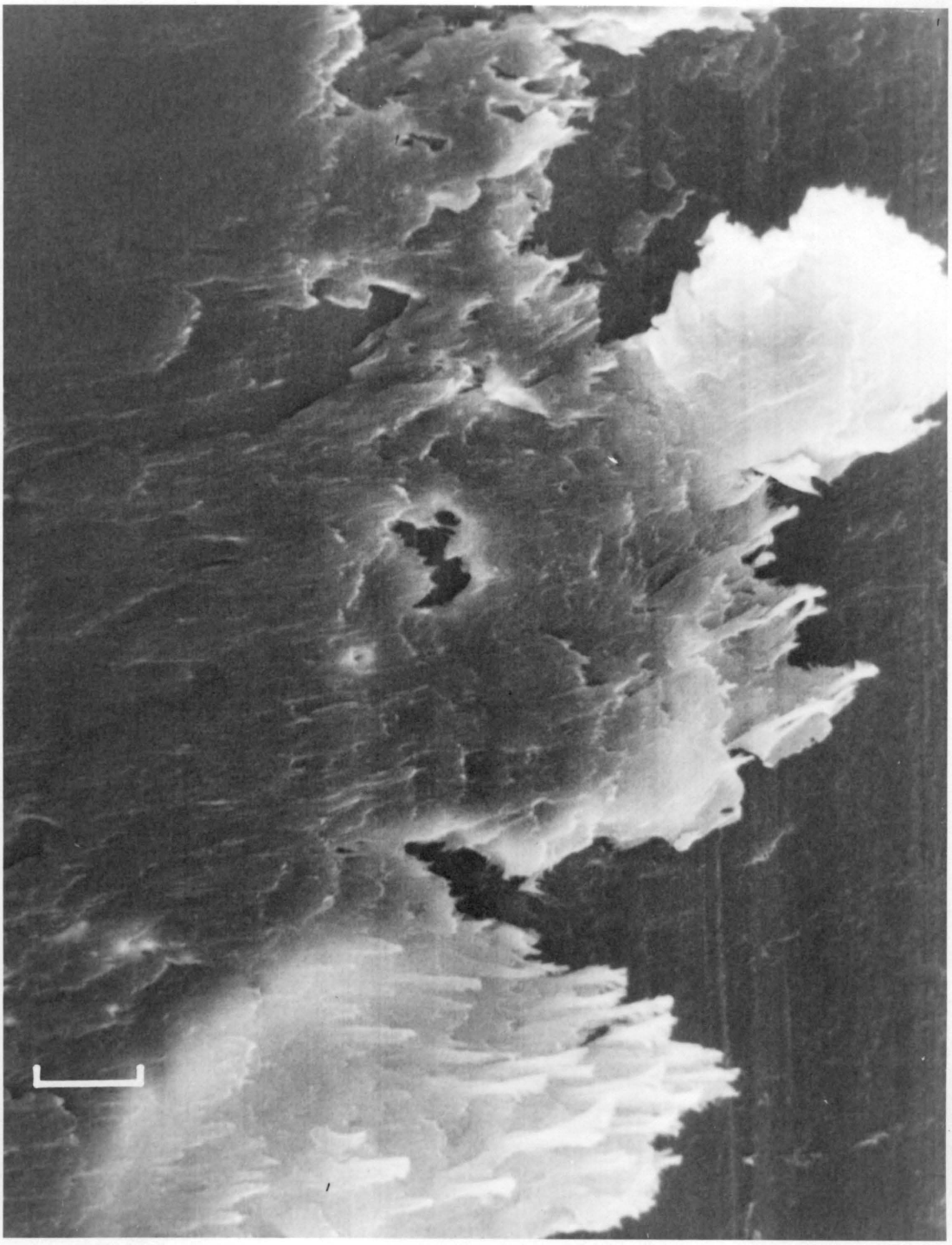

Figure 31. Scanning electron microscope picture of a pin after 57600 passes on a smooth disk at 128 cm/sec. Index mark is 20 μm.

polymer are cut off by the asperities of the steel surface. Most of this abrasion is done during perpendicular sliding, because the polymer surface encounters more asperities than it would during parallel sliding. Large amounts of loose debris are generated, although the polymer tends to fill the grooves first. Most of the heat energy is removed by the formation of loose wear particles and the temperature of the contact zone remains lower than the softening temperatures of the polymer.

Parallel Sliding

Very little polymer transfers to the disk at the low speed. The thin films that do transfer at a low number of passes are caused by adhesive forces [Fig. 32]. As the number of passes increase large amounts of loose debris are generated [Fig. 33], but only small amounts of deposits can be seen on the steel surface [Fig. 34].

At the high speed of sliding deposits are caused only by the asperities which are perpendicular to the sliding direction [Fig. 35]. Although the wear mechanism is abrasive, some adhesive shearing can be seen in the top layers of thick films, which form tongues as the number of passes increase [Fig. 36]. Loose debris particles are made up of rolls of abraded polymer [Fig. 37] and do not have the layered structure of adhesive debris.

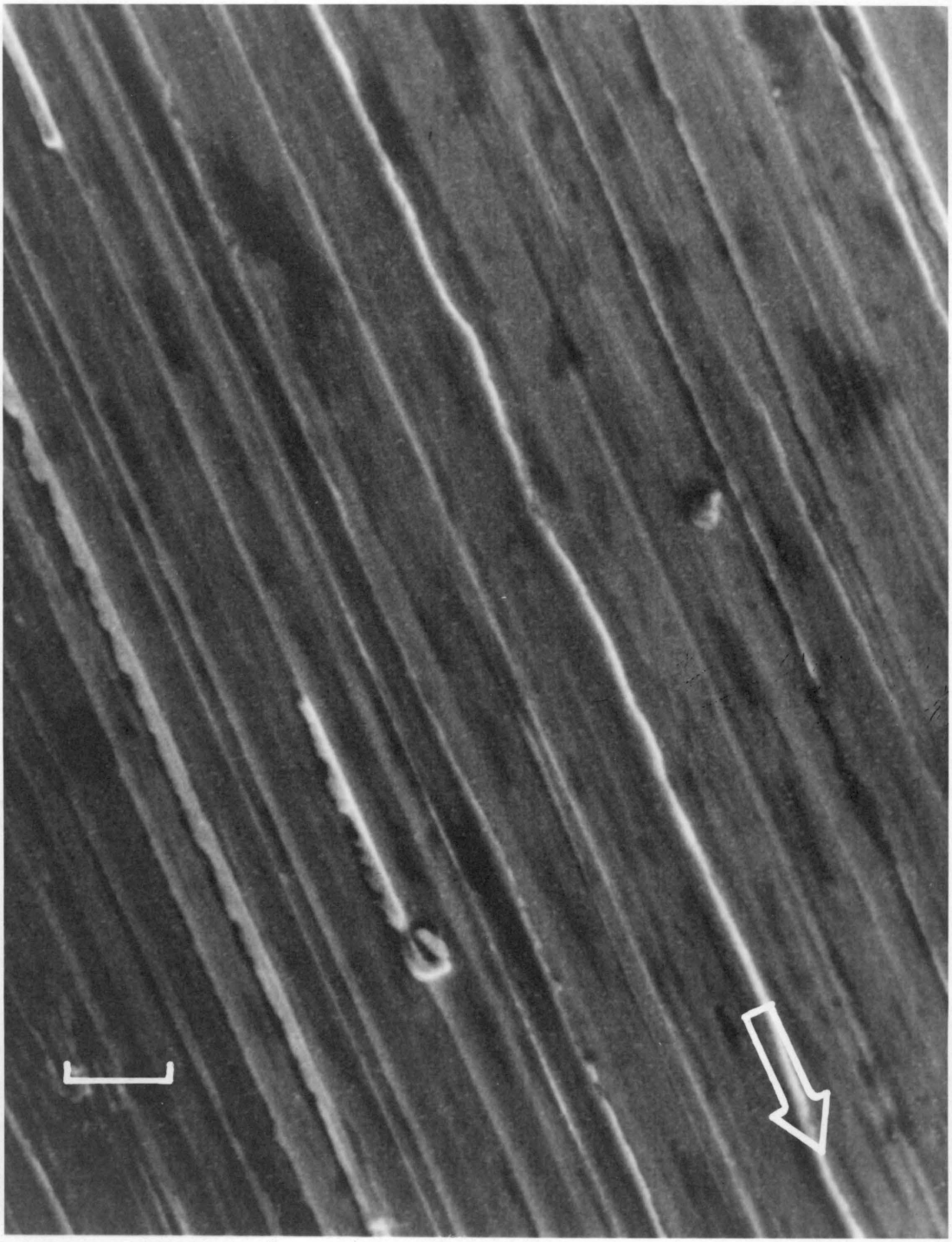

Figure 32. Scanning electron microscope picture of a rough disk after 2400 passes at 32 cm/sec. Index mark is 10 μm. Arrow shows the direction of sliding of the pin.

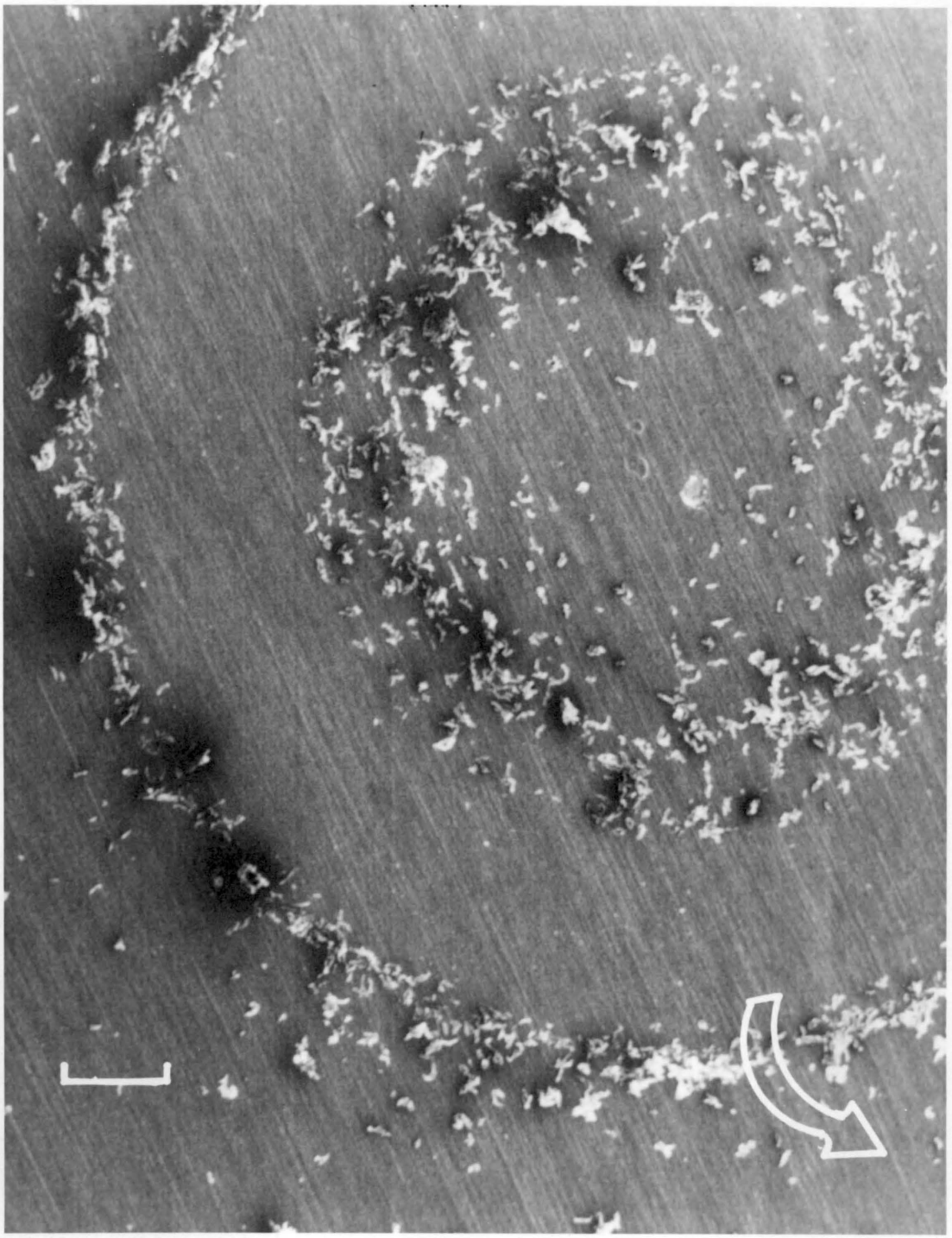

Figure 33. Scanning electron microscope picture of a rough disk after 9600 passes at 32 cm/sec. Index mark is 833 μm. Arrow shows the direction of sliding of the pin.

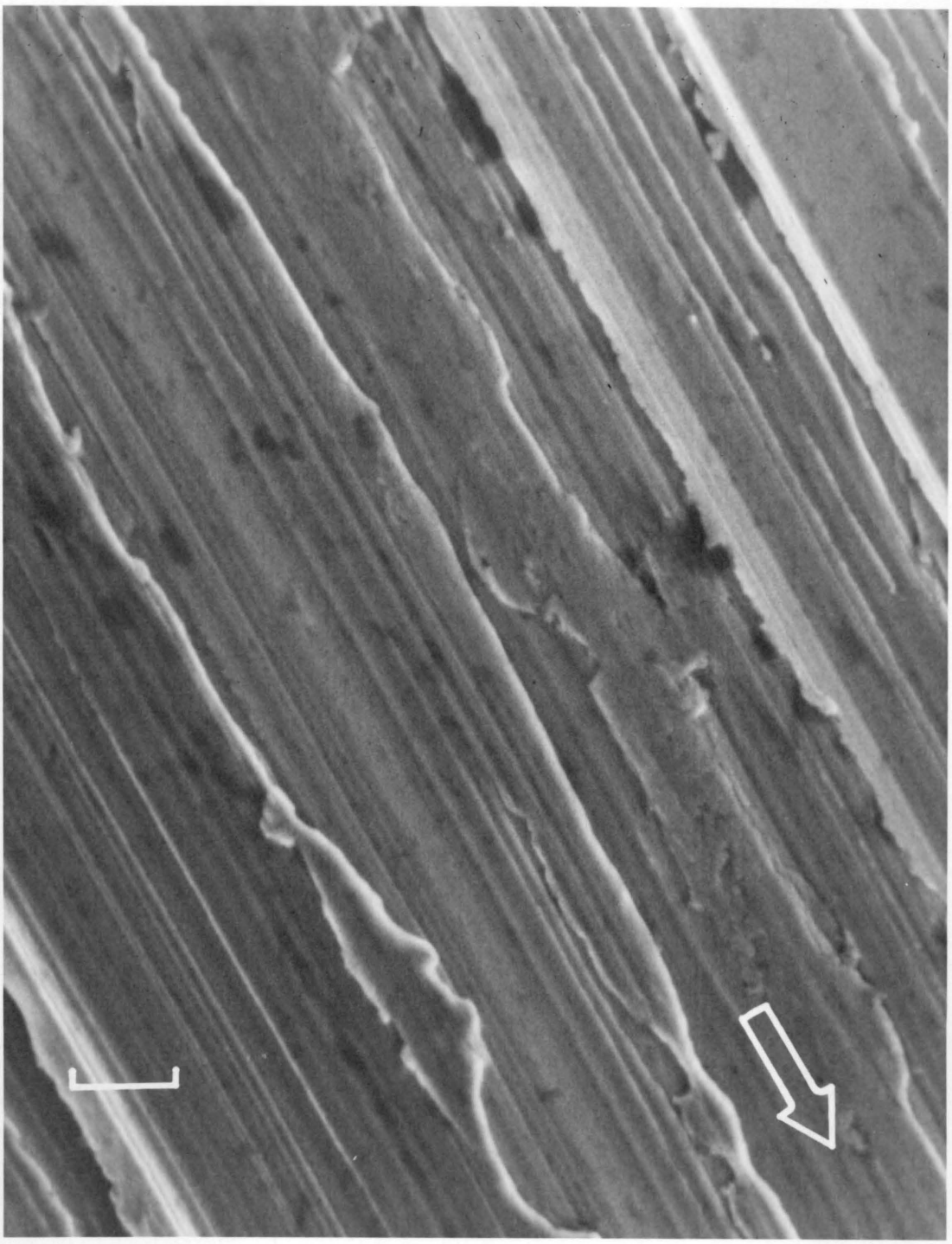

Figure 34. Scanning electron microscope picture of a rough disk after 76800 passes at 32 cm/sec. Index mark is 10 μm. Arrow shows the direction of sliding of the pin.

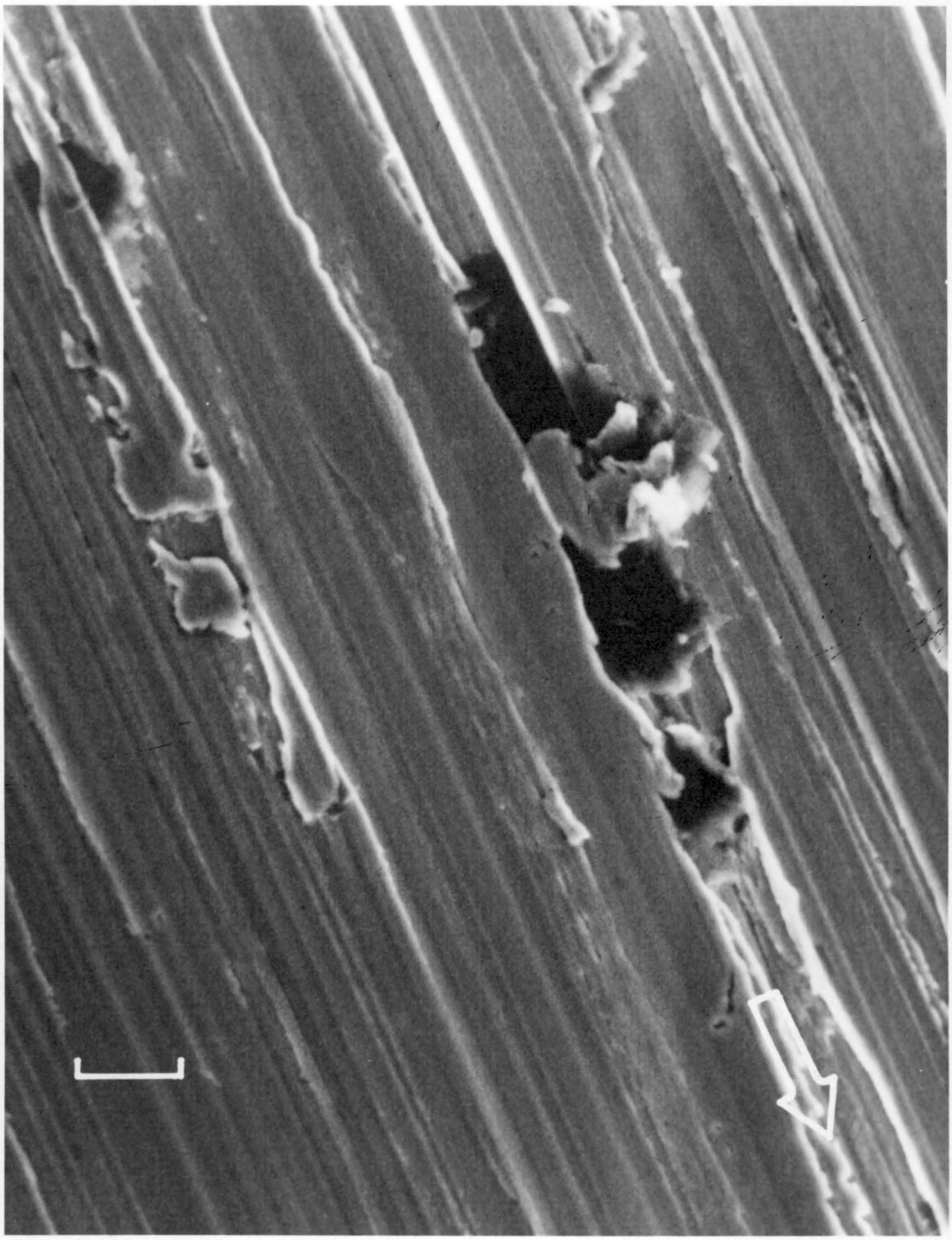

Figure 35. Scanning electron microscope picture of a rough disk after 2400 passes at 32 cm/sec. Index mark is 10 μm. Arrow shows the direction of sliding of the pin.

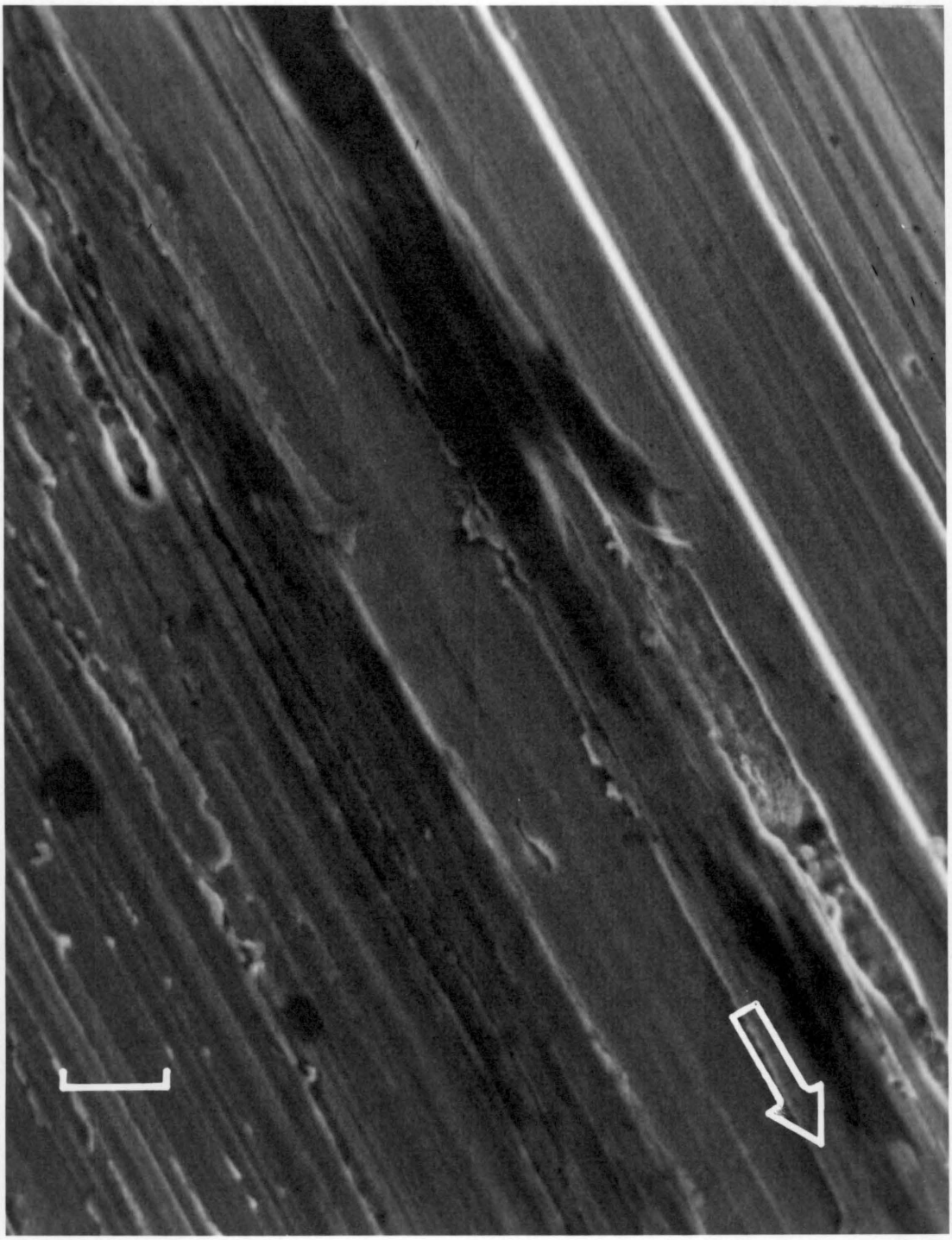

Figure 36. Scanning electron microscope picture of a rough disk after 76800 passes at 128 cm/sec. Index mark is 10 μm. Arrow shows the direction of sliding of the pin.

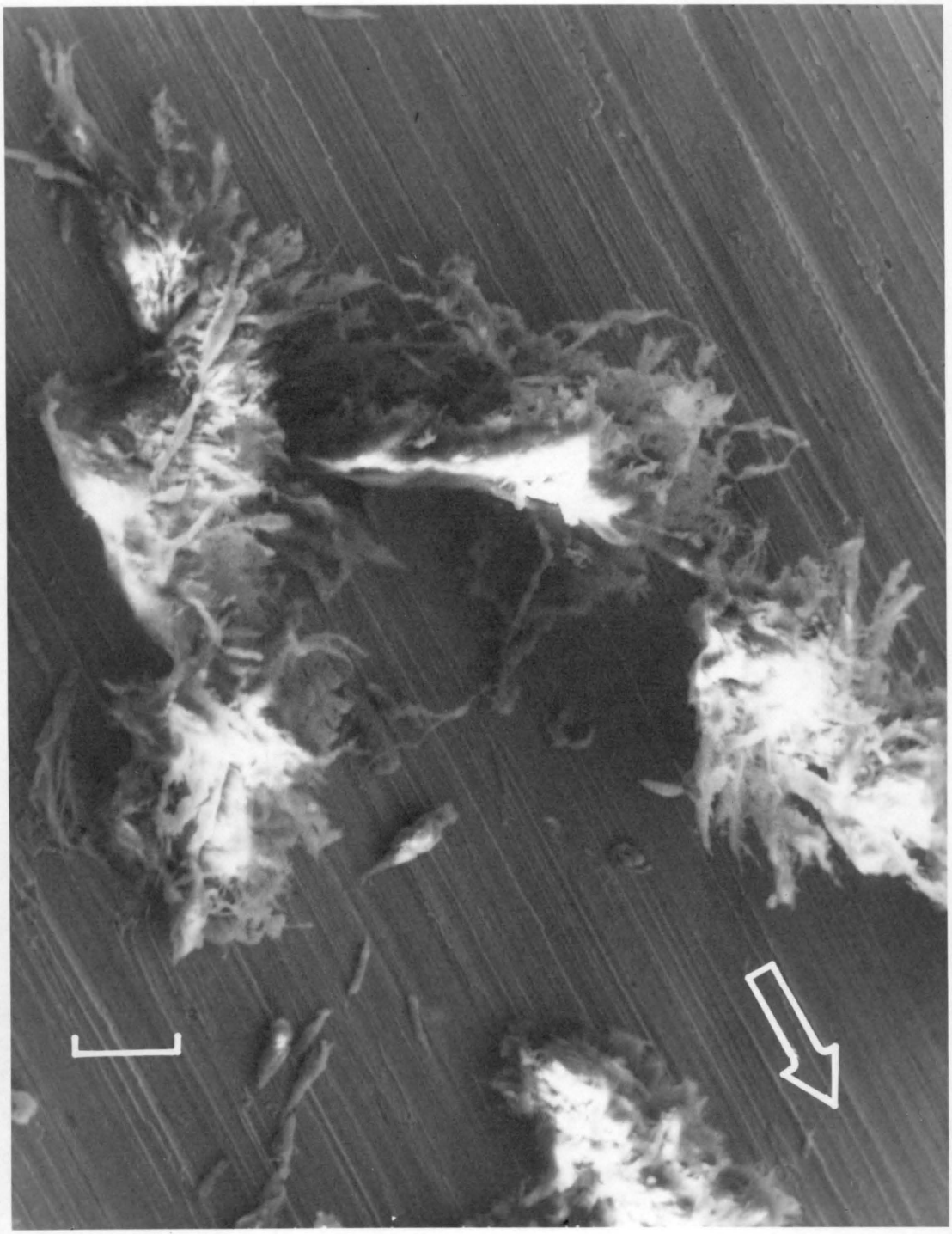

Figure 37. Scanning electron microscope picture of a rough disk after 76800 passes at 128 cm/sec. Index mark is 50 μm. Arrow shows the direction of sliding of the pin.

Perpendicular Sliding

An abrasive mechanism governs the wear process at the low speed of sliding, where the polymer is cut by the asperities and piles up in the trailing edge of the grooves [Fig. 38]. When the abraded particles can not go into the grooves loose debris are generated in the form of rolls [Fig. 39], which sometimes group together to form larger debris particles as the number of passes increase [Fig. 40]. Some adhesive films can also be seen on the plateaus at those high number of passes [Fig. 41].

Abrasive tearing is observed at the high speed of sliding. Large particles of polymer are cut off from the pin [Fig. 42] by the asperities of steel surface. As the number of passes increase this process results in the formation of many loose chunks of polymer [Fig. 43], which are sometimes pressed together between the pin and the disk to form bigger particles [Fig. 44].

Wear Surfaces of the Pins

Examination of the pins, which are worn at the low speed, shows an abrasive cutting mechanism, which tends to get milder as the number of passes increase.

Shearing and tearing of the polymer surface can be seen at low number of passes [Fig. 45, 46]. However, as the process continues some of the debris is caught between the pin and disk and abrasion is decreased [Fig. 47]. The load is carried by those squeezed particles and the rest of the pin obtains a smooth topography, because of the

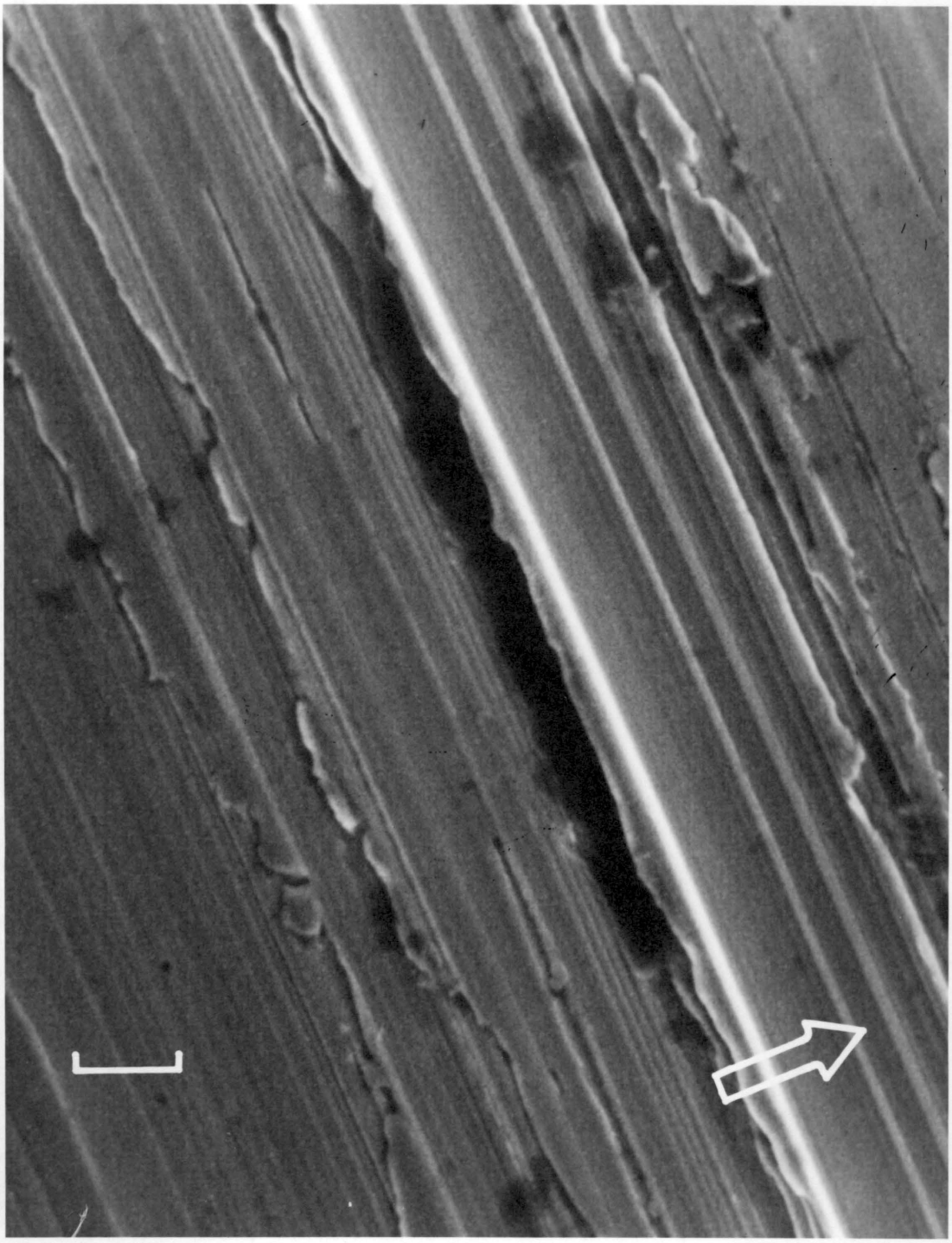

Figure 38. Scanning electron microscope picture of a rough disk after 2400 passes at 32 cm/sec. Index mark is 10 μm. Arrow shows the direction of sliding of the pin.

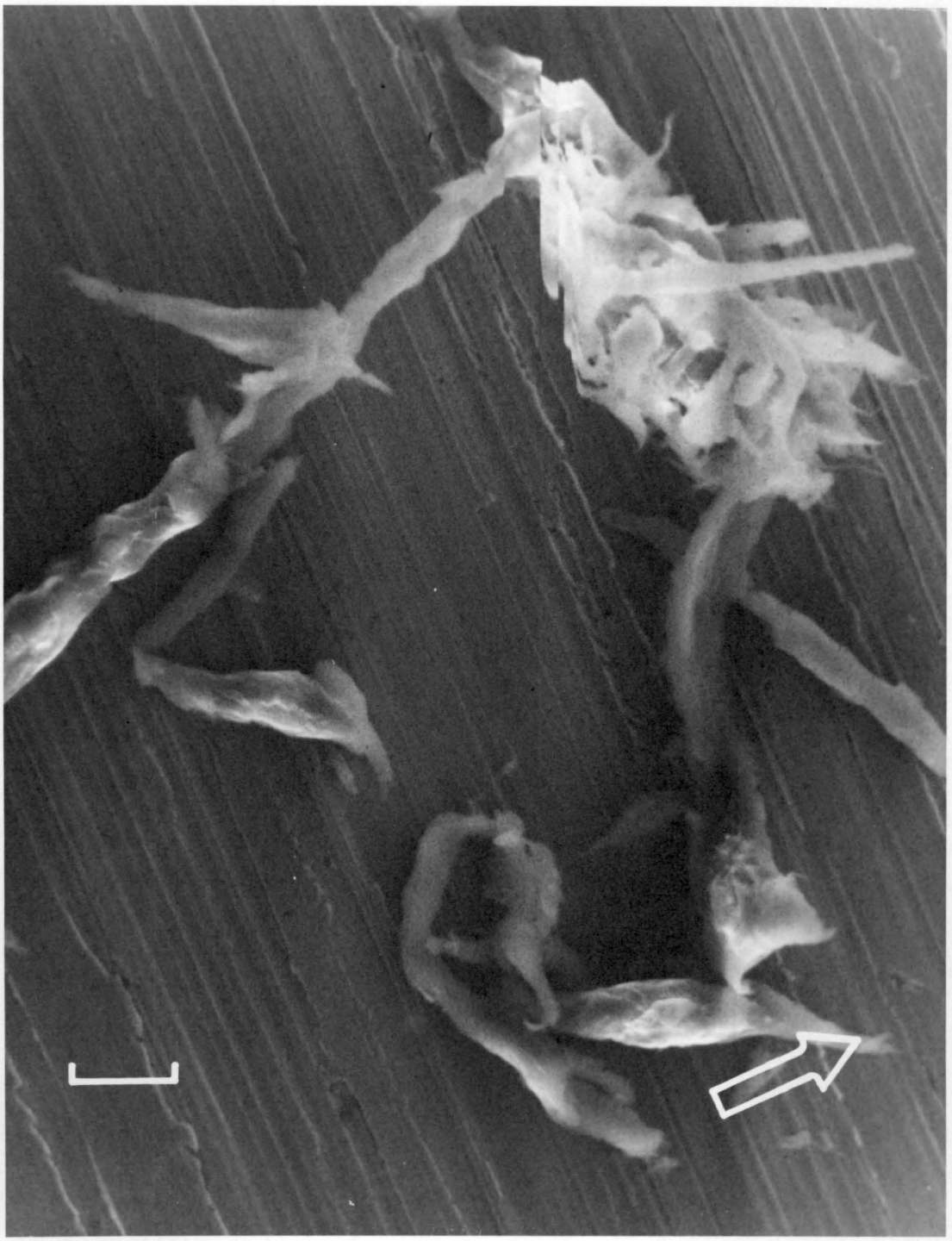

Figure 39. Scanning electron microscope picture of a rough disk after 2400 passes at 32 cm/sec. Index mark is 20 μm. Arrow shows the direction of sliding of the pin.

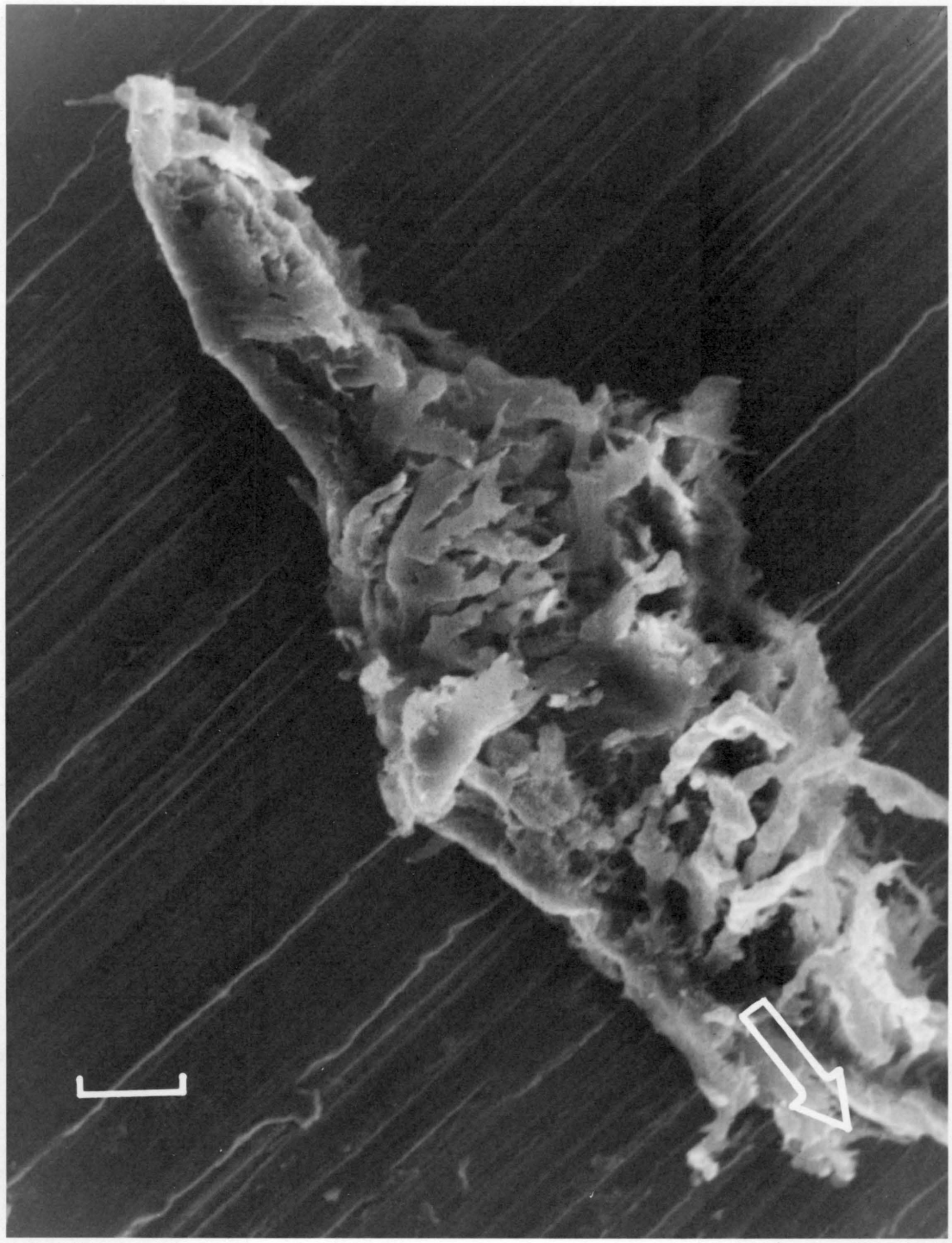

Figure 40. Scanning electron microscope picture of a rough disk after 38400 passes at 32 cm/sec. Index mark is 20 μm. Arrow shows the direction of sliding of the pin.

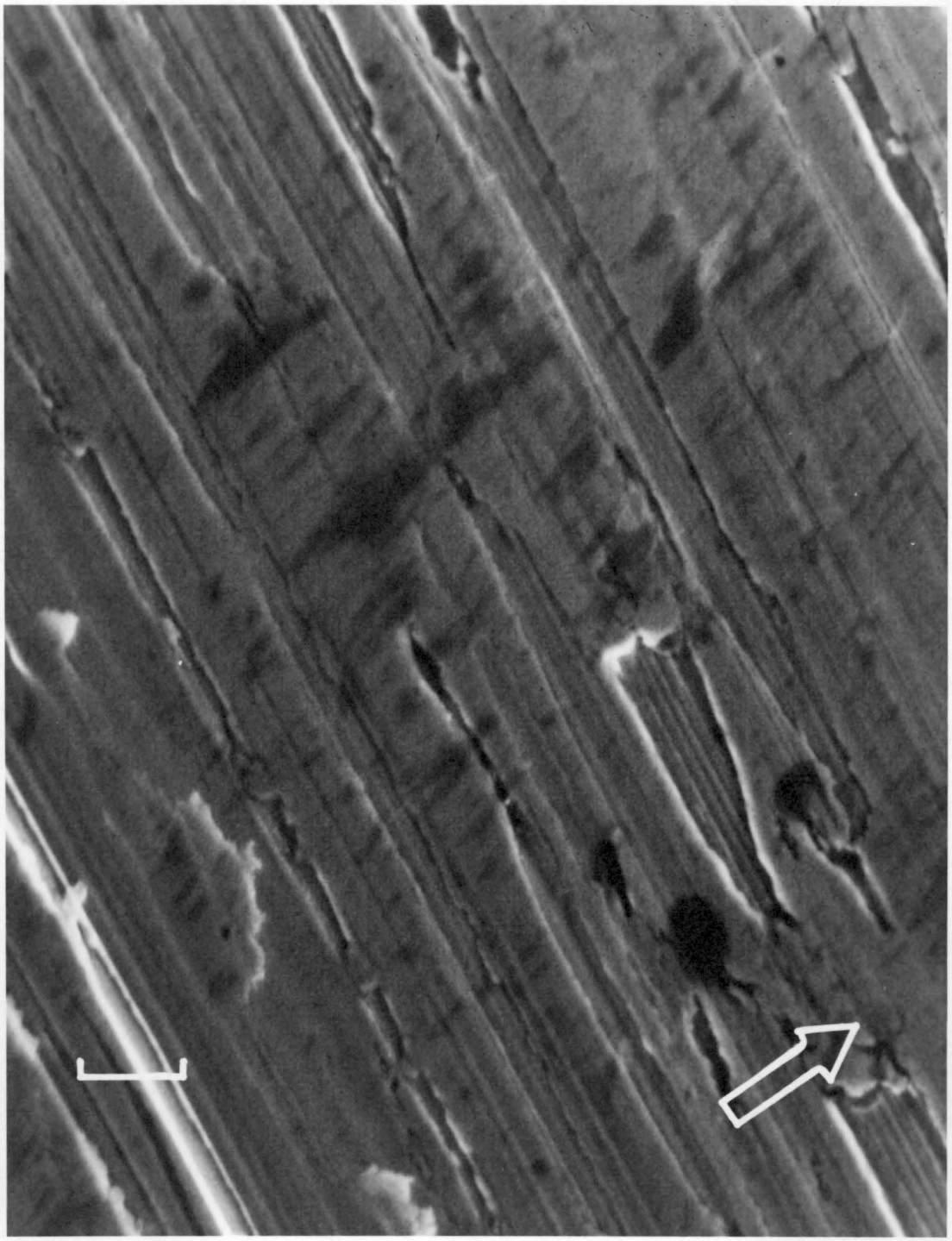

Figure 41. Scanning electron microscope picture of a rough disk after 76800 passes at 32 cm/sec. Index mark is 10 μm. Arrow shows the direction of sliding of the pin.

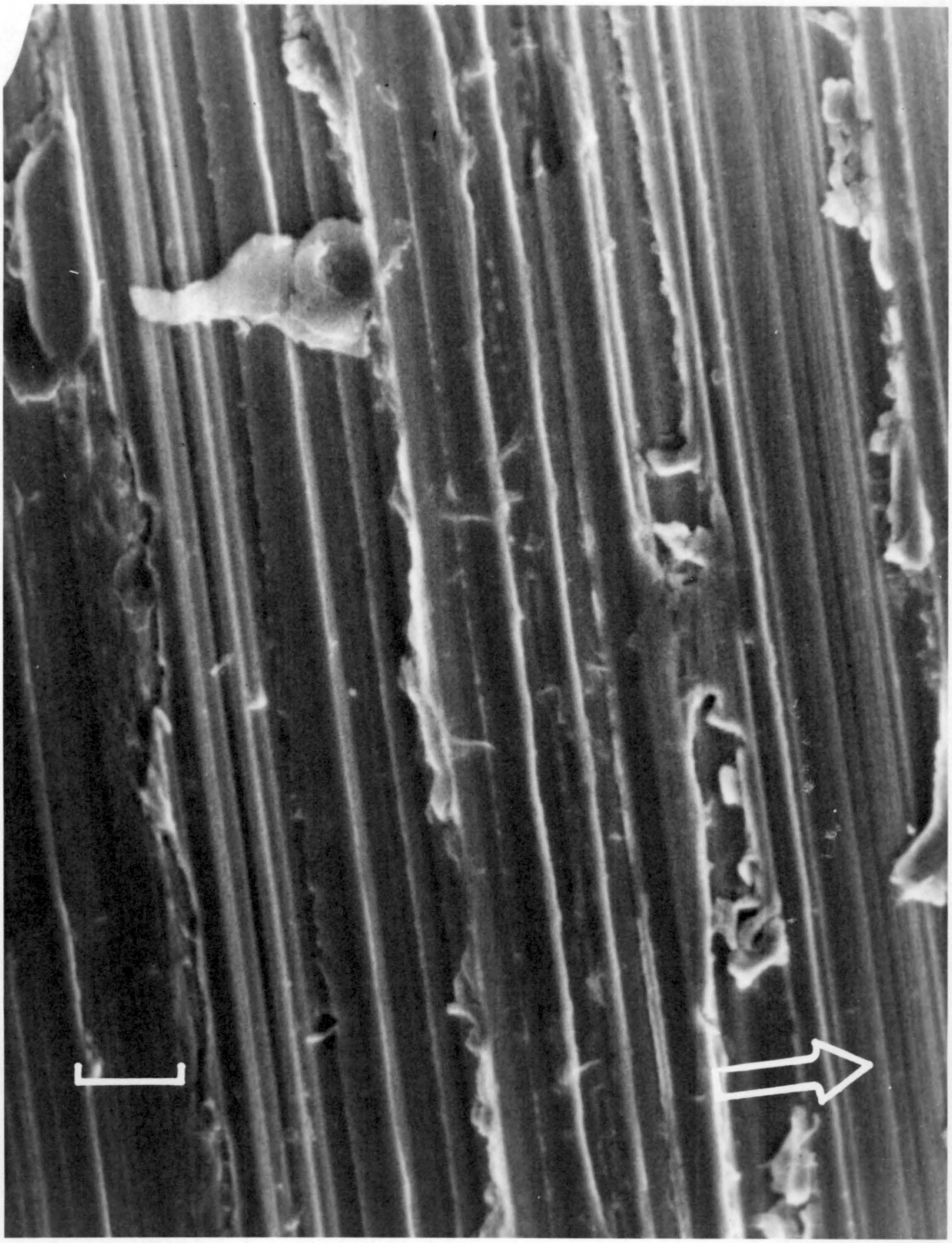

Figure 42. Scanning electron microscope picture of a rough disk after 9600 passes at 128 cm/sec. Index mark is 10 μm. Arrow shows the direction of sliding of the pin.

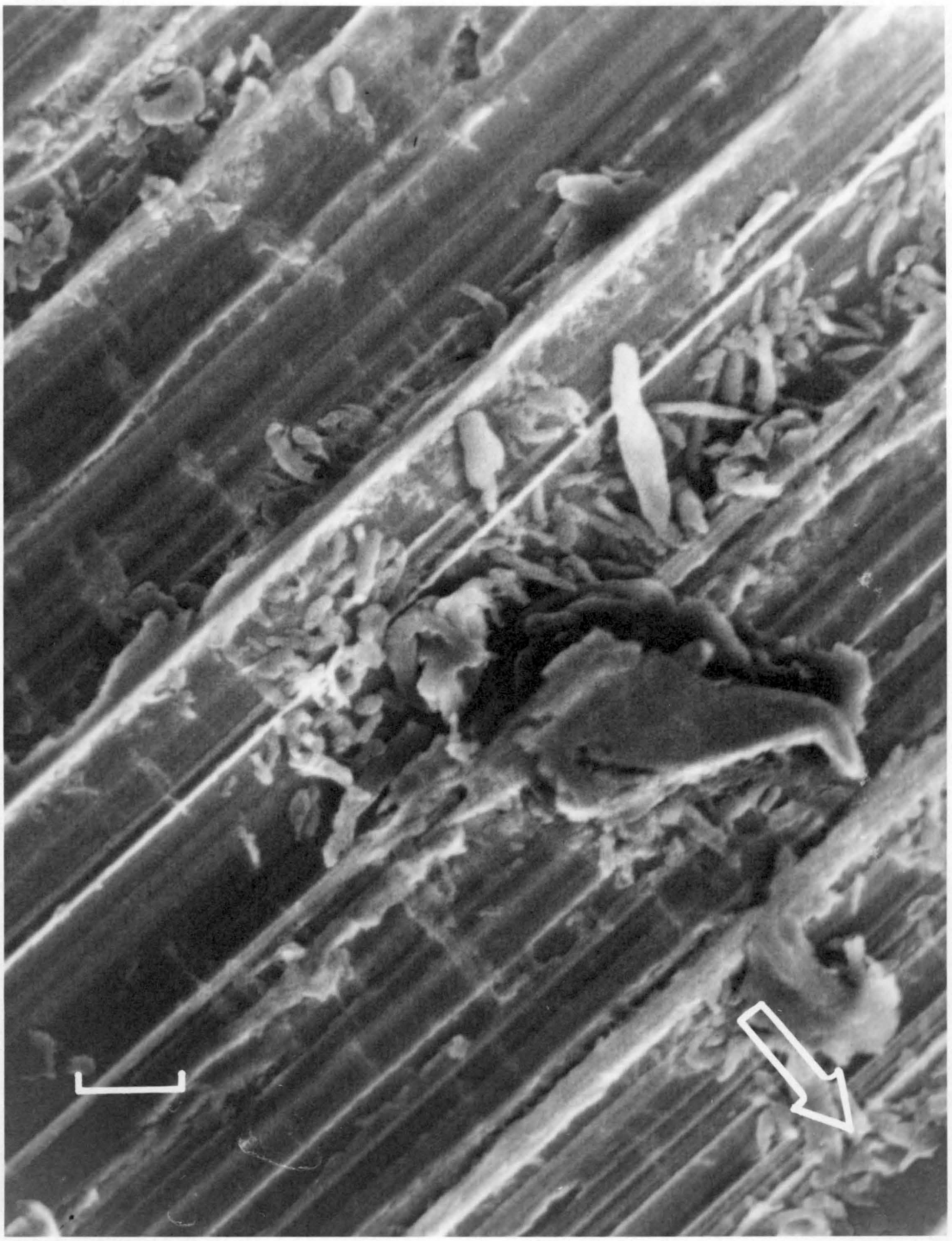

Figure 43. Scanning electron microscope picture of a rough disk after 38400 passes at 128 cm/sec. Index mark is 10 μm. Arrow shows the direction of sliding of the pin.

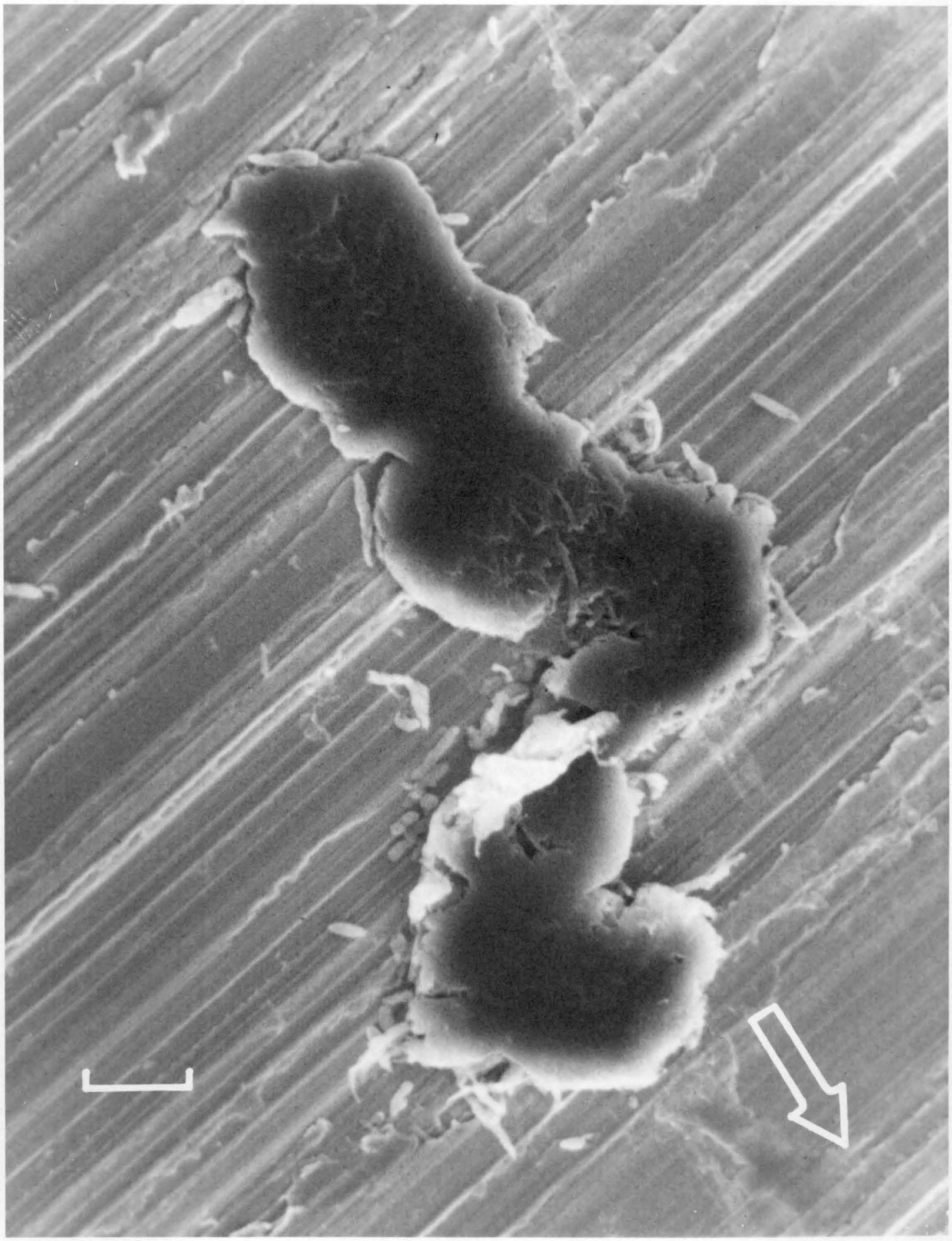

Figure 44. Scanning electron microscope picture of a rough disk after 38400 passes at 128 cm/sec. Index mark is 10 μm. Arrow shows the direction of sliding of the pin.

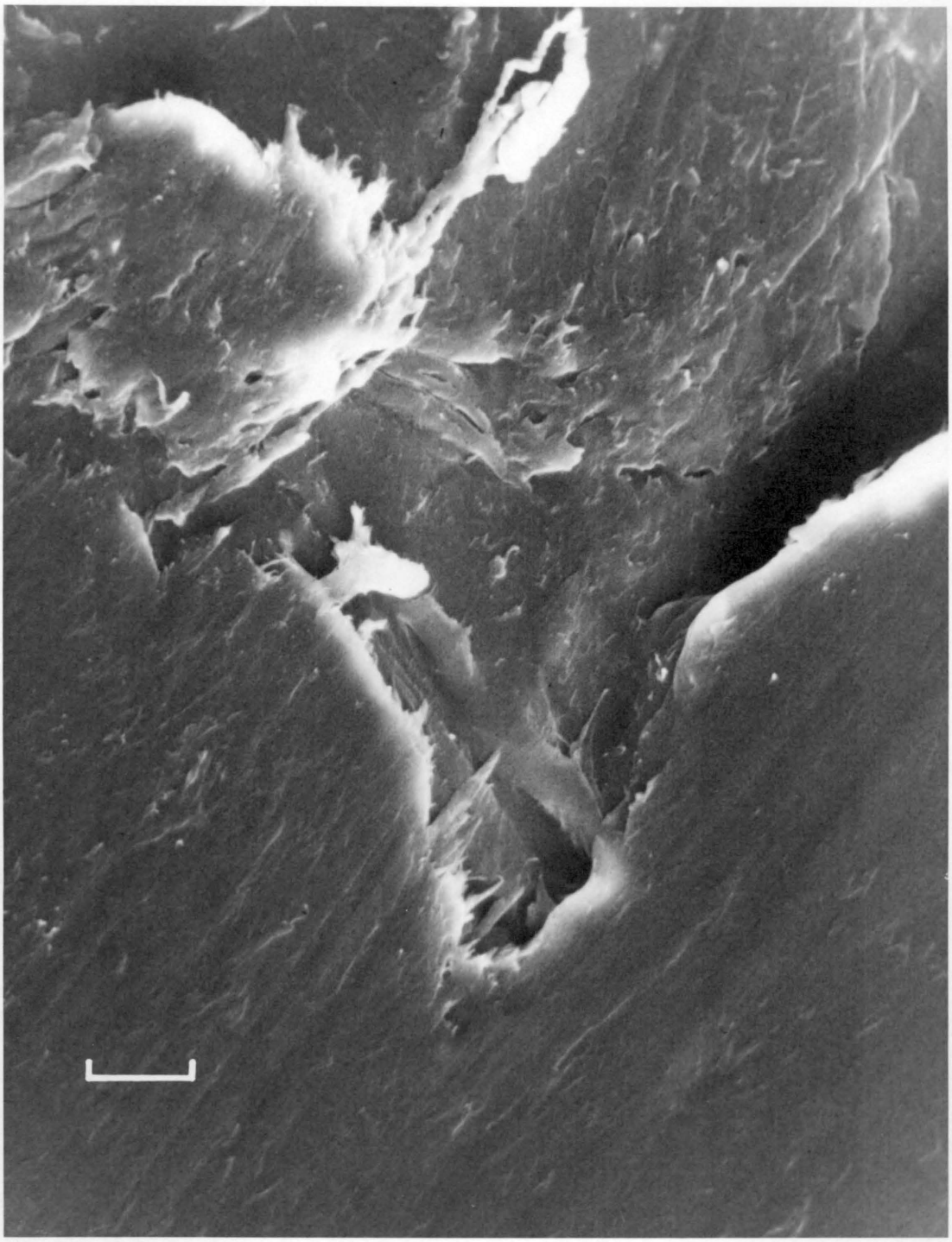

Figure 45. Scanning electron microscope picture of a pin after 2400 passes on a rough disk at 32 cm/sec. Index mark is 20 μm.

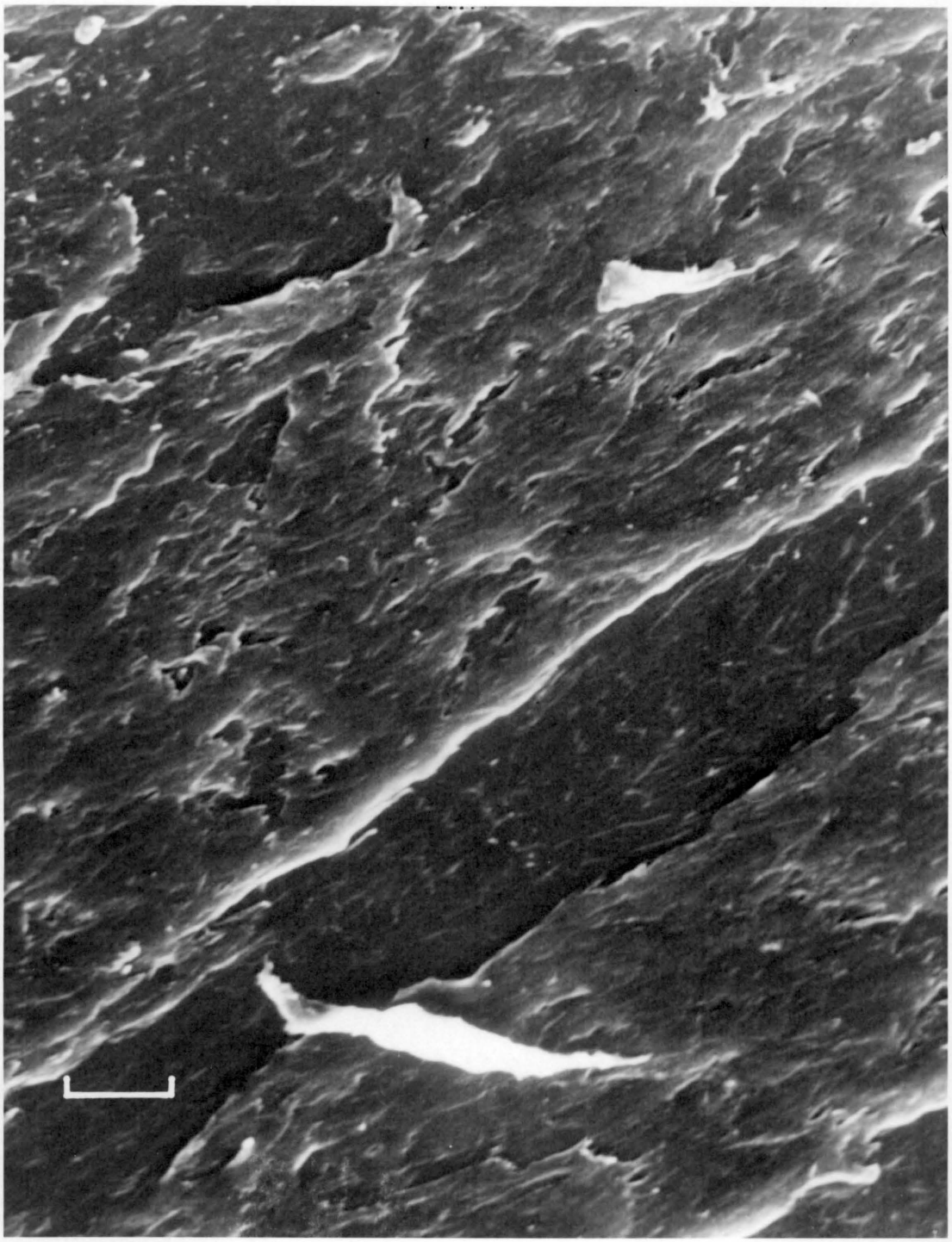

Figure 46. Scanning electron microscope picture of a pin after 9600 passes on a rough disk at 32 cm/sec. Index mark is 20 μm.

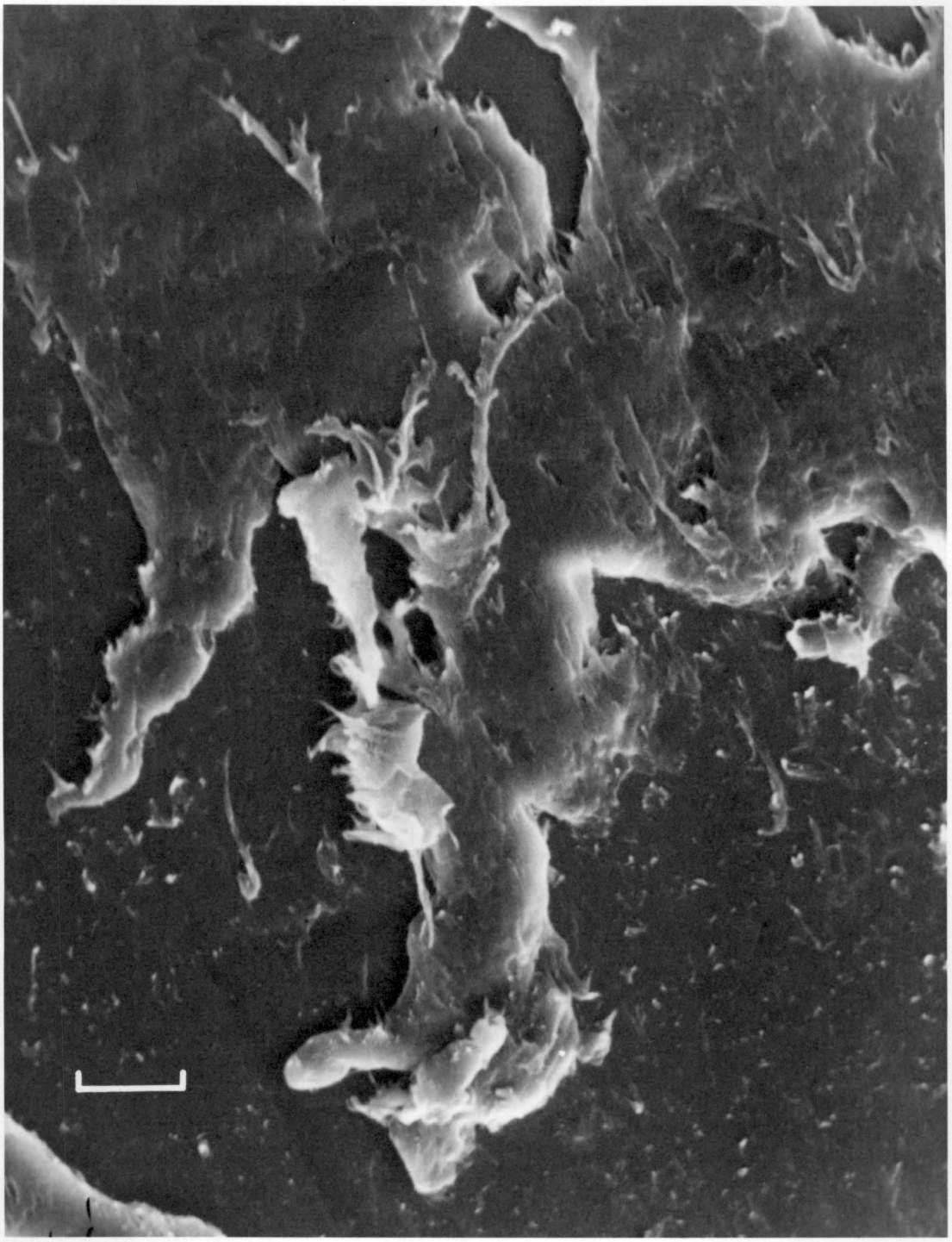

Figure 47. Scanning electron microscope picture of a pin after 19200 passes on a rough disk at 32 cm/sec. Index mark is 20 μm.

decrease in the depth of penetration of the pin area. When the squeezed particles are worn off, the asperities of the steel surface sink into the polymer and the abrasion process starts.

Depth of penetration is lower at the high speed and the surfaces of the worn out pins look smoother than those that are worn at the low speed. Tearing can still be observed [Fig. 48], although some portions of the pin are very smooth [Fig. 49]. The high wear rate results in the total removal of surfaces. Thus, new surfaces are formed and, therefore, changes can not be observed as the number of passes increase [Fig. 50, 51].

The basic characteristic of these surfaces is the existence of a smooth zone [Fig. 52] and a rough zone [Fig. 53] side by side. This is because the surface of the pin is subject to localized wearing, which moves from place to place as the surface topography changes.

c. Medium Roughness Surfaces

Sliding of the polymer pin on the medium roughness surface results in both abrasive and adhesive wear. Chunks of polymer are removed by the asperities of the steel surface and form loose debris, whereas layers are removed by adhesive forces between the two surfaces and form tightly bonded films.

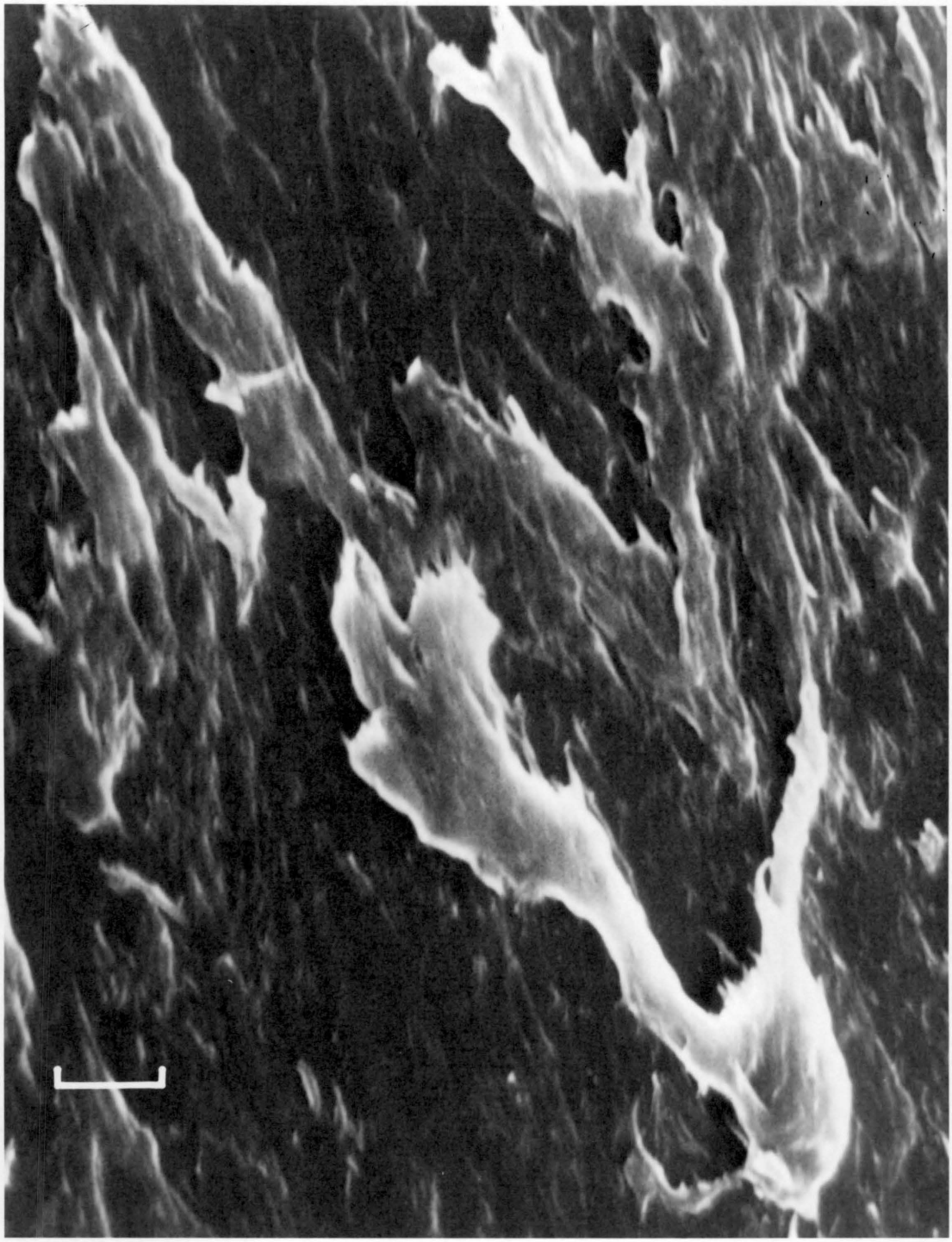

Figure 48. Scanning electron microscope picture of a pin after 2400 passes on a rough disk at 128 cm/sec. Index mark is 10 μm.

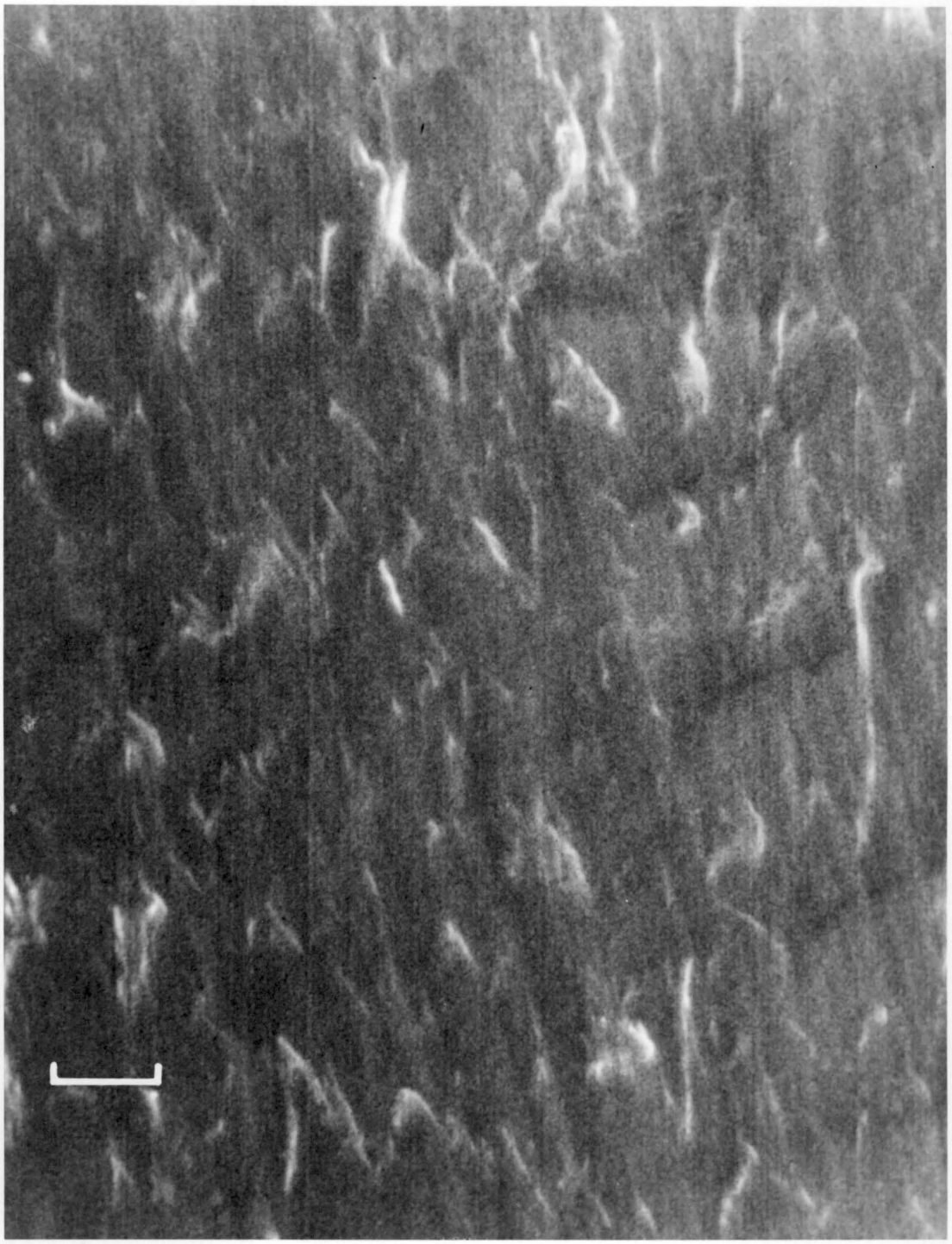

Figure 49. Scanning electron microscope picture of a pin after 2400 passes on a rough disk at 128 cm/sec. Index mark is 5 μm.

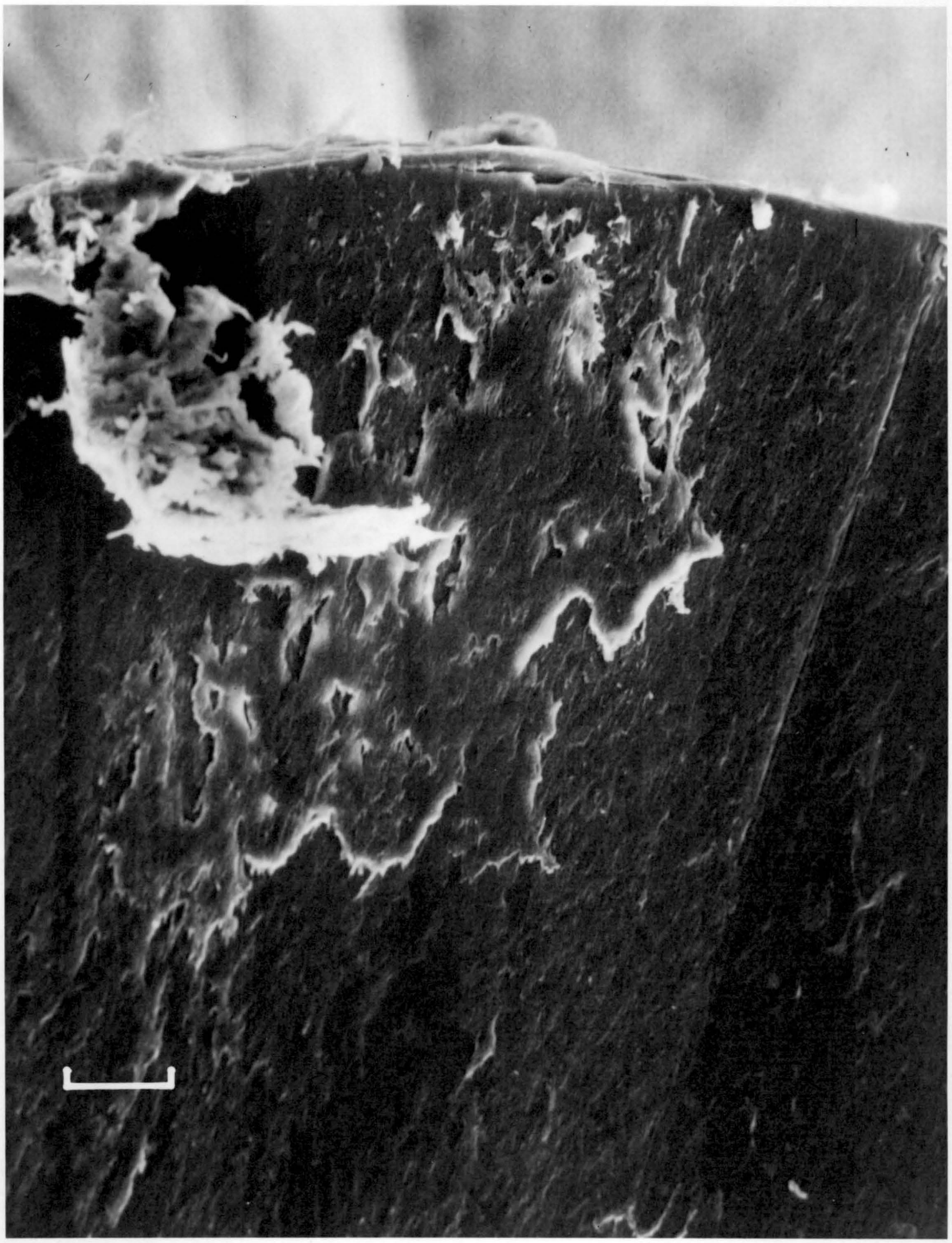

Figure 50. Scanning electron microscope picture of a pin after 9600 passes on a rough disk at 128 cm/sec. Index mark is 50 μm.

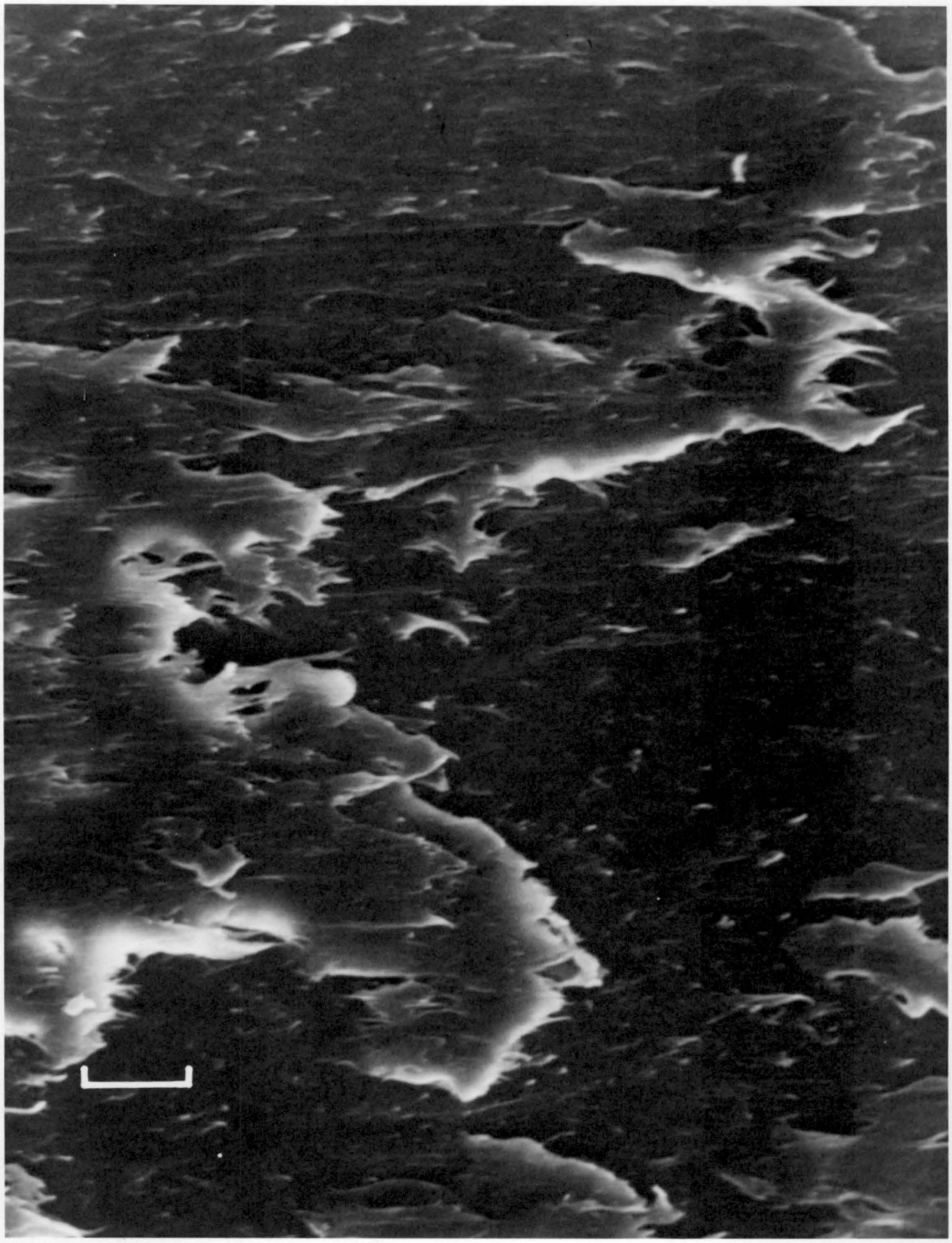

Figure 51. Scanning electron microscope picture of a pin after 38400 passes on a rough disk at 128 cm/sec. Index mark is 20 μm.

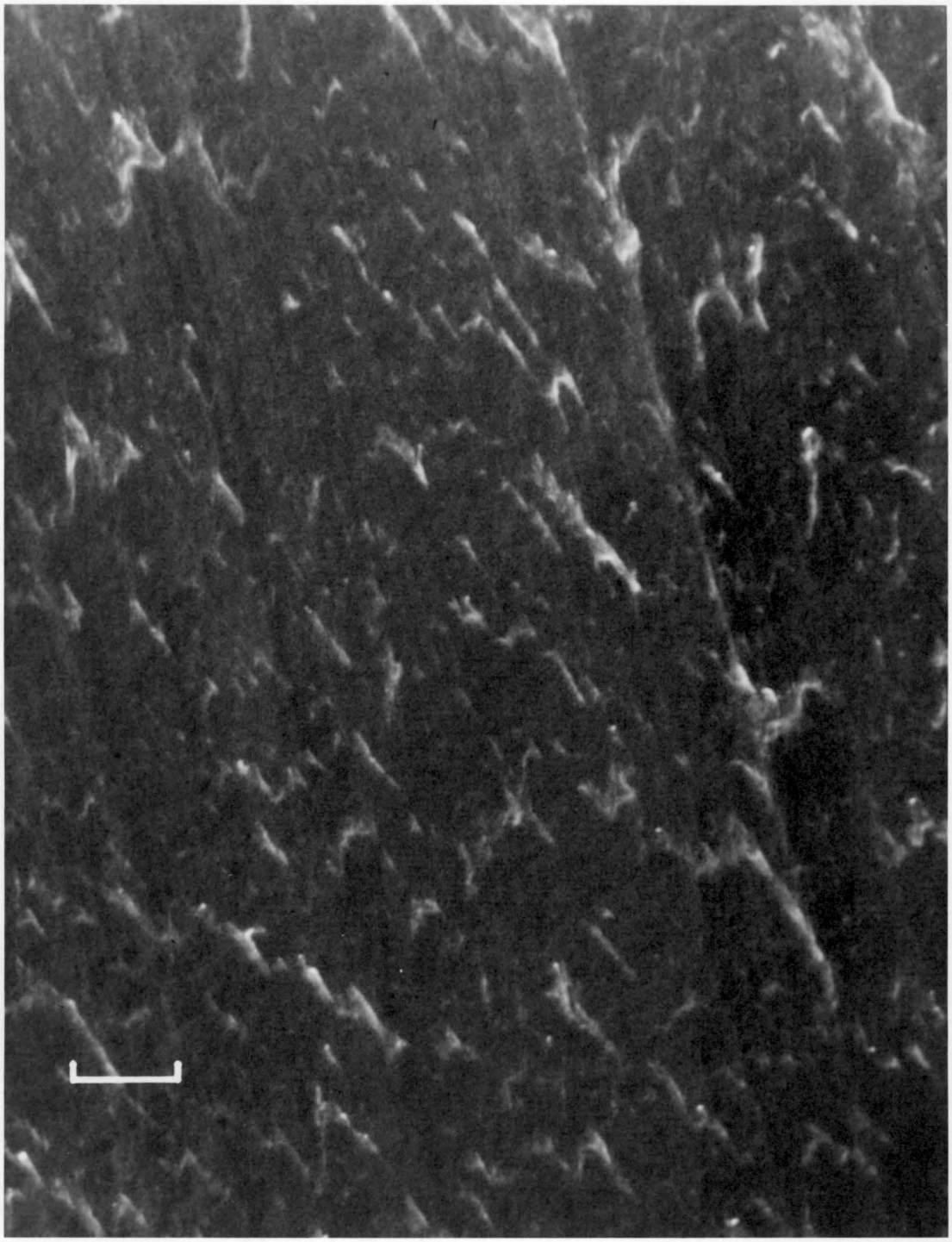

Figure 52. Scanning electron microscope picture of a pin after 76800 passes on a rough disk at 128 cm/sec. Index mark is 10 μm.

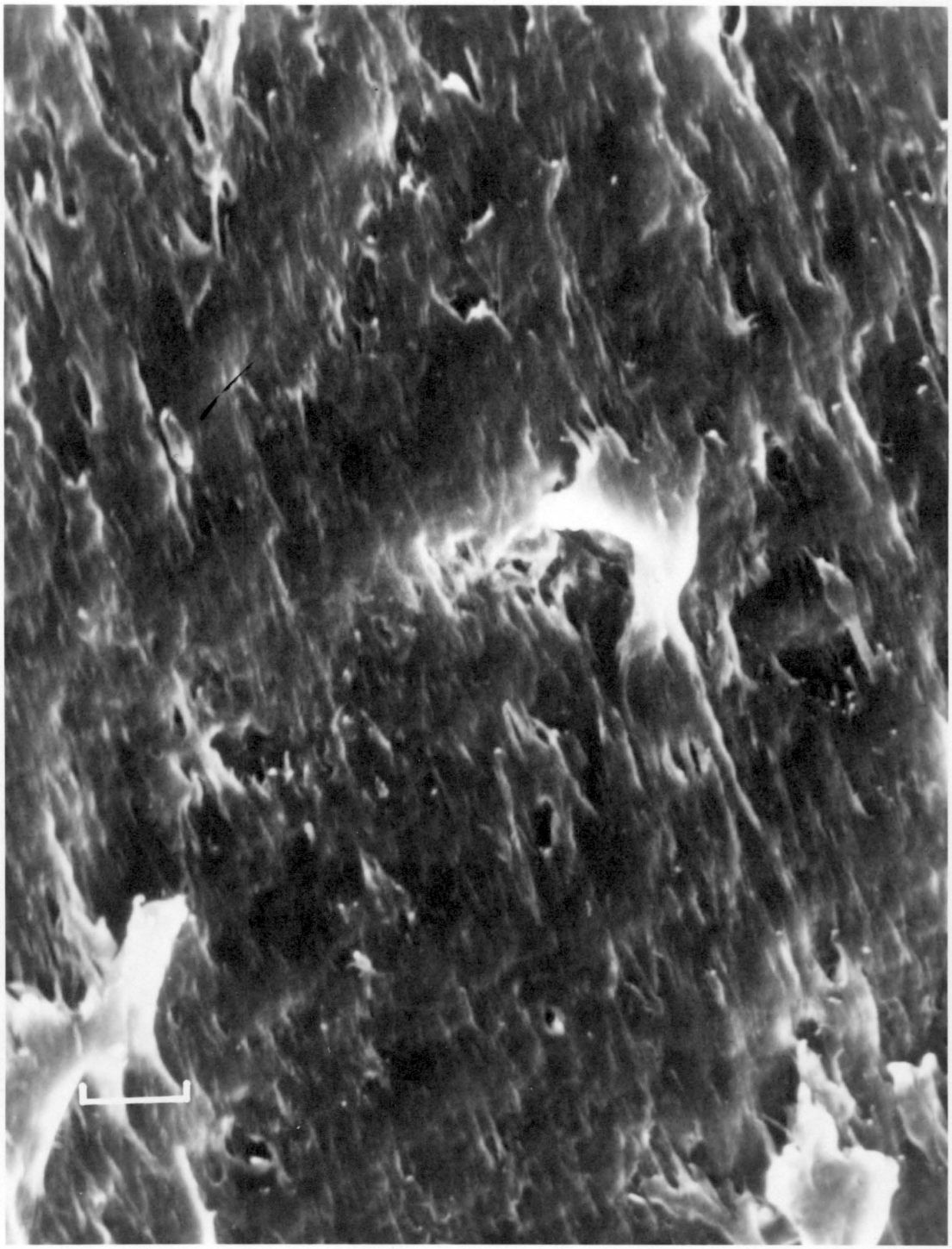

Figure 53. Scanning electron microscope picture of a pin after 76800 passes on a rough disk at 128 cm/sec. Index mark is 10 μm.

Parallel Sliding

Abrasive and adhesive wear can be seen at very low number of passes during low speed sliding [Fig. 54], and becomes more obvious as the number of passes and speed increase [Fig. 55].

At the high speed of sliding the higher temperatures cause thick, non-uniform layers to adhere to the surface [Fig. 56]. These layers become more uniform as the number of passes increase and form tongues as a result of adhesive shearing [Fig. 57].

45 degree Sliding

The heaviest deposit zones form when the direction of sliding is 45 degrees to the lay of the surface [Fig. 58]. This is because abrasion is favored by perpendicular sliding and adhesion is favored by parallel sliding. A joint mechanism controls the transfer process during 45 degree sliding and particles which are abraded during perpendicular sliding adhere to the surface when the sliding direction changes.

Perpendicular Sliding

At 600 passes at the high speed of sliding the abraded particles tend to fill the grooves and the sheared films cover the surfaces of the plateaus [Fig. 59]. Polymer is transferred to the surface by adhesive forces [Fig. 60]. However, observations of the loose debris reveals that it was generated by abrasive action. In fact, a closer examination of the loose debris shows that abraded particles form

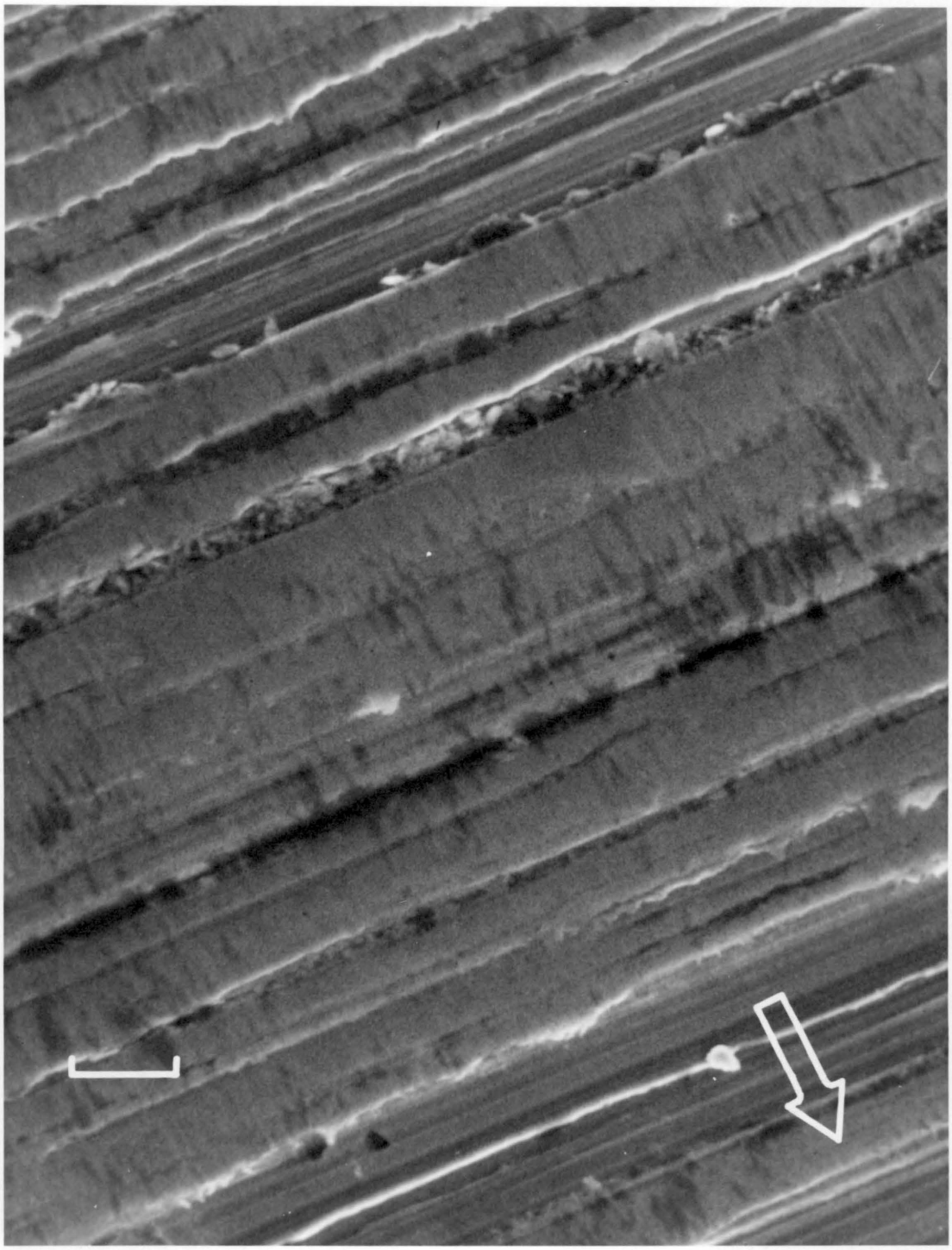

Figure 54. Scanning electron microscope picture of a medium roughness disk after 75 passes at 32 cm/sec. Index mark is 10 μm. Arrow shows the direction of sliding of the pin.

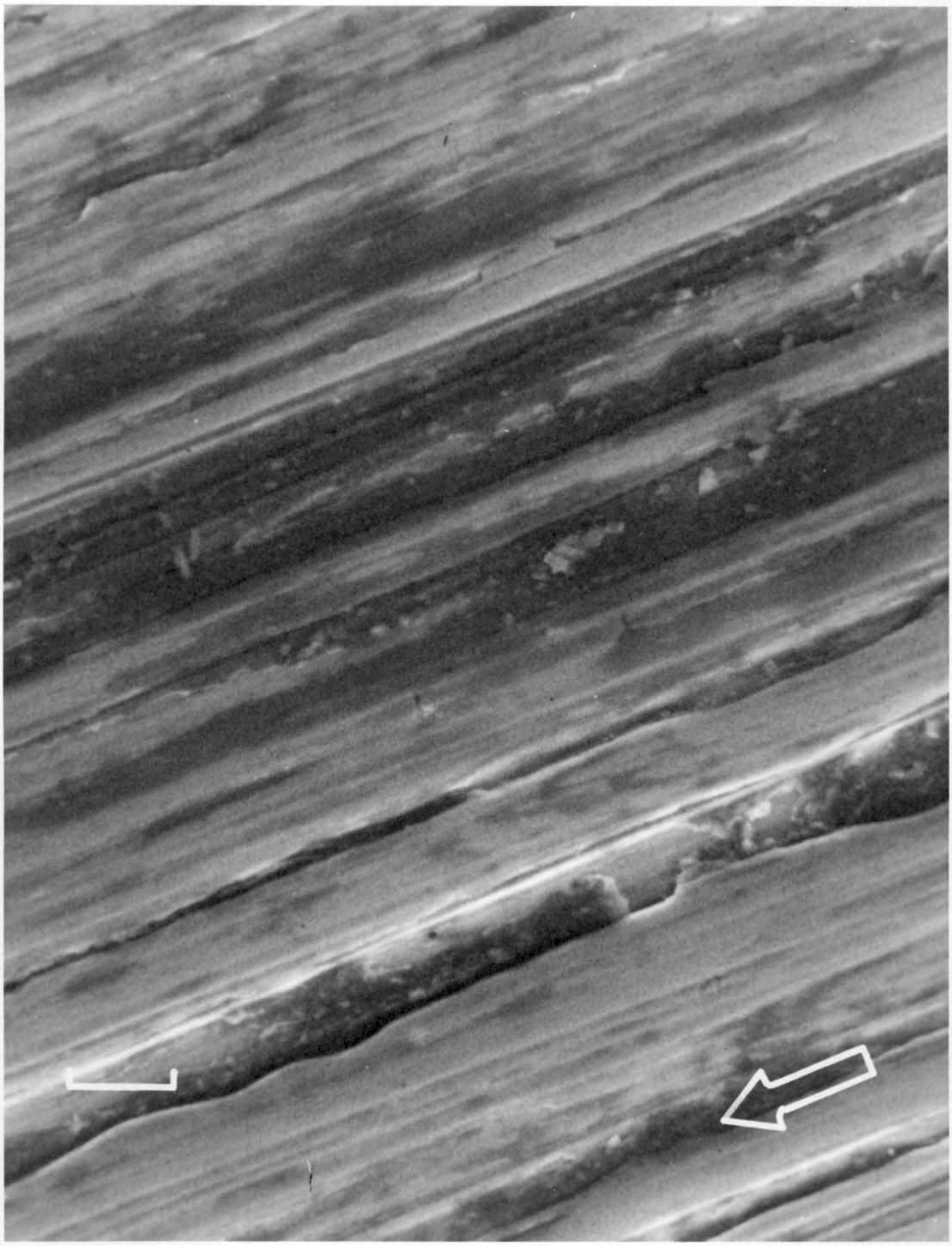

Figure 55. Scanning electron microscope picture of a medium roughness disk after 225 passes at 96 cm/sec. Index mark is 10 μm. Arrow shows the direction of sliding of the pin.

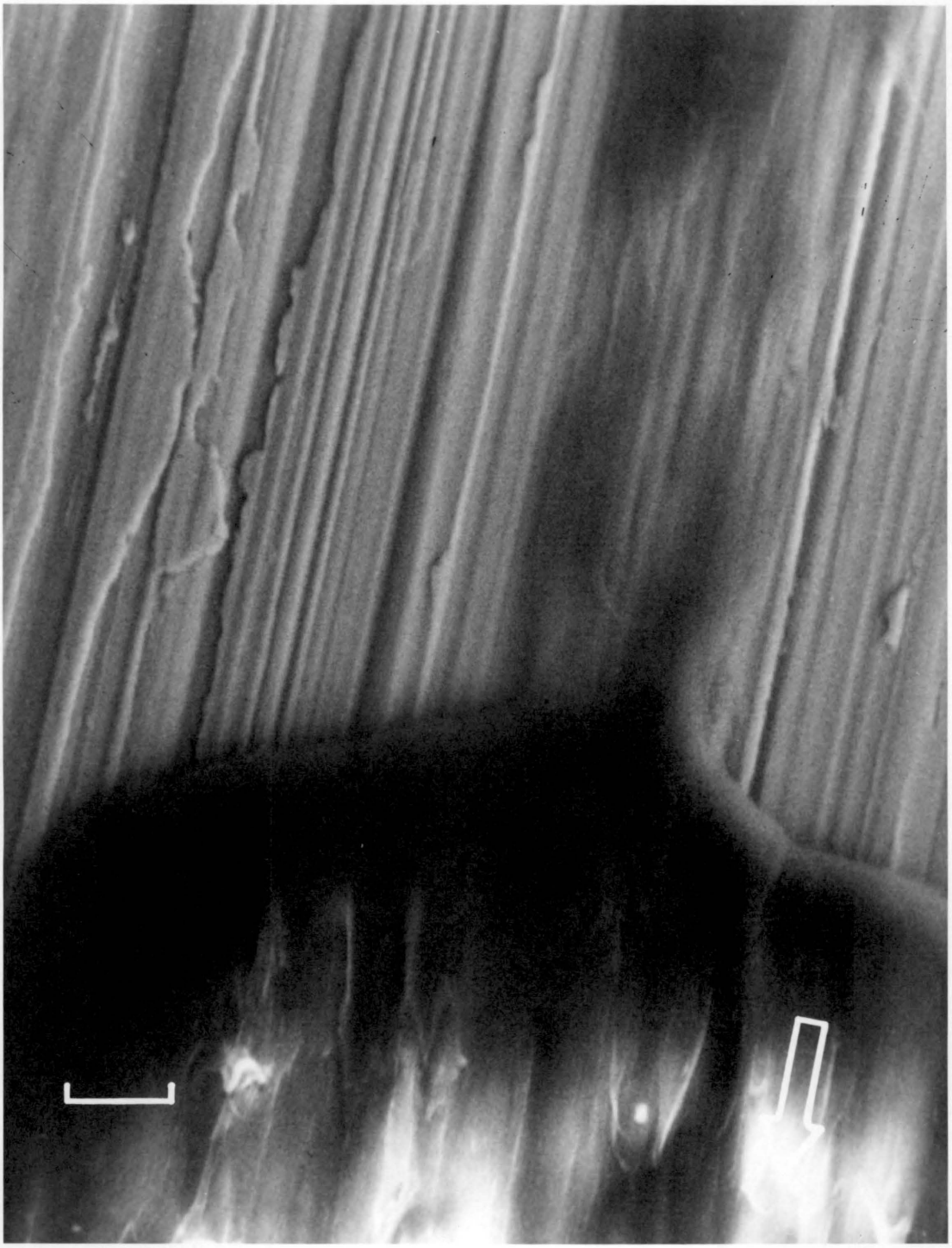

Figure 56. Scanning electron microscope picture of a medium roughness disk after 9600 passes at 128 cm/sec. Index mark is 10 μm. Arrow shows the direction of sliding of the pin.

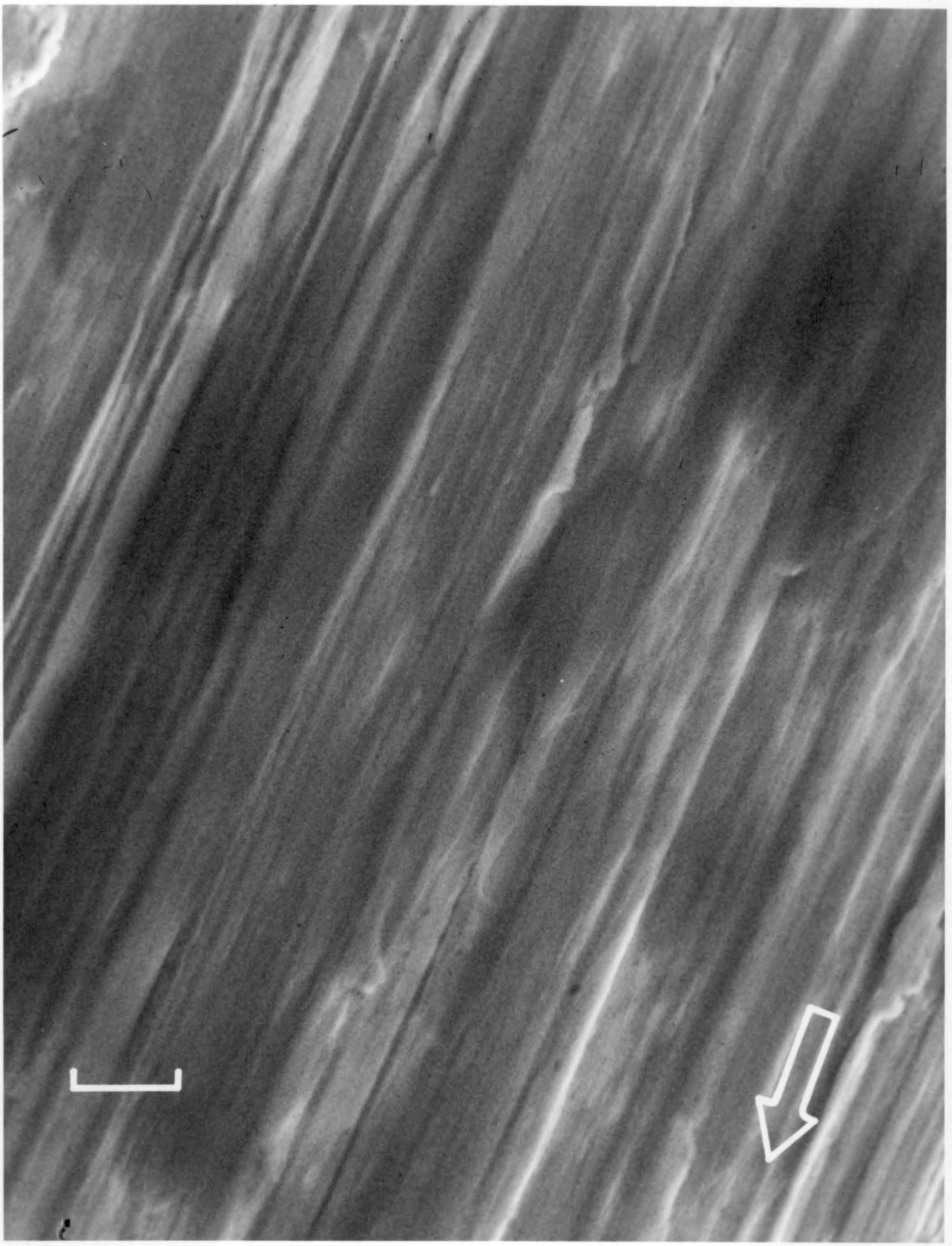

Figure 57. Scanning electron microscope picture of a medium roughness disk after 38400 passes at 128 cm/sec. Index mark is 10 μm. Arrow shows the direction of sliding of the pin.

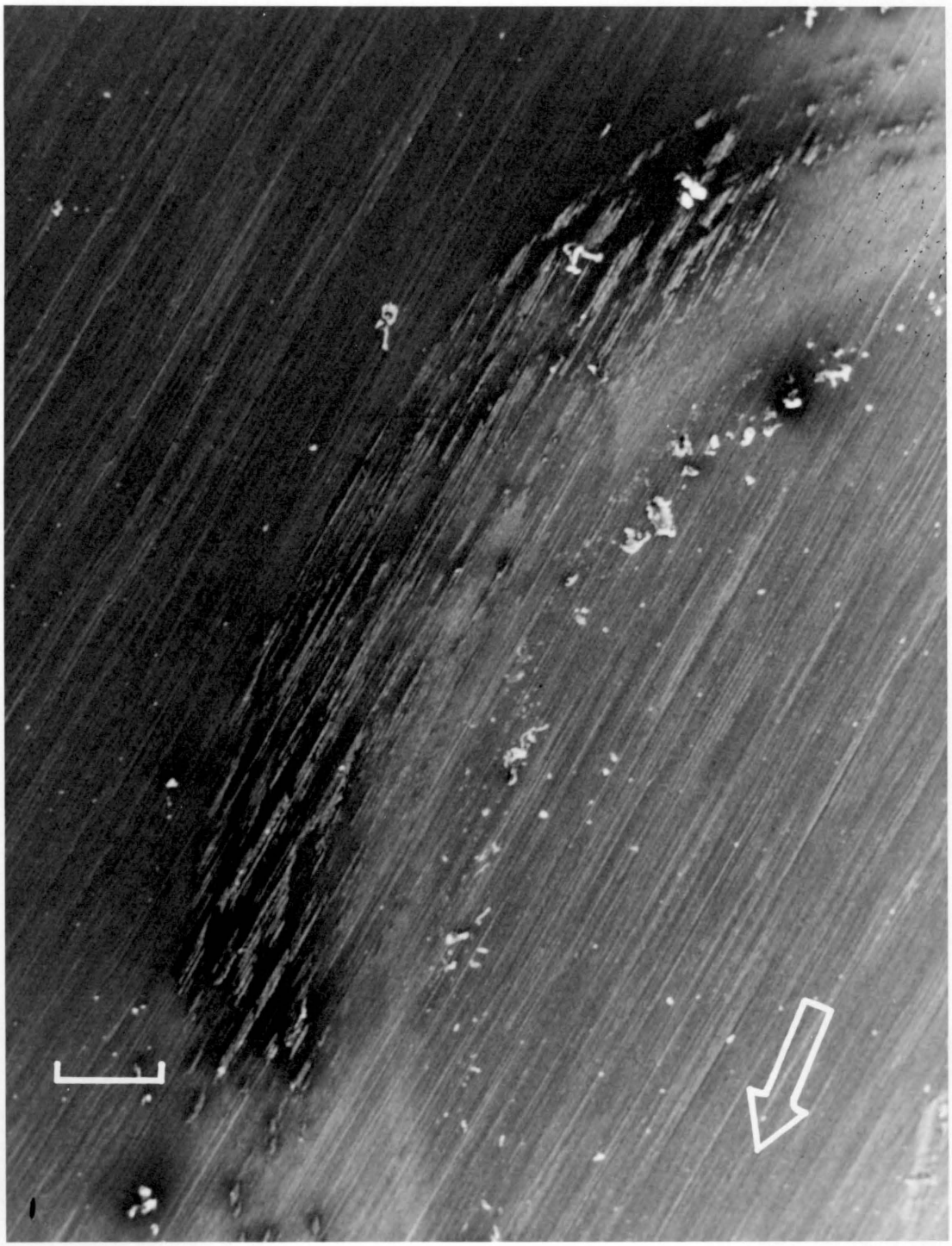

Figure 58. Scanning electron microscope picture of a medium roughness disk after 4800 passes at 32 cm/sec. Index mark is 500 μm. Arrow shows the direction of sliding of the pin.

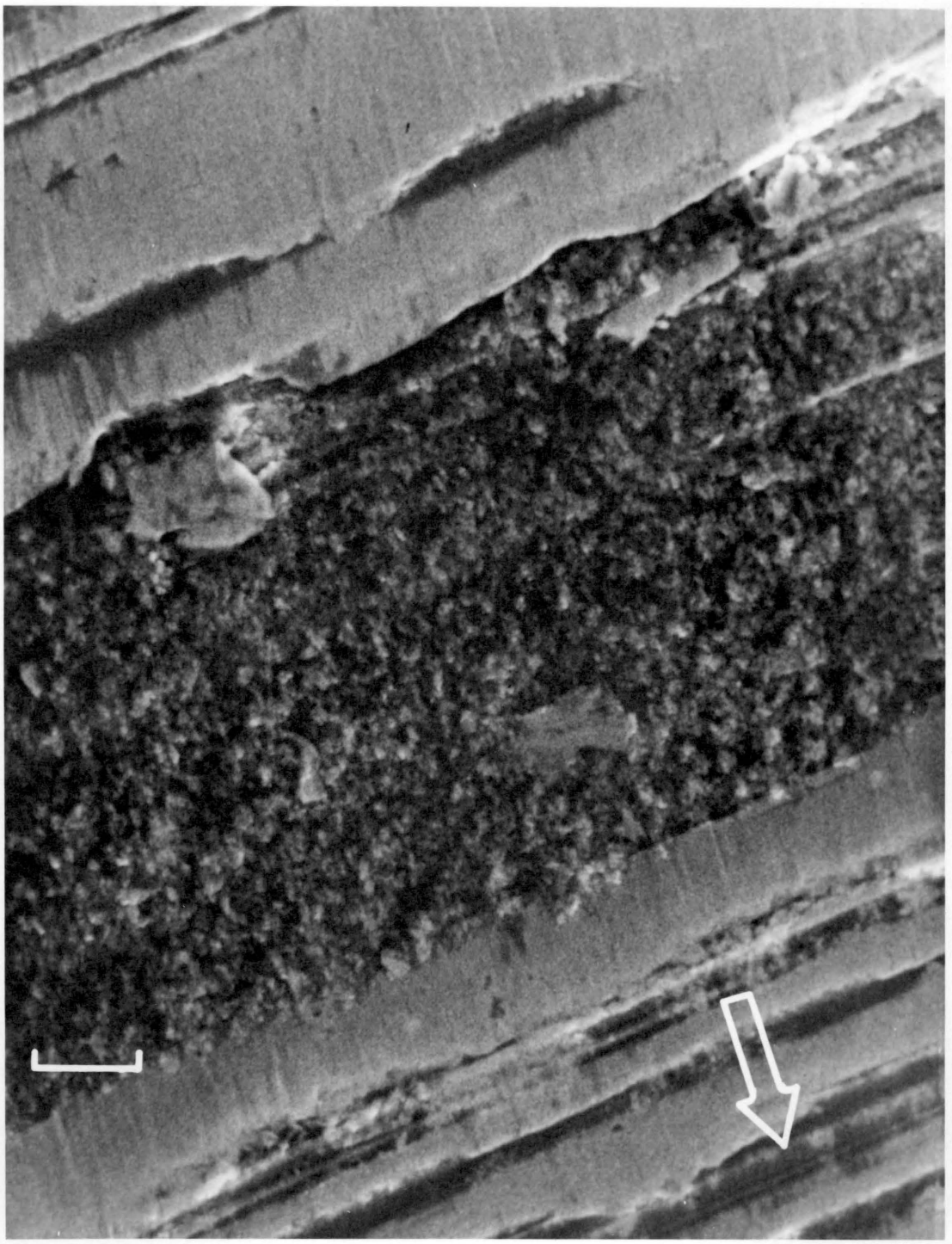

Figure 59. Scanning electron microscope picture of a medium roughness disk after 600 passes at 128 cm/sec. Index mark is 10 μm. Arrow shows the direction of sliding of the pin.

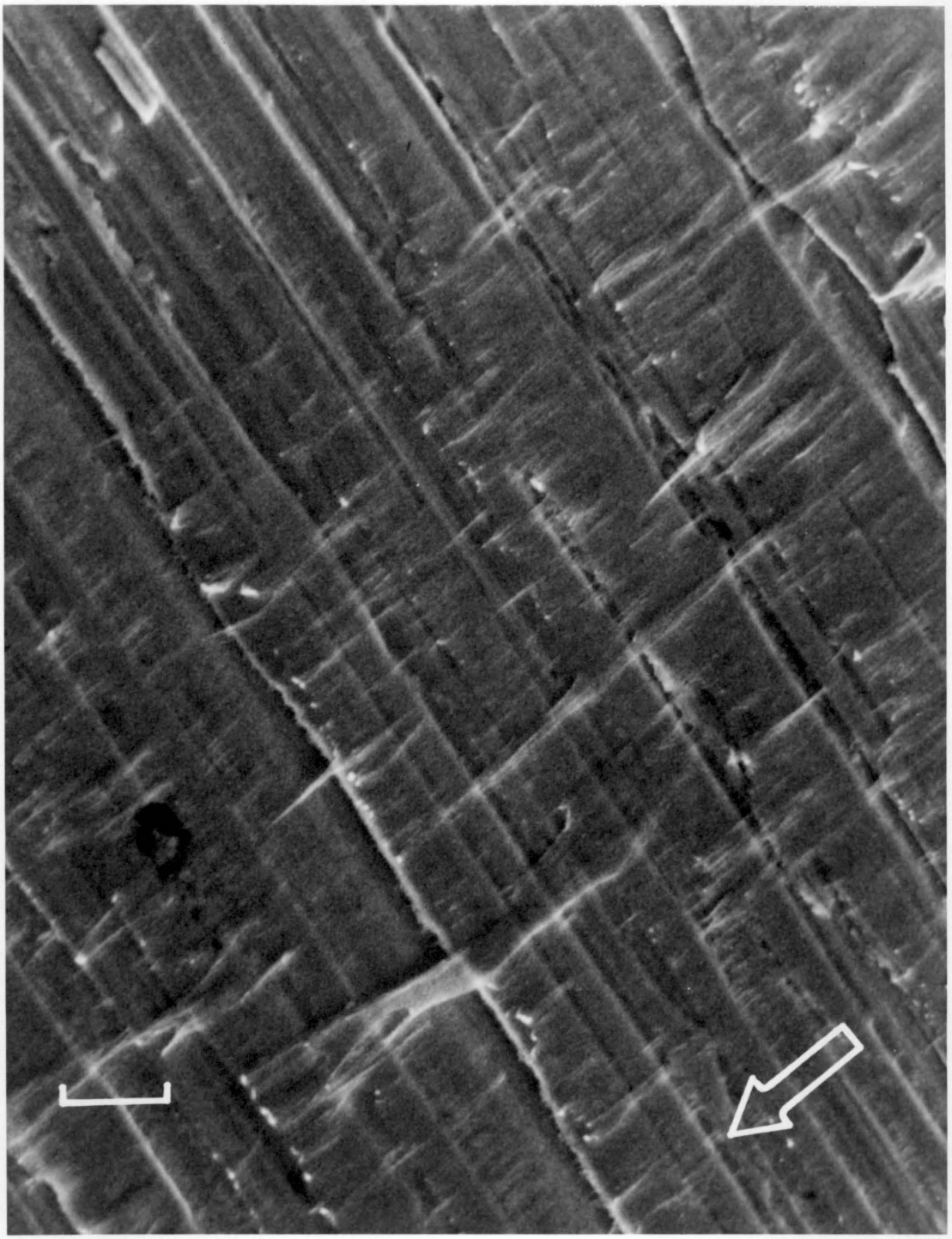

Figure 60. Scanning electron microscope picture of a medium roughness disk after 19200 passes at 128 cm/sec. Index mark is 10 μm. Arrow shows the direction of sliding of the pin.

rolls, which later stick together to form the more massive particles [Fig. 61].

Wear Surfaces of the Pins

Pins that are worn at the high speed show a combination of abrasive and adhesive processes. Surface layers are cut by the asperities of the steel surface and pile on top of each other [Fig. 62] as a result of abrasive cutting. Meanwhile, tongues are formed on these layers due to the adhesive forces. These forces cause the layers of polymer to flow over each other and a multi-layered surface topography results [Fig. 63].

B. Wear of the Pins

The amounts of wear were plotted versus the number of passes for each surface roughness at the two speeds of sliding. The best fitting curves were chosen from 8 different regression models by the method of least squares. These curves turned out to be straight lines of the form $y = a + bx$, where y is the wear in milligrams and x is the number of passes [Fig. 64-68]. The slopes of these straight lines were used to find the constant wear rates [Table 2].

These results have shown that surface roughness is the major parameter in determining the wear rates. In fact, the wear rates are increased by two orders of magnitude in going from the smooth surface to the rough surface. This behaviour is due to the change in the wear mode, which is adhesive on the smooth surface and abrasive

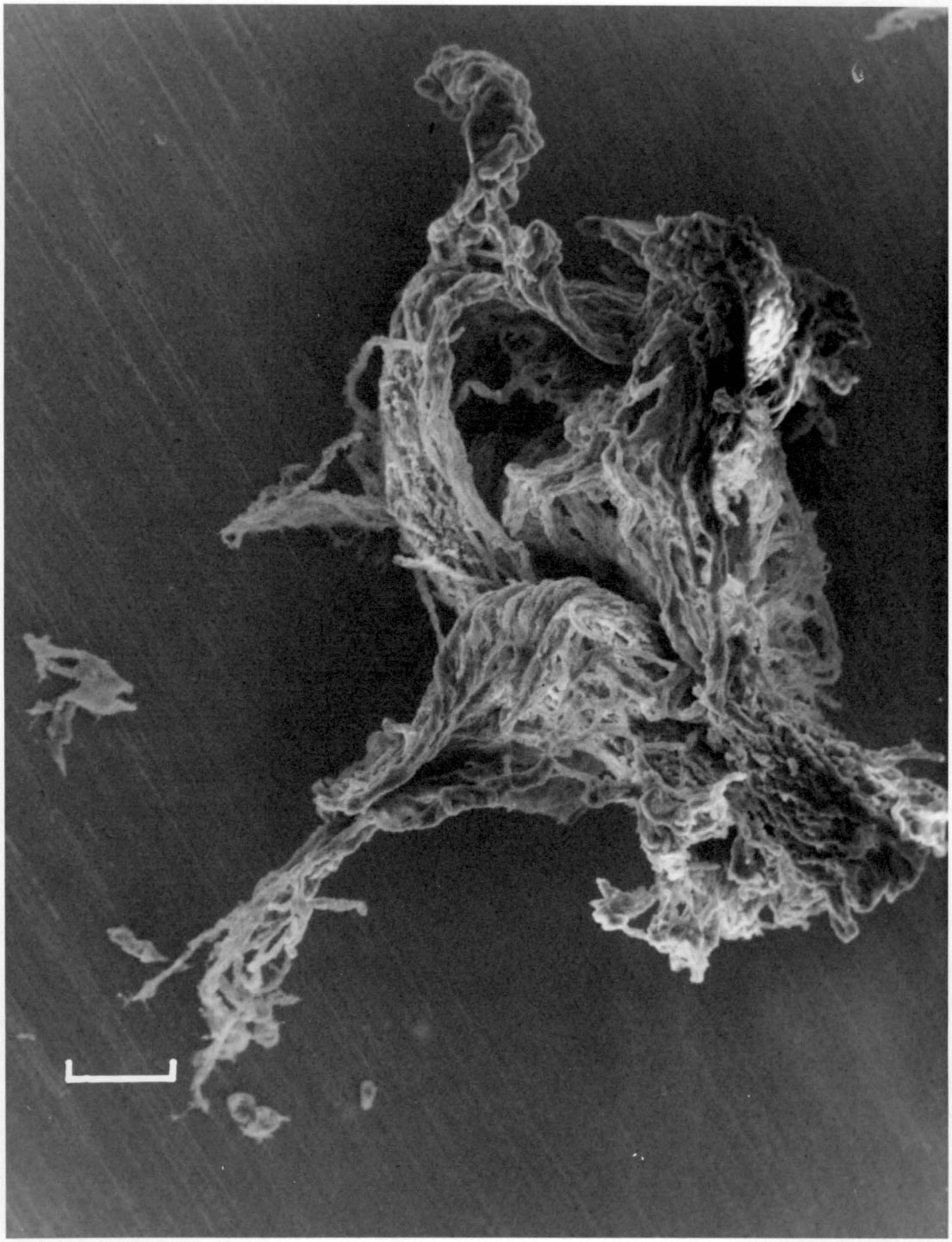

Figure 61. Scanning electron microscope picture of a medium roughness disk after 19200 passes at 128 cm/sec. Index mark is 100 μm.

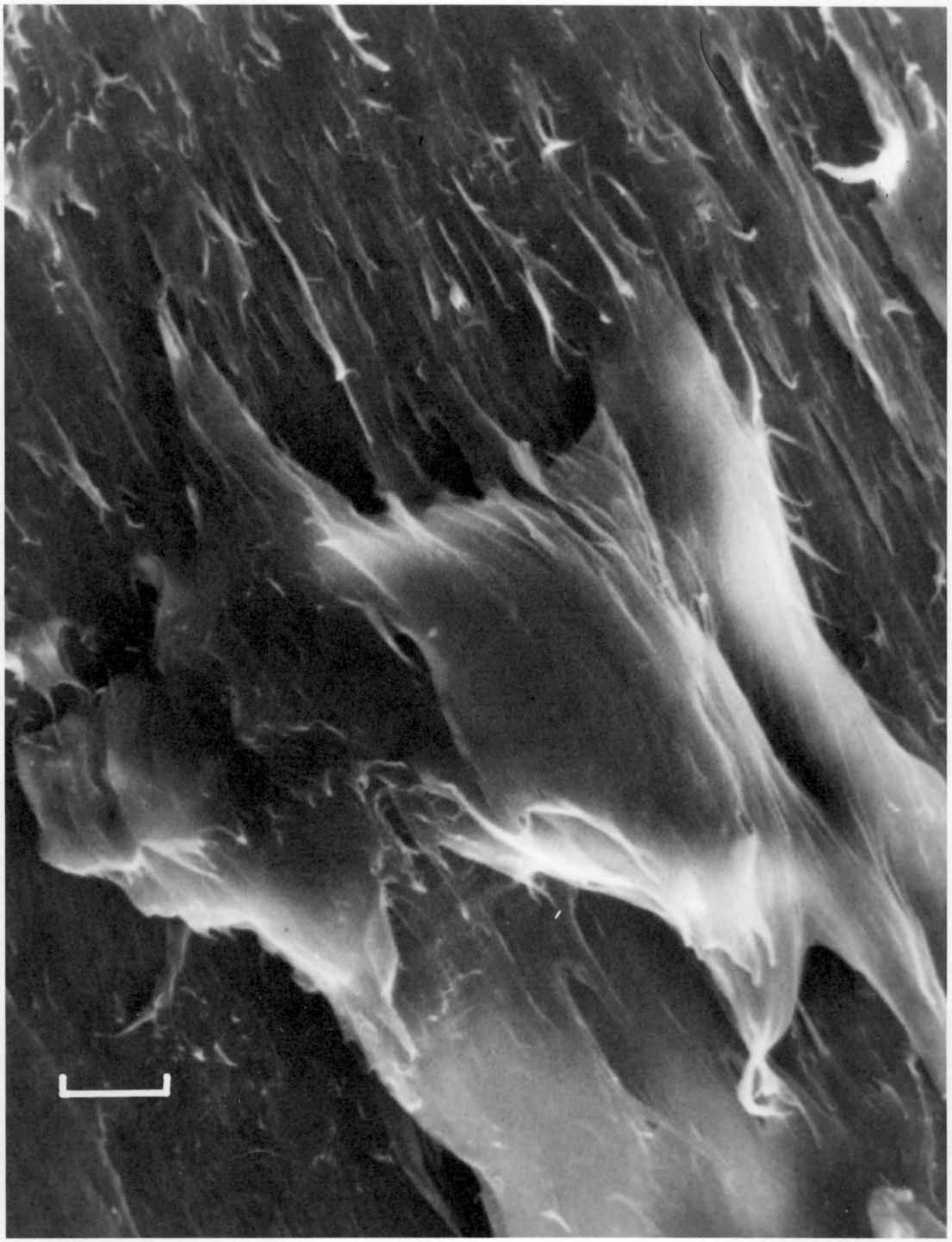

Figure 62. Scanning electron microscope picture of a pin after 9600 passes on a medium roughness disk at 128 cm/sec. Index mark is 10 μm.

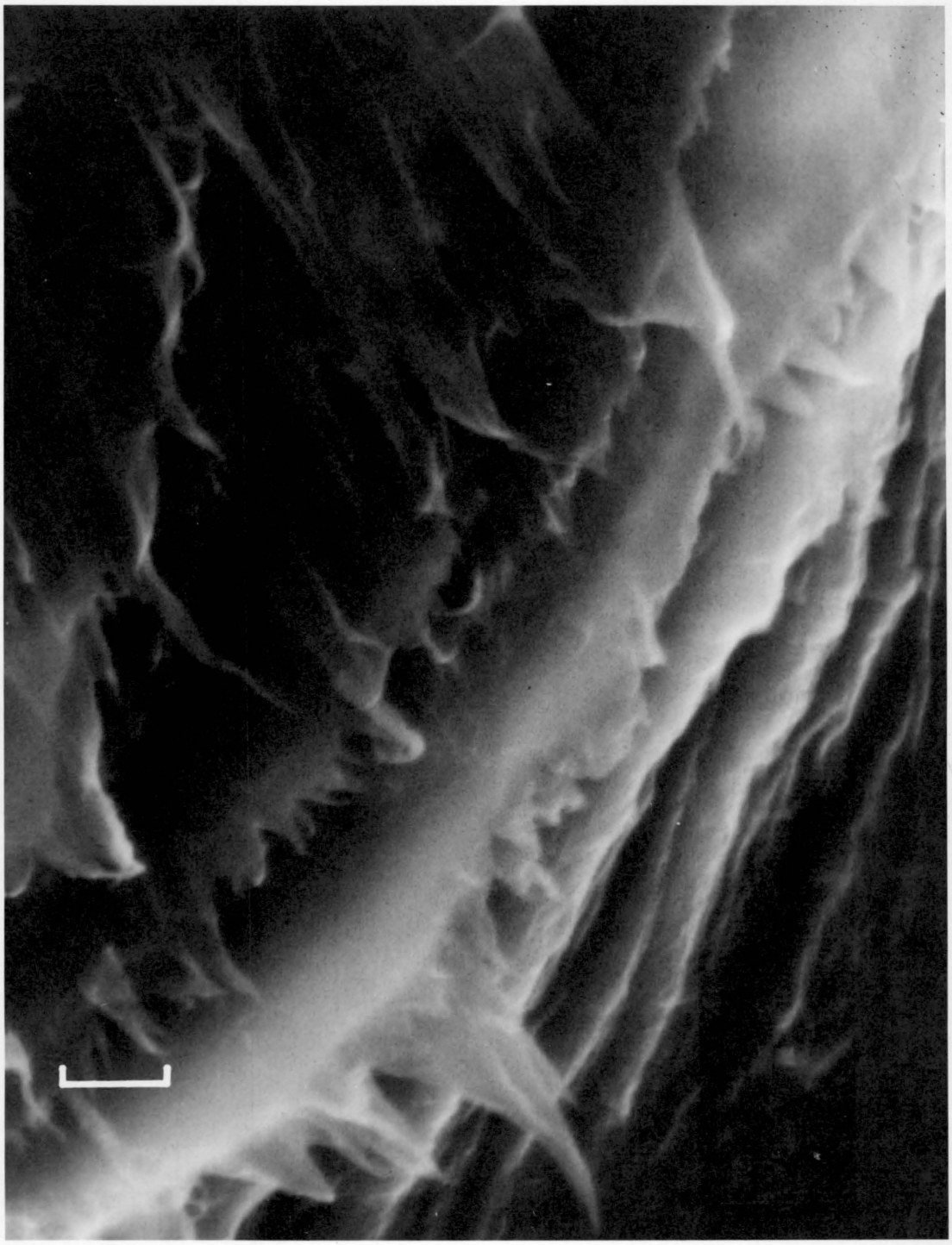

Figure 63. Scanning electron microscope picture of a pin after 9600 passes on a medium roughness disk at 128 cm/sec. Index mark is 5 μm.

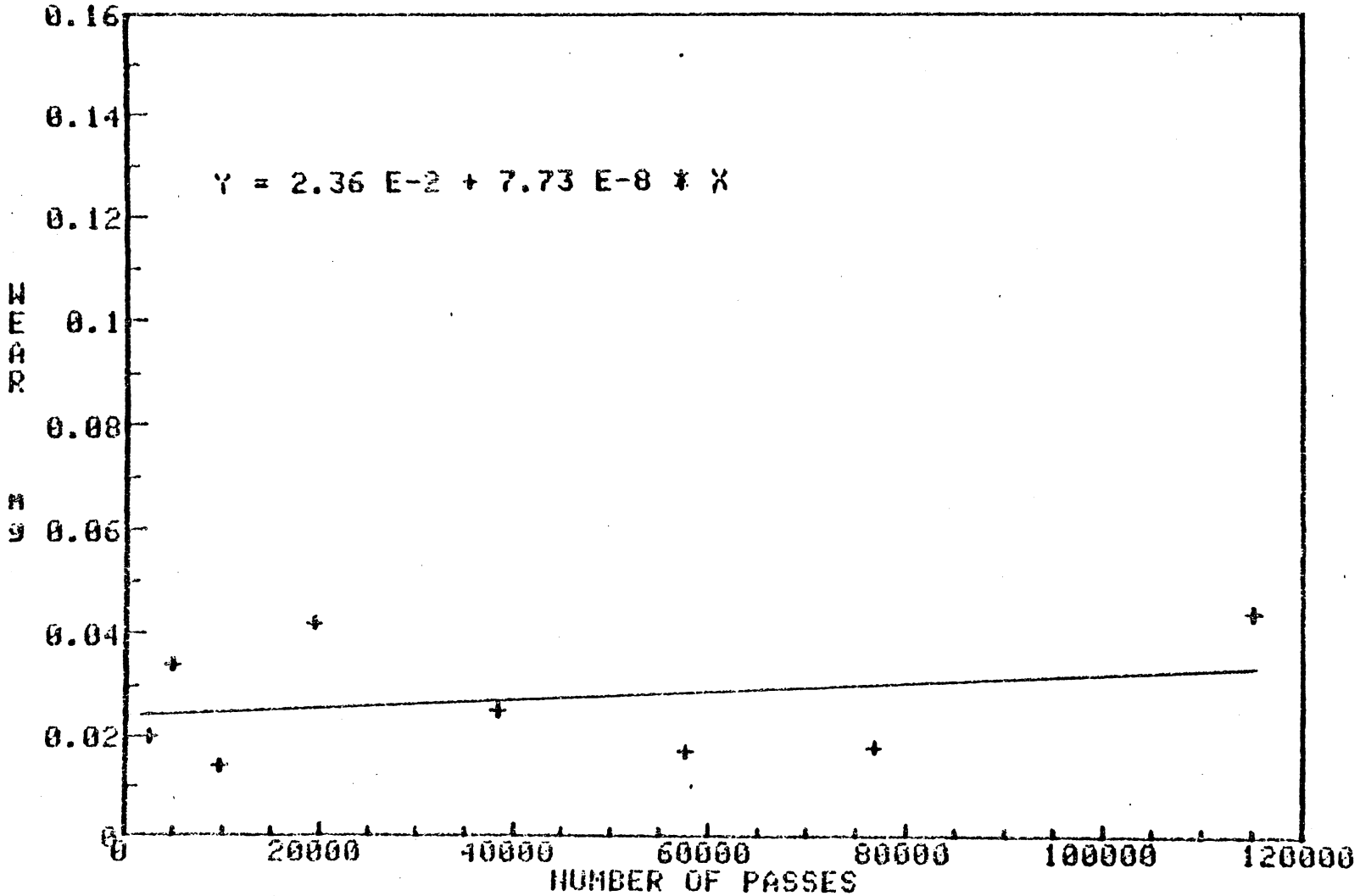

Figure 64. Wear of LDPE pins on the smooth surface at the low speed

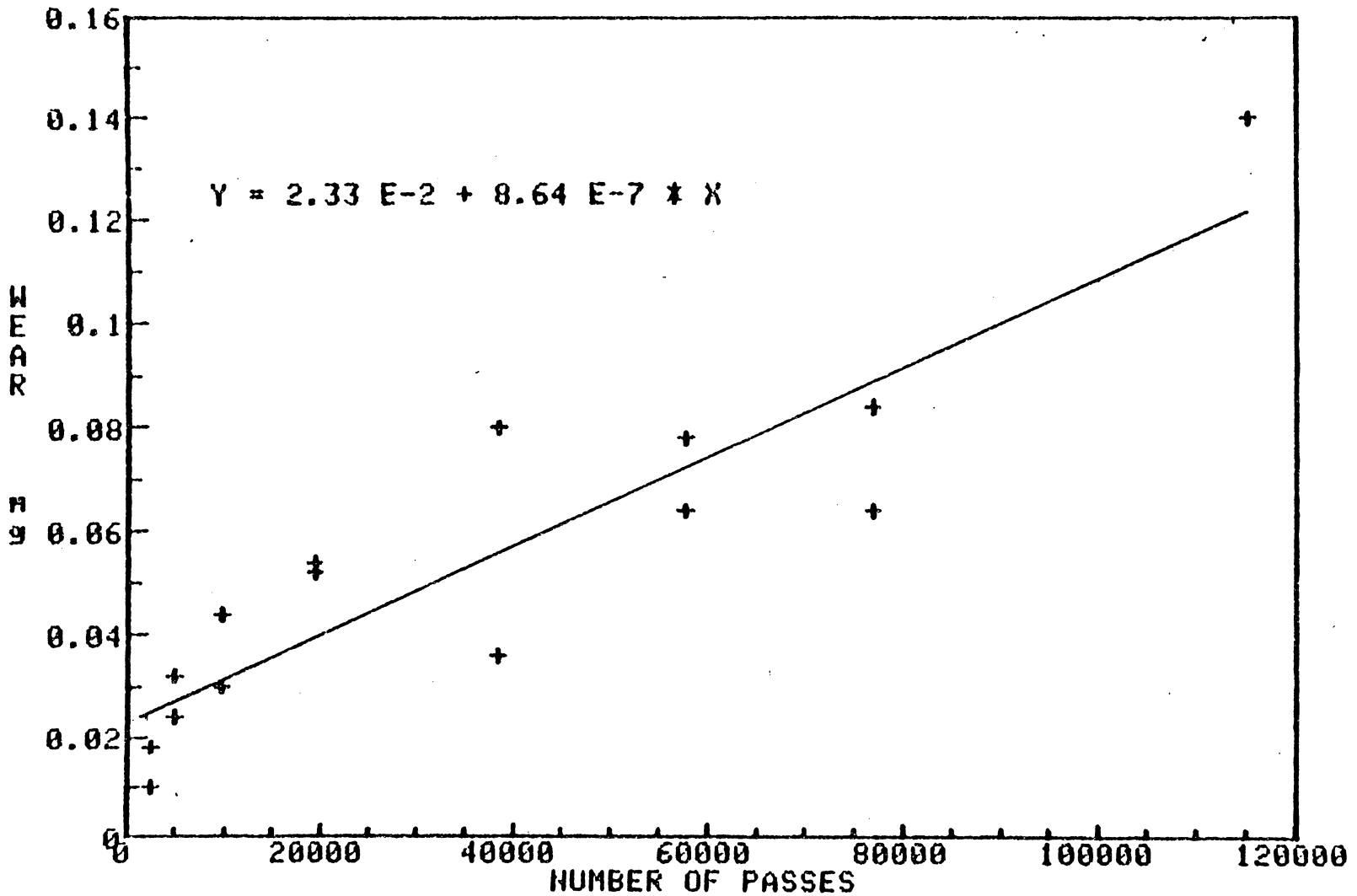

Figure 65. Wear of LDPE pins on the smooth surface at the high speed

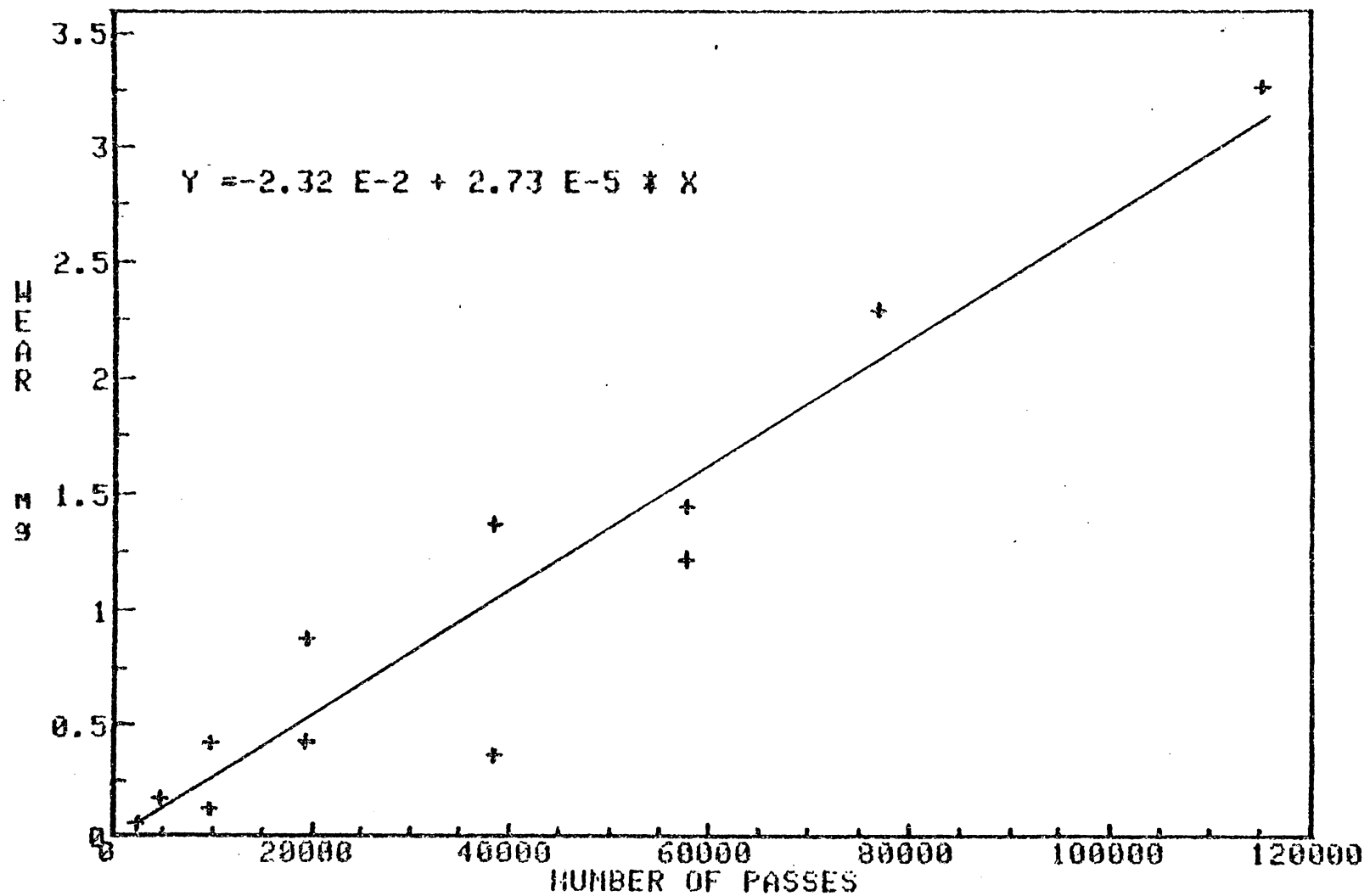

Figure 66. Wear of LDPE pins on the medium surface at the high speed

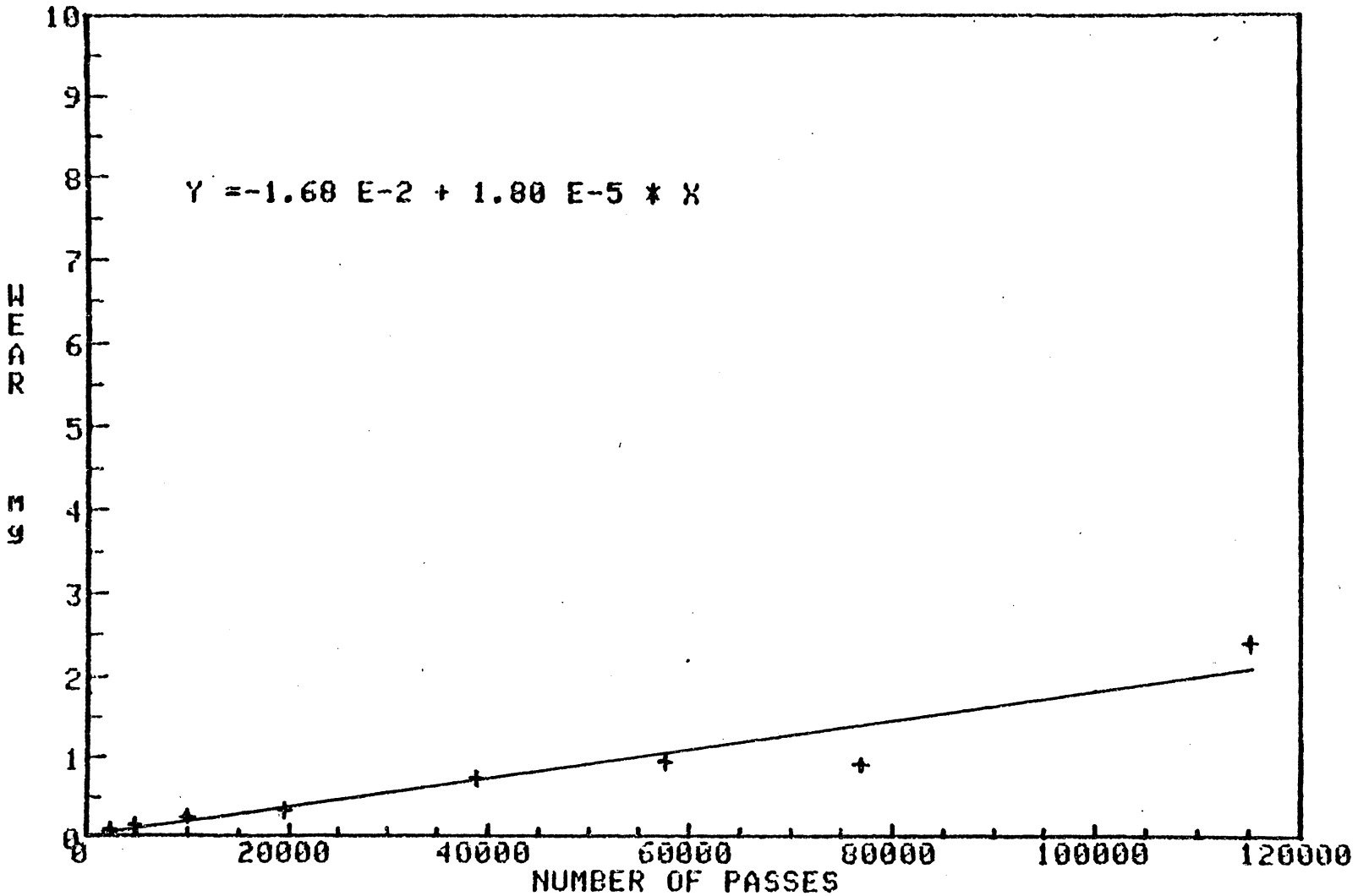

Figure 67. Wear of LDPE pins on the rough surface at the low speed

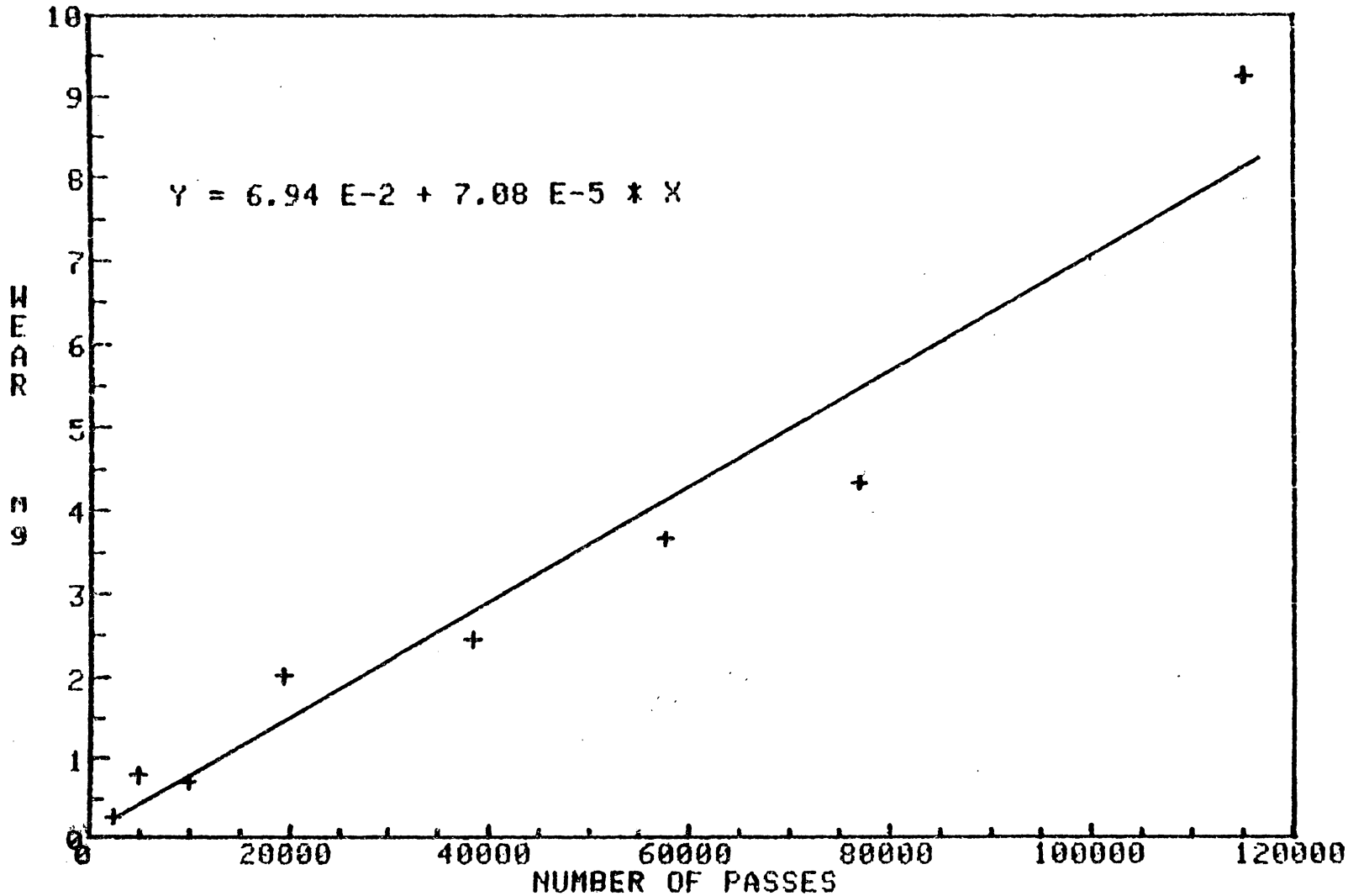

Figure 68. Wear of LDPE pins on the rough surface at the high speed

TABLE 2

WEAR RATES FOR LDPE PINS SLIDING ON STEEL DISKS

SURFACE ROUGHNESS CLA (μm)	WEAR RATE* (g/m) at 32 cm/sec	WEAR RATE (g/m) at 128 cm/sec
$6.52\ (10)^{-2}$	$(2.42\pm8.78)(10)^{-9}$	$(6.75\pm1.10)(10)^{-9}$
$6.45\ (10)^{-1}$		$(2.13\pm0.47)(10)^{-7}$
1.16	$(5.64\pm1.66)(10)^{-8}$	$(5.53\pm1.32)(10)^{-7}$

*Mean and 95% confidence limits are tabulated. The confidence limits are obtained by determining the variance in the slope of the wear lines.

on the rough surface. A medium wear rate was observed for the medium roughness surface, where the wear mode is both adhesive and abrasive.

The effect of speed on the wear rate can only be seen for sliding on the smooth surface, where the wear rate at the high speed is about three times as much as the wear rate at the low speed. This is mainly due to the increase in temperature with speed, which causes the softening of the polymer at the high speed. The low wear rates at the low speed could also be due to transfer occurring from the disk to the pin as films break from the steel surface. This behaviour is suggested by the scatter in the low speed wear data, where for some intervals wear seems to decrease as the number of passes increases [Fig. 64]. Transfer from the steel surface to the pin is not significant in the other cases where wear increases with number of passes. The wear rates do not change with speed for sliding on the rough surface, where no temperature effects are observed.

The straight lines of wear versus number of passes do not pass through the origin, although the origin could be considered as an exact data point. (Values of the y-intercept of the straight lines are listed in Table 3.) The values of the y-intercept for the smooth surface are significant compared to the amounts of wear [Table 4]. This is due to the fact that the initial wear rates (i.e., the wear rates before 2400 passes is reached) are much higher than the constant wear rates calculated for the higher number of passes. For the rougher surfaces the uncertainty in the y-intercept is too large to detect the initial wear rates. This large uncertainty range is due to the

TABLE 3

VALUES OF THE Y-INTERCEPT IN WEAR EQUATIONS

SURFACE ROUGHNESS CLA (μm)	Y-INTERCEPT* (mg) at 32 cm/sec	Y-INTERCEPT* (mg) at 128 cm/sec
$6.52\ (10)^{-2}$	$(2.36\pm1.15)(10)^{-2}$	$(2.33\pm0.07)(10)^{-2}$
$6.45\ (10)^{-1}$		$(-2.32\pm2.99)(10)^{-2}$
1.16	$(-1.78\pm27.9)(10)^{-2}$	$(6.94\pm88.5)(10)^{-2}$

*Mean and 95% confidence limits are tabulated. The confidence limits are found by determining the intersections of the 95% confidence bands with the Y-axis.

TABLE 4

WEAR OF LDPE PINS ON SMOOTH STEEL DISKS

NUMBER OF PASSES	WEAR (mg) at 32 cm/sec	WEAR* (mg) at 128 cm/sec	WEAR* (mg) at 128 cm/sec
2400	0.020	0.010	0.018
4800	0.034	0.032	0.024
9600	0.014	0.080	0.044
19200	0.042	0.054	0.052
38400	0.025	0.086	0.080
57600	0.017	0.064	0.078
76800	0.018	0.084	0.064
115200	0.044	0.140	-

*Replicate experiments were performed to measure repeatability.

high amounts and the variability of wear on the rougher surfaces [Table 5 and 6].

In examining Tables 4, 5, and 6 one has to keep in mind that the amounts of wear are given with respect to the number of passes, and that the circumference of the high speed track is four times the circumference of the low speed track.

C. Friction of the Pins

Friction coefficients were plotted versus the number of passes for the smooth and rough surfaces at the two speeds of sliding. The best fitting curves were chosen from 8 different regression models by the method of least squares. These curves turned out to be straight lines of the form $y = a + bx$, where y is the friction coefficient and x is the number of passes [Fig. 69, 70]. The equations are listed in Table 7.

These results have shown that the coefficient of friction stays relatively constant throughout the experiments, except for low speed sliding on the smooth surface. In this case, the friction coefficient decreases as the number of passes increase. This shows that the process has not reached a steady state. For the smooth surfaces the friction coefficients at the high speed sliding are lower than the friction coefficients at the low speed of sliding [Table 8]. This is probably due to the high temperature at the high speed, which results in a decrease in the shear resistance of the polymer due to softening.

TABLE 5

WEAR OF LDPE PINS ON MEDIUM ROUGHNESS STEEL DISKS

NUMBER OF PASSES	WEAR* (mg) at 128 cm/sec	WEAR* (mg) at 128 cm/sec
2400	0.052	-
4800	0.172	-
9600	0.124	0.414
19200	0.874	0.426
38400	0.364	1.364
57600	1.218	1.442
76800	-	2.288
115200	-	3.264

*Replicate experiments were performed to measure repeatability.

TABLE 6

WEAR OF LDPE PINS ON ROUGH STEEL DISKS

NUMBER OF PASSES	WEAR (mg) at 32 cm/sec	WEAR (mg) at 128 cm/sec
2400	0.062	0.263
4800	0.148	0.798
9600	0.229	0.705
19200	0.319	2.014
38400	0.717	2.462
57600	0.938	3.673
76800	0.914	4.332
115200	2.387	9.238

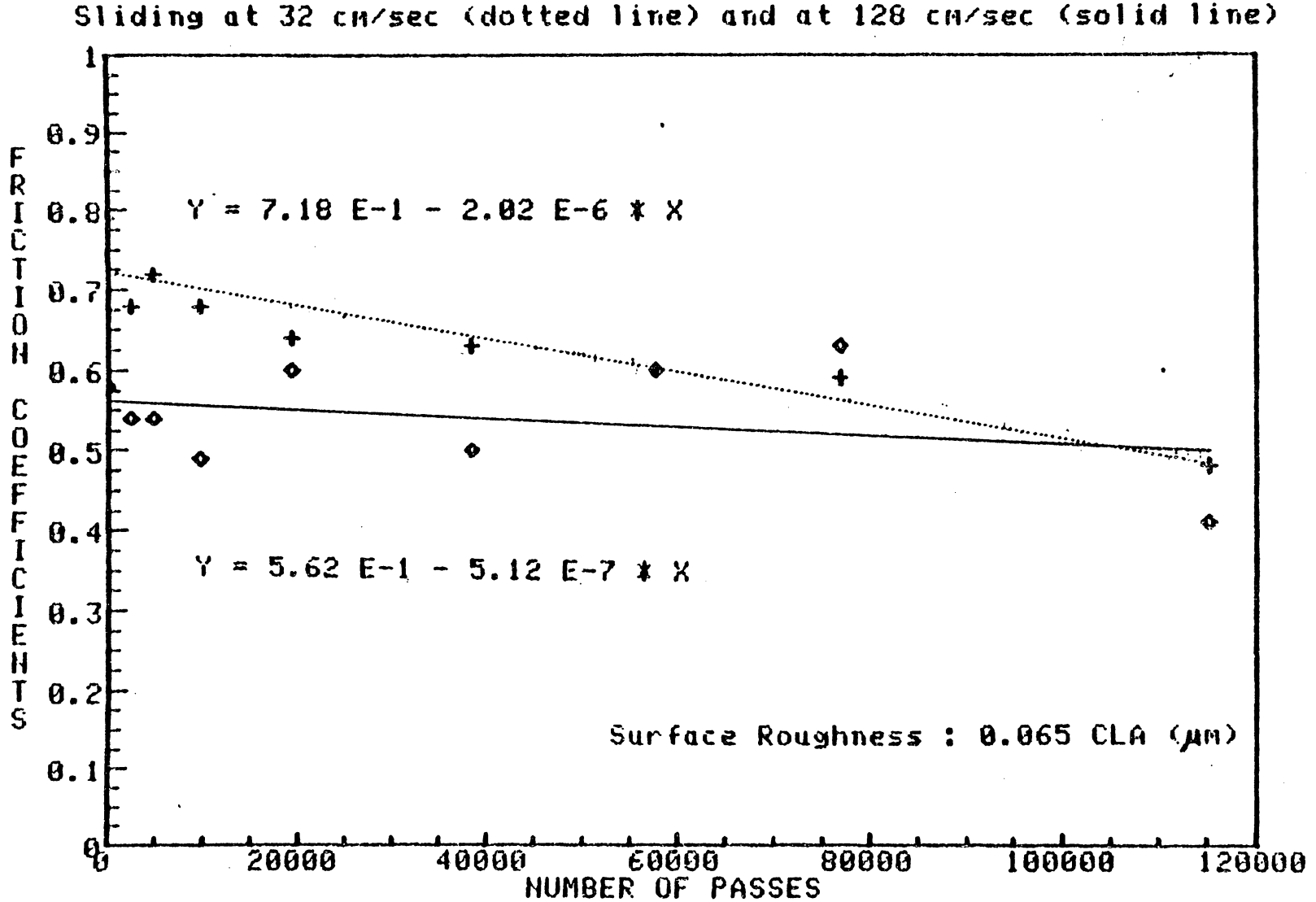

Figure 69. Friction coefficients for LDPE pins on smooth steel surfaces

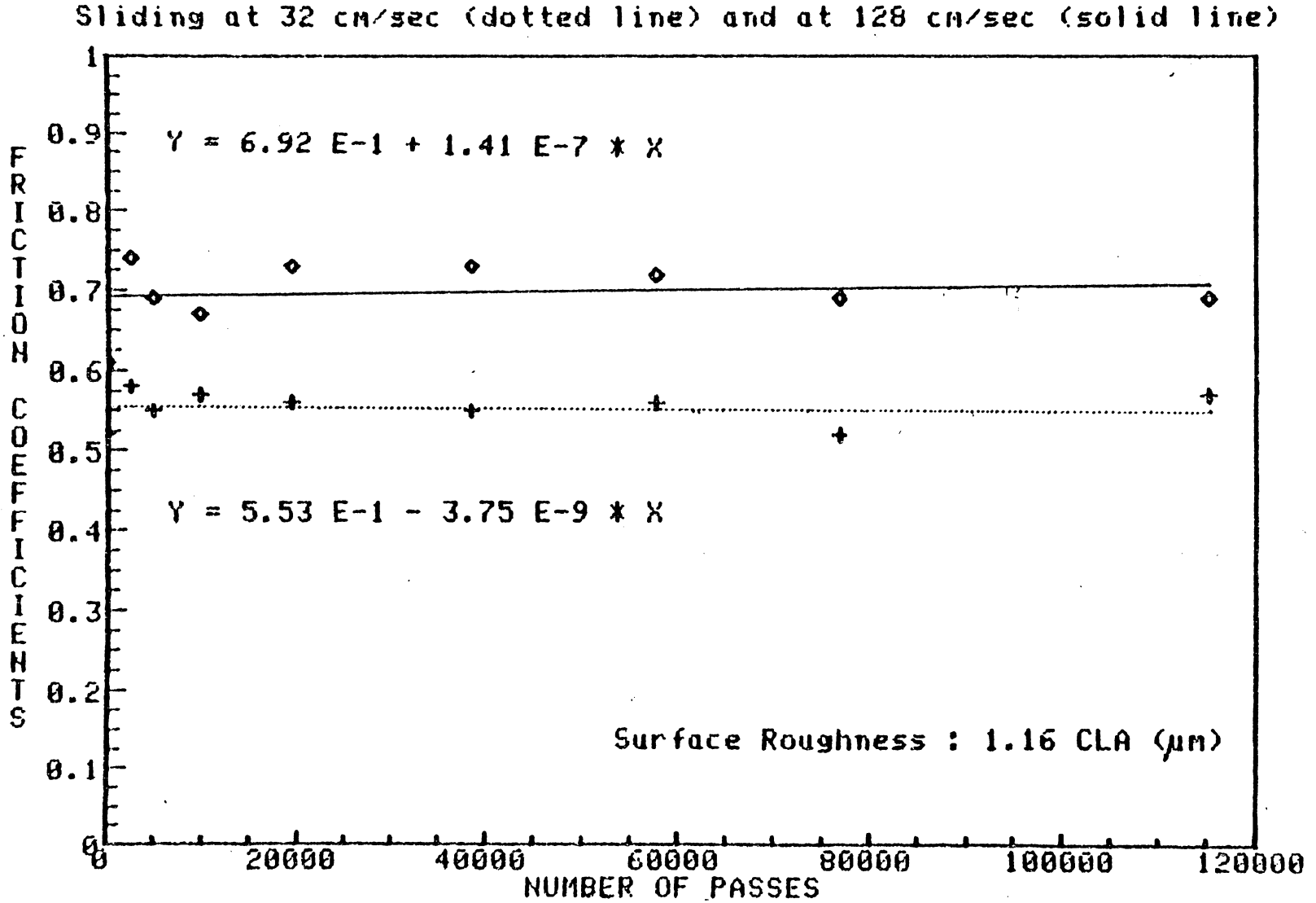

Figure 70. Friction coefficients for LDPE pins on rough steel surfaces

TABLE 7

EQUATIONS OF FRICTION

SURFACE ROUGHNESS CLA (μm)	SPEED (cm/sec)	EQUATION $y = a + bx$*	
		a**	b**
$6.52\ (10)^{-2}$	32	$(7.18\pm0.38)(10)^{-1}$	$(-2.02\pm0.76)(10)^{-6}$
$6.52\ (10)^{-2}$	32	$(5.62\pm0.77)(10)^{-1}$	$(-5.12\pm14.6)(10)^{-9}$
1.16	128	$(5.53\pm0.25)(10)^{-1}$	$(-3.75\pm474.)(10)^{-7}$
1.16	128	$(6.92\pm0.47)(10)^{-1}$	$(1.41\pm8.93)(10)^{-7}$

*y is the friction coefficient, x is the number of passes.

**Mean and 95% confidence limits are tabulated. The confidence limits in a are found by determining the intersections of the 95% confidence bands with the y-axis. The confidence limits in b are obtained by determining the variance in the slope of the wear lines.

TABLE 8

FRICTION COEFFICIENTS FOR LDPE PINS

ON SMOOTH STEEL DISKS

NUMBER OF PASSES	FRICTION COEFFICIENTS at 32 cm/sec	FRICTION COEFFICIENTS at 128 cm/sec
0	0.79	0.58
2400	0.68	0.54
4800	0.72	0.54
9600	0.68	0.49
19200	0.64	0.60
38400	0.63	0.50
57600	0.60	0.60
76800	0.59	0.63
115200	0.48	0.41

For the rough surfaces friction coefficients at the high speed of sliding are higher than the friction coefficients at the low speed of sliding [Table 9].

Figures 71 through 74 show the actual plots of friction coefficients versus the number of passes up to 9000 passes. Examination of these figures show that there are periods of change in the order of 0.05 in the coefficients of friction. These changes are random in nature and are due to the changes in the surface films on the disks.

A spectrum analysis of the friction data was made to find the frequency of vibrations of the pivot arm. It was possible to do this because the friction coefficients are proportional to the motion of the pivot arm. A sample plot of these frequencies shows a major peak at 10 Hertz which corresponds to the rotational frequency of the disk [Fig. 75]. The next peak at 20 Hertz is a harmonic of the 10 Hertz vibration.

The natural frequency of the pivot arm was found by the frequency analysis of the response of the pivot arm to an impulse force. The response to the impulse is shown in Fig. 76 and the frequency analysis is shown in Fig. 77. A peak search in this frequency analysis has shown the natural frequency of the pivot arm to be around 6 Hertz. This has explained the relatively high magnitudes of vibration during operation, but it was not feasible to change the system parameters to alter this frequency. However, a damper was added to the system to decrease the magnitude of the vibrations, but

TABLE 9

FRICTION COEFFICIENTS FOR LDPE PINS

ON ROUGH STEEL DISKS

NUMBER OF PASSES	FRICTION COEFFICIENTS at 32 cm/sec	FRICTION COEFFICIENTS at 128 cm/sec
0	0.52	0.61
2400	0.58	0.74
4800	0.55	0.69
9600	0.57	0.67
19200	0.56	0.73
38400	0.55	0.73
57600	0.56	0.72
76800	0.52	0.69
115200	0.57	0.69

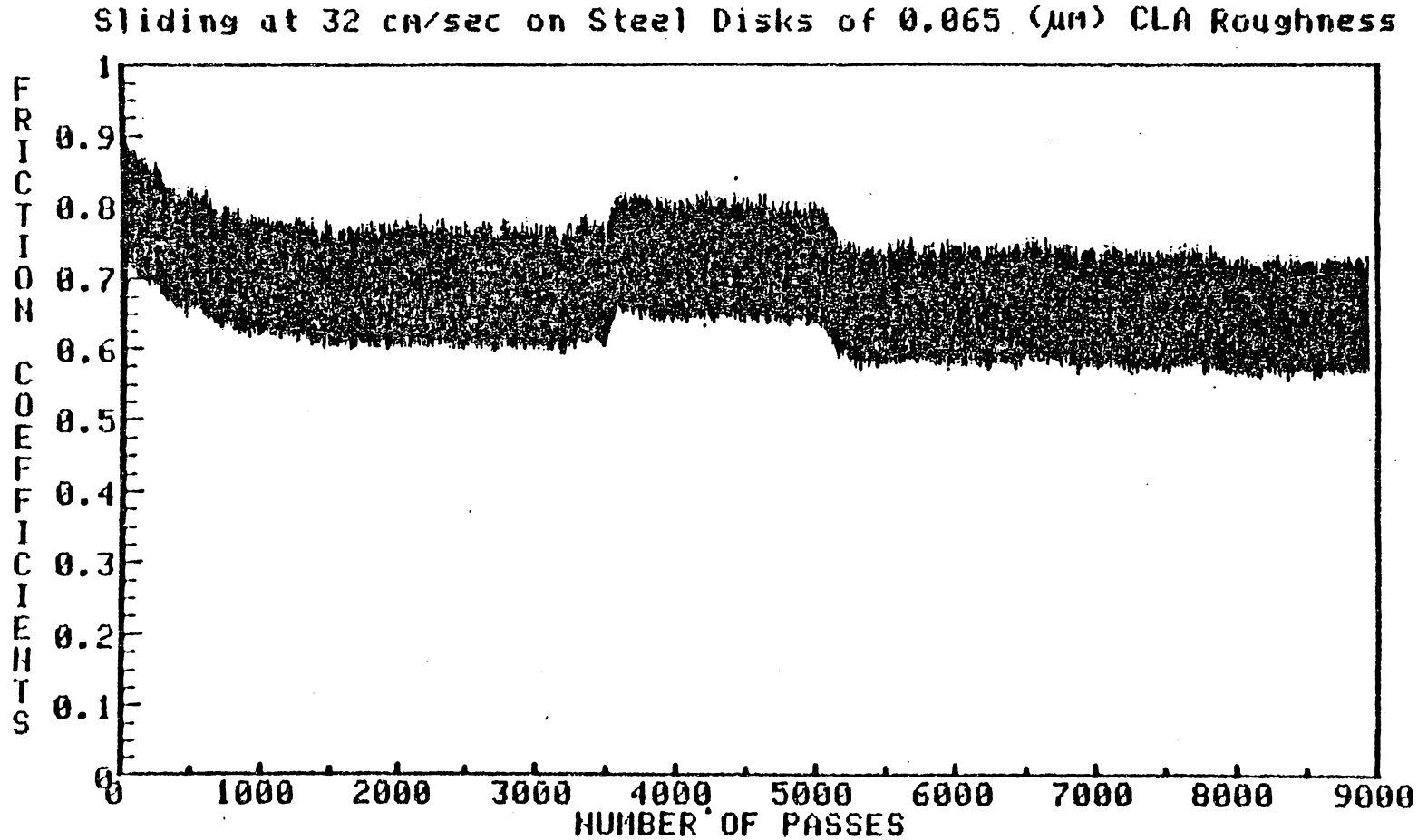

Figure 71. Friction coefficients for LDPE pins on smooth steel surfaces at the low speed

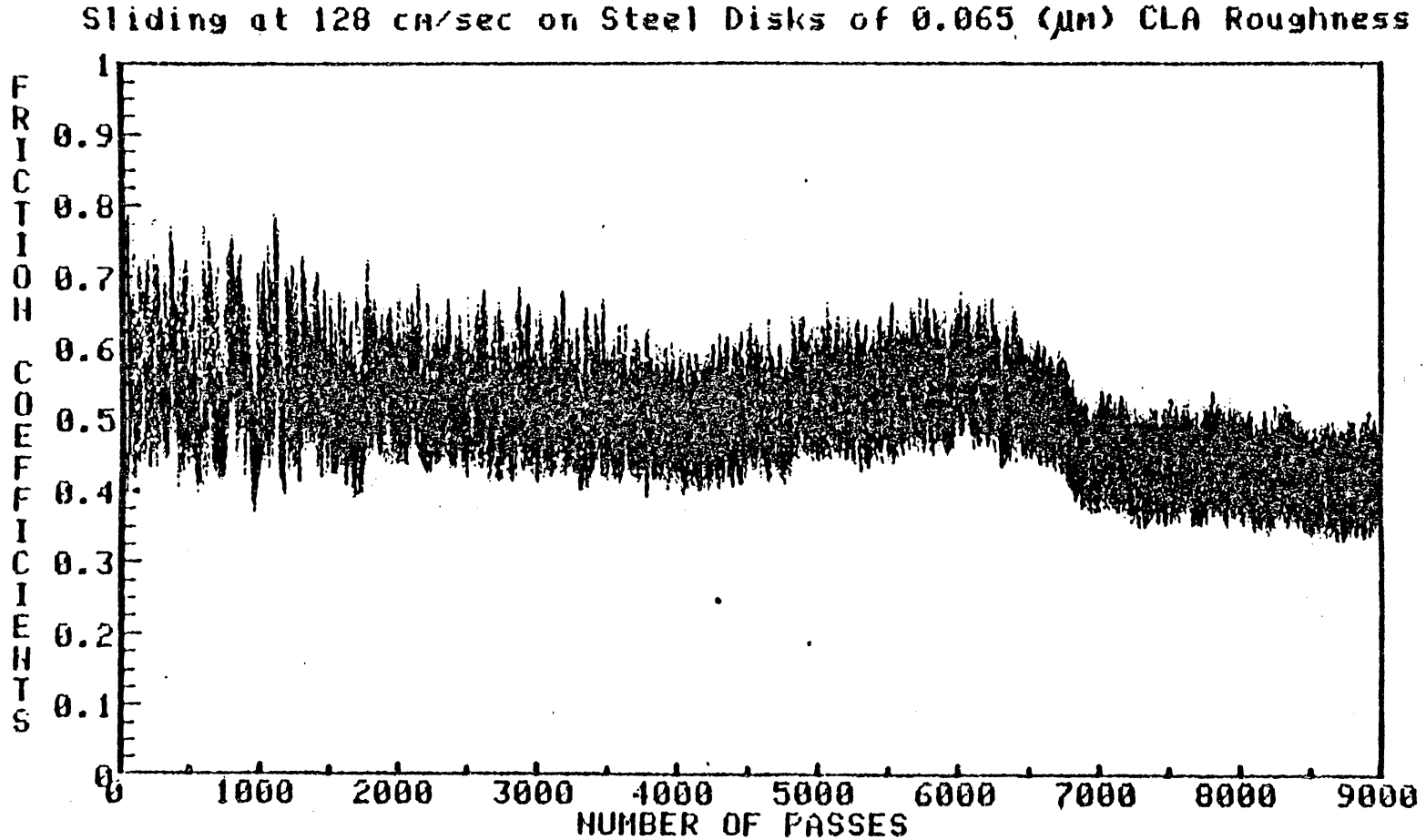

Figure 72. Friction coefficients for LDPE pins on smooth steel surfaces at the high speed

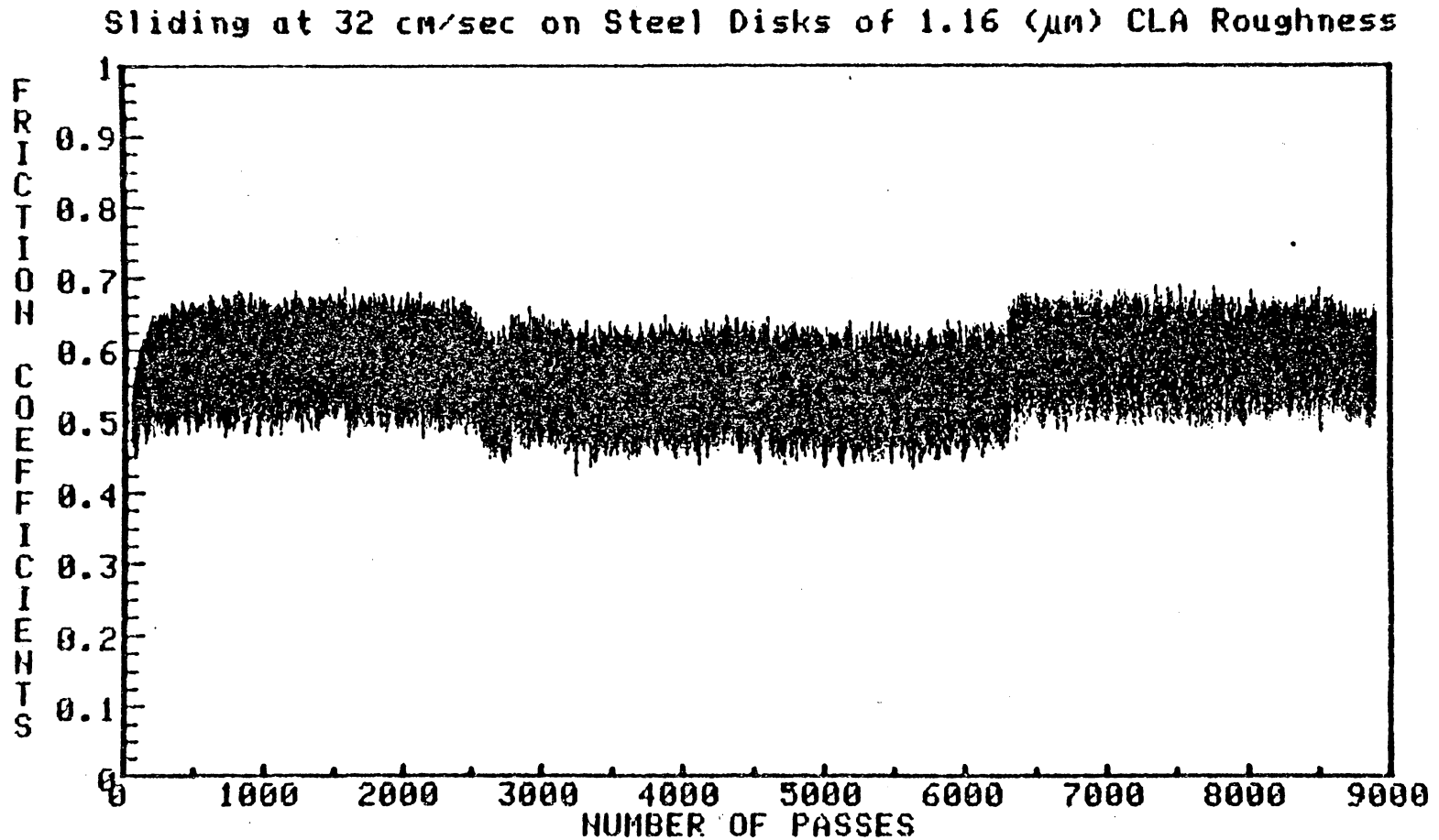

Figure 73. Friction coefficients for LDPE pins on rough steel surfaces at the low speed

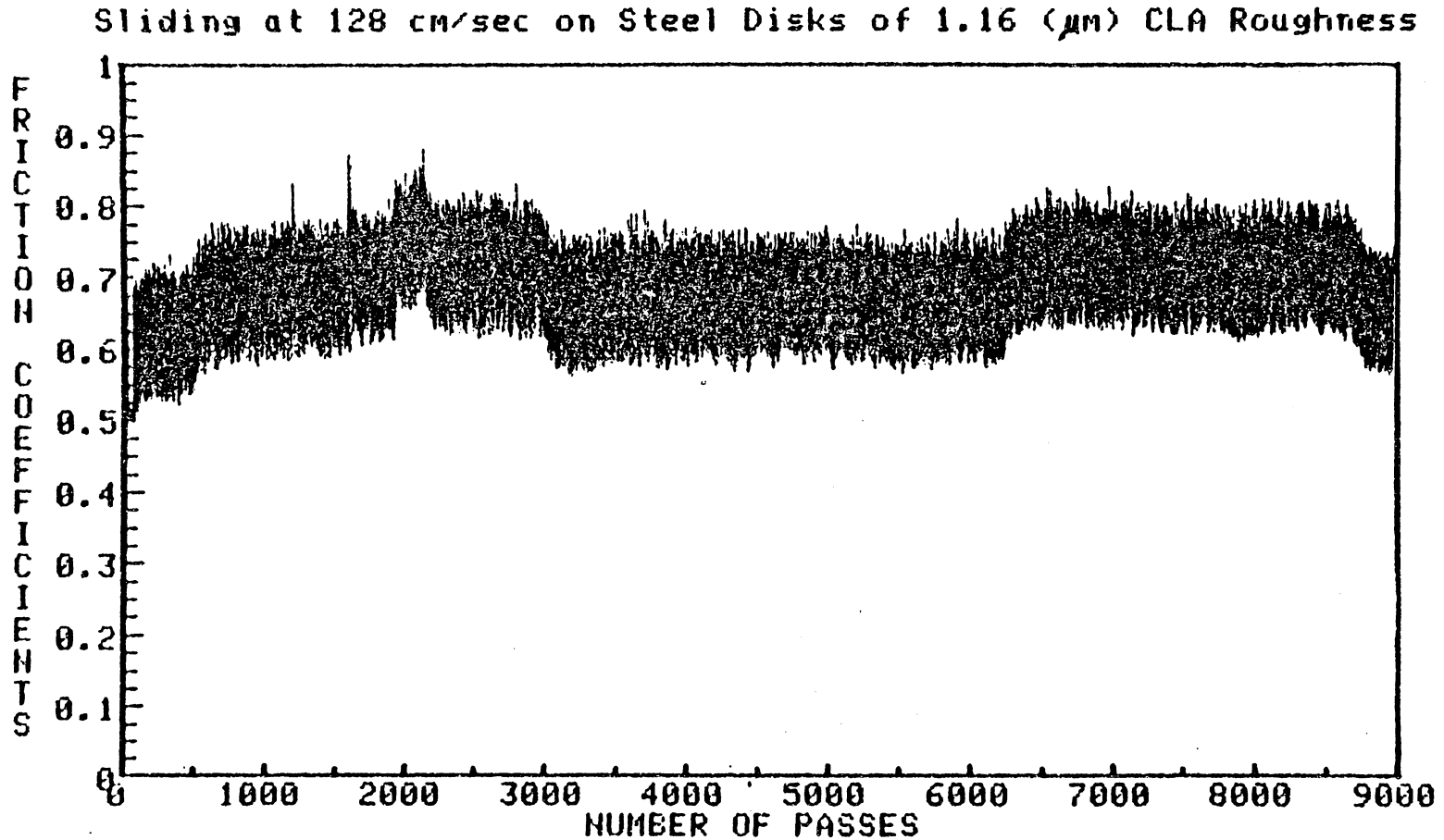

Figure 74. Friction coefficients for LDPE pins on rough steel surfaces at the high speed

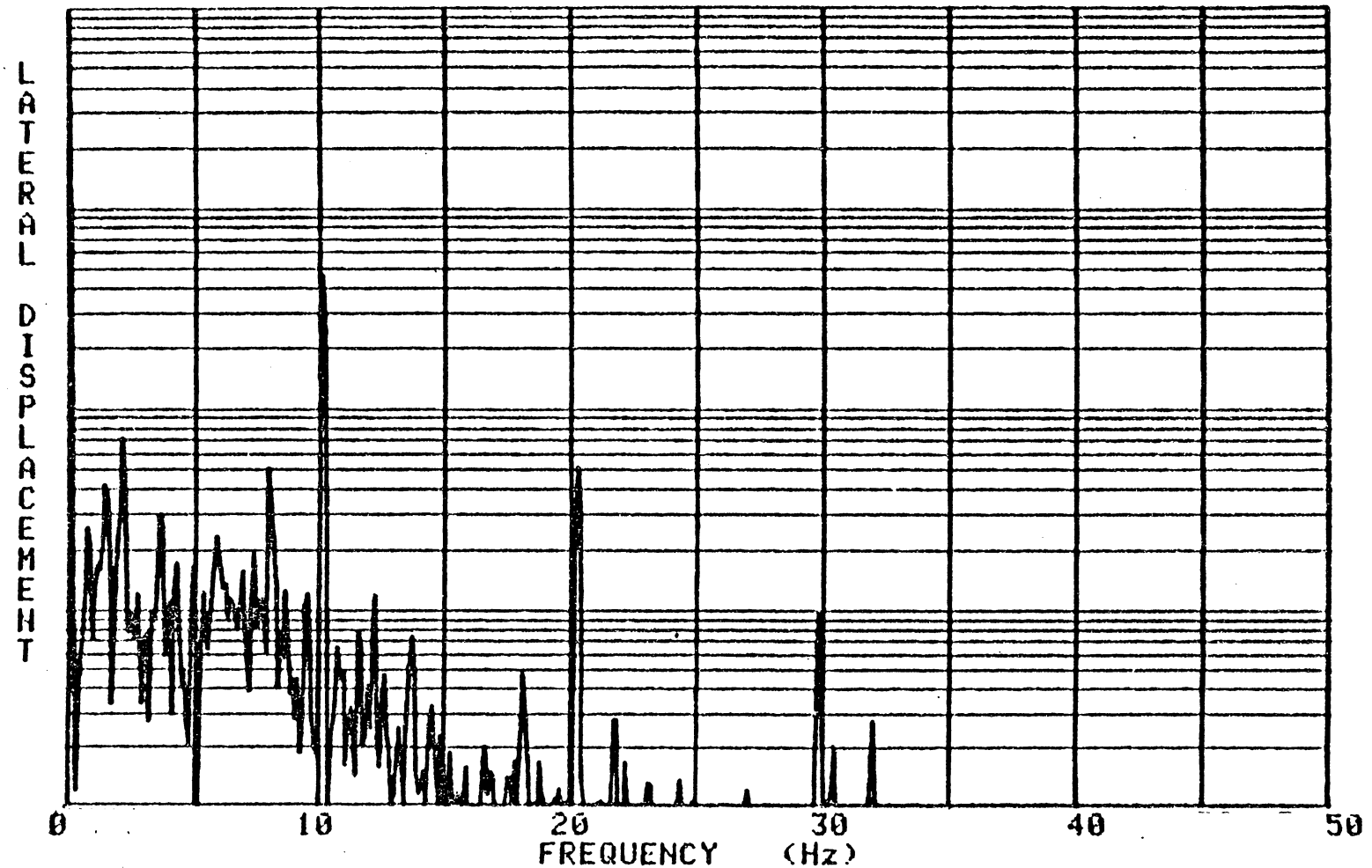

Figure 75. A sample spectrum analysis of the response of the pivot arm during the friction measurements

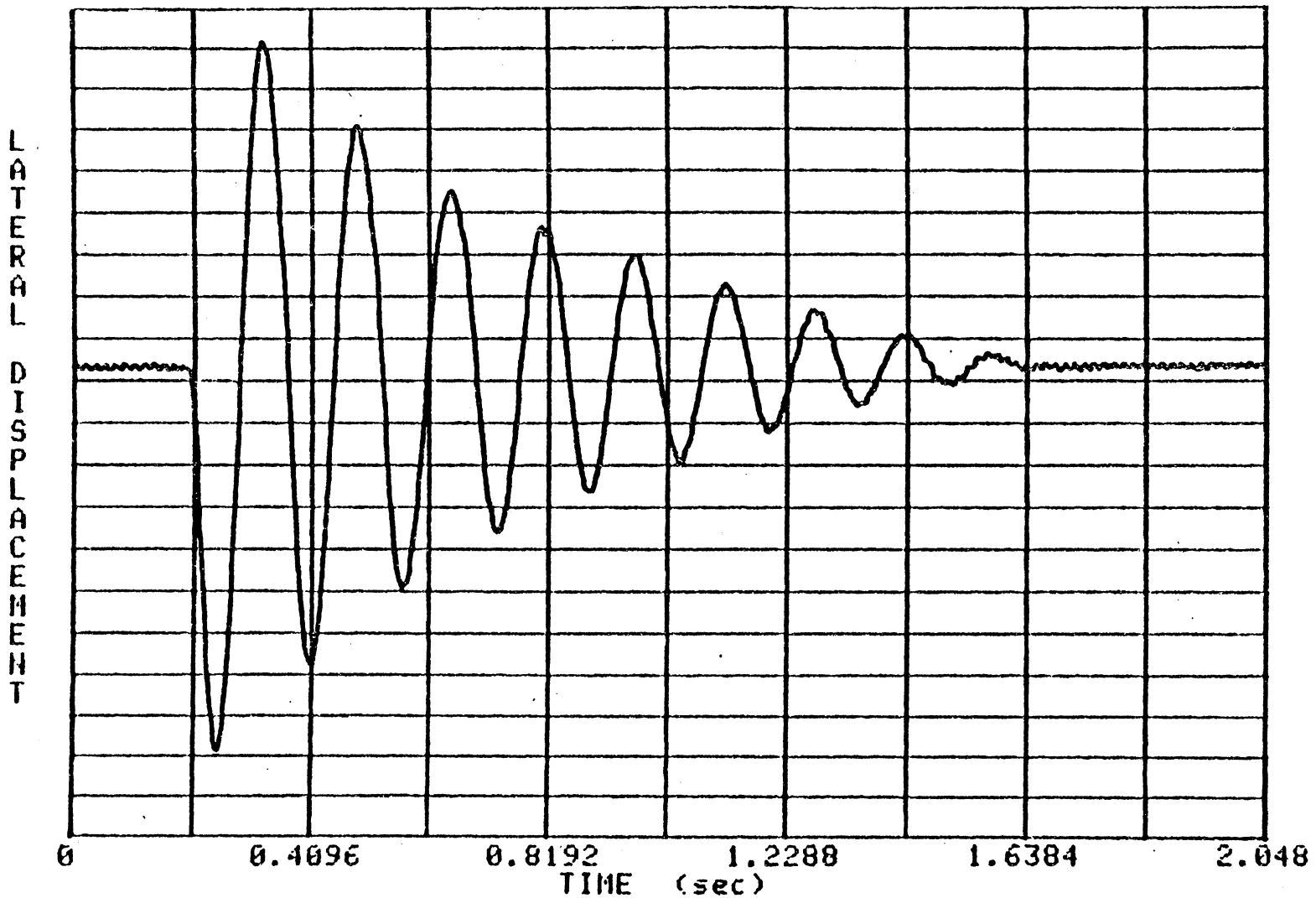

Figure 76. Displacement response of the pivot arm to a force impulse

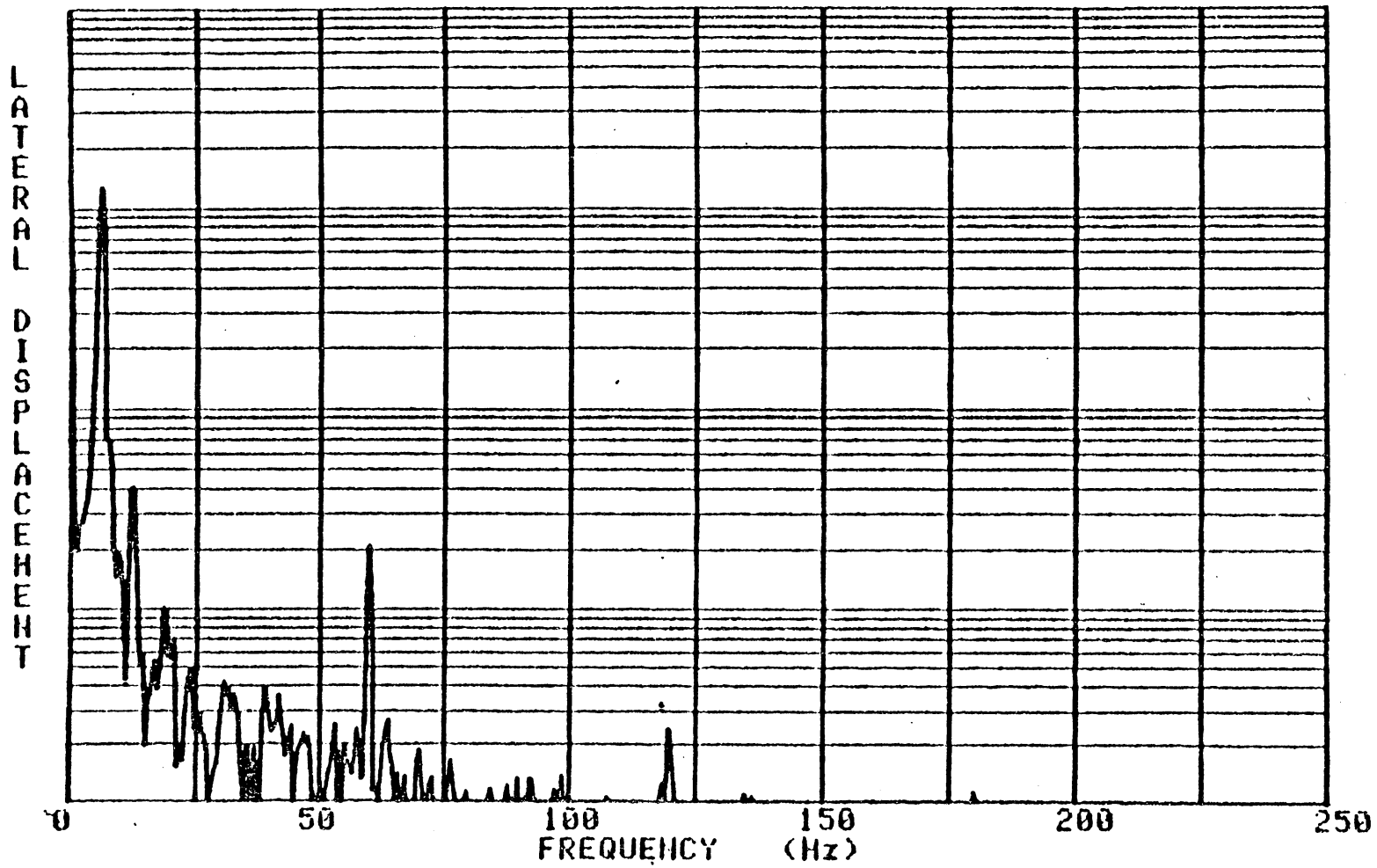

Figure 77. Spectrum analysis of the displacement response of the pivot arm to a force impulse

the damping coefficient was not large enough to cause any significant decrease.

DISCUSSION

The effects of surface roughness and sliding speed on the friction and wear of LDPE pins on steel disks were studied. The results showed that surface roughness is the major parameter in determining the wear mode of the polymer for the speeds and surface roughnesses examined.

The complex nature of the wear mechanisms led to separate studies of the adhesive and abrasive wear mechanisms. The adhesive mechanism was studied on a smooth surface and the abrasive mechanism was studied on a rough surface to determine the effects of surface roughness.

Visual observations of wear on smooth surfaces showed that wear occurred by the formation of surface films. These films were sheared from the polymer by the bonds formed between the steel surface and the polymer pin. The first deposits were in the form of localized thin films, which formed the basis for the building up of thick films at the local area. These thick films were then sheared and uniform thickness films were formed by the flow of the polymer. Plastic deformations like the formation of tongues and the flow of surface films over each other proved that the adhesional bonds caused the wear. There was a strong possibility of back transfer from the surface of the steel disk to the polymer pin. Very small amounts of loose debris were formed.

The energy theory proposed by Rabinowicz (4) for adhesive processes can be used to explain the generation of the loose debris

particles [Fig. 37, 61]. Visual observations had shown that the plastic deformations led to the formation of uniform thickness surface films by removing polymer from the thicker parts of the films. Since these surface films were similar to adhesive films described by Rabinowicz, it is hypothesized that subsequent loadings would cause elastic deformations. As the film thickness increased the amount of elastic energy that could be stored in the films also increased. When the elastic energy exceeded the energy of adhesion the films broke off [Fig. 13, 14]. These broken films formed the debris particles, which had the layered characteristic of the surface films [Fig. 15].

Experiments were carried out at two different speeds to examine the effect of speed on the wear of the polymer. Tanaka and Uchiyama (10) had examined the wear of LDPE on smooth surfaces and showed that temperature effects would play an important role at the high speeds of sliding. Experiments reported in this thesis showed that softening and even melting of surface layers occurred at the high speed of sliding on the smooth surfaces. Temperatures high enough to cause melting were caused by the heat generated at the sliding interface. Most of this heat energy remained in the interface, although some of it was removed by the formation of the small quantities of loose debris. Softening resulted in an increase in the wear rate [Table 2] and in a decrease in the friction force [Table 8]. The calculated wear rate (6.75×10^{-9} g/m) was in good agreement with the data presented by Tanaka and Uchiyama (10), who had found a wear rate of

(2.40×10^{-8} g/m).* The decrease in the friction force was due to the decrease in the shear strength, resulting from the increase in temperature, as was predicted by Lancaster (35, 36).

The unidirectional grinding of the steel disks caused the polymer to encounter different types of surfaces during passes. Visual observations showed that surface films were formed more readily during parallel sliding. This led to the conclusion that adhesion was favored by parallel sliding due to the surface topography. The formation of adhesional bonds was easier during parallel sliding than it was during perpendicular sliding.

Visual observations of wear on rough surfaces showed an abrasive mode, where wear was caused by the cutting of chunks of polymer by the asperities of the steel surface. Large amounts of wear debris were produced as a result of this process and the debris that was not pushed aside was piled up in the leading edge of the asperities. Piling up in this manner was a unique characteristic of the rough surfaces [Fig. 38, 42]. In the smooth surfaces, the small amounts of debris that was generated was pushed around and some of it was piled up in the leading edge of the grooves [Fig. 23, 24]. Therefore, observations of the loose debris in the grooves was found to be a means of distinguishing between the adhesive and abrasive processes.

---

*Data by Tanaka and Uchiyama is converted with the assumption of linear dependence on normal load.

Sliding on the rough surface was studied for the low and high speeds of sliding, but the wear rates were about the same for both speeds. The temperature of the polymer remained below the softening temperatures and melting was not observed. This was due to the fact that the frictional energy was carried away by the formation and separation of loose particles.

The wear rates for the rough surface were much higher than the wear rates for the smooth surface, because of the excessive amounts of debris produced by the cutting processes. The cutting processes caused wear marks parallel to the direction of sliding and were believed to result from plastic behaviour of the polymer [Ref. 22, 25].

The abrasive processes were favored by perpendicular sliding, because the sliding velocity was perpendicular to the lay direction and many asperities made contact with the polymer. During parallel sliding there was a small component of velocity perpendicular to the lay direction due to the circular shape of the track. This component of velocity and the irregularities in the surface caused small amounts of abrasion during parallel sliding.

Medium roughness surfaces showed the combined effects of adhesive and abrasive processes on the wear rates. The combination of the processes caused a wear rate, which was between those for the smooth and rough surfaces. Abrasive processes resulted in the generation of loose debris particles and adhesive processes resulted in the adhesion of these particles to the steel surfaces. The wear

rate was lower than the wear rate for sliding on the rough surface because of the decreased abrasion. Adhesion was not strong enough to compensate for this decrease, because the surface was not smooth enough. In fact, the surface had to be much smoother than the smooth surface for such a contribution from the adhesive processes.

In both the smooth and the rough surfaces there were periods of change in the friction coefficients due to the changes occurring on the worn surfaces. The changes probably were the formation and breaking of the films in adhesive wear and squeezing of a loose debris particle in between the pin and the disk in abrasive wear. Determination of the exact causes of these changes would require an intensive study of the surfaces before, during, and after the change periods. However, these changes were an order of magnitude smaller than the friction coefficients and the study to determine their causes was not justified.

The friction coefficients for the smooth surfaces were compared with the data given by Tanaka and Uchiyama (10), who had reported coefficients in the order of 1.0. The coefficients reported in this thesis [Table 8] were lower than this value. However, the surfaces used in this thesis were rougher than the surfaces used in the above reference. This caused the lower values of the coefficients by decreasing the adhesive forces.

Room temperature and humidity were not controlled and changes occurred in these parameters during the experiments. However, the temperatures of the sliding interface were much higher than the room

temperatures [Ref. 30] and therefore, the room temperature had no effect on the process. The effect of humidity was also neglected because the changes in humidity were believed to be small enough not to affect the properties of the polymer.

CONCLUSIONS

Surface roughness was found to be the major parameter in determining the wear mode of LDPE on steel surfaces for the speeds covered at the experimental conditions. The wear mode was shown to control the friction and wear rate of the polymer. The following observations and conclusions were made:

[1] Sliding on the smooth surface resulted in adhesive wear, where the surface films were laid on the steel surface by the shearing of the polymer.

[2] Adhesive processes resulted in the generation of very small amounts of loose debris, which were produced in two ways. One was the breaking of the bonds by the plastic deformations to generate the small sized debris particles. The other way was the removal of the surface films by the stored elastic energy to form the massive debris particles.

[3] The temperature of the contact area increased with speed on the smooth surfaces and caused melting of the polymer. This resulted in an increase in the wear rate.

[4] Sliding on the rough surfaces resulted in abrasive wear, where chunks of polymer were cut off by the penetrating asperities of the steel surfaces.

[5] Abrasive processes resulted in the generation of large amounts of loose debris, and the wear rate was high.

[6] The frictional energy was removed by the formation of loose debris particles in the abrasive processes. SEM pictures showed no evidence of melting and the wear rates were comparable in both speeds.

[7] Both the adhesive and abrasive wear modes occurred on the medium roughness surfaces and their effects were comparable. This process resulted in a medium wear rate.

A means of determining the wear modes by the examination of the loose debris in the grooves was established. According to this method loose debris with a layered structure in the leading edge of the grooves would imply adhesion and loose debris squeezed in the trailing edge of the grooves would imply abrasion.

RECOMMENDATIONS

Temperature is an important factor in determining the friction and wear of polymers. Results have shown that softening and probably melting occurs at the high speed of sliding on the smooth surfaces. However, there was no evidence of the effect of temperature on the rough surfaces. Therefore, it is necessary to do experiments at higher speeds of sliding to determine the change in the friction and wear due to increasing temperatures.

The unidirectional lay of the disks has been a hindering factor in the analysis of parallel and perpendicular sliding. It will be helpful to do experiments, where these processes are isolated by the use of surfaces which are radially or concentrically ground.

Properties of polymers have a major influence on the friction and wear. Therefore, it is necessary to isolate the effects of properties and examine them separately. This could be done by experimenting on different polymers under identical conditions (e.g. the effect of hardness can be determined by running tests on polymers with different hardnesses but with similar properties). These studies would also help to determine the effect of temperature on the wear rate, because the effect of temperature is to change the material properties, which in turn affect the wear rate.

Friction measurements have shown periods of change in the wear processes. It might be useful to make visual observations of the wear surfaces before, during, and after these periods of change to

determine the mechanism that is causing it. In this way, the changes in the wear mode during the experiments can be studied.

The vibration of the pivot arm during friction measurements caused fluctuations in the sliding speed. The effects of these fluctuations were believed to be negligible. However, it would be worthwhile to redesign the wear machine to attenuate the response to sliding forces.

REFERENCES

1. Archard, J. F., "Contact and Rubbing of Flat Surfaces", Journal of Applied Physics, 24, 1953, pp. 981-988.

2. Bowden, F. P., Tabor, D., The Friction and Lubrication of Solids, Part 1, Oxford, Cleardon Press, 1964, pp. 10-22, 285-287.

3. Green, A. P., "Friction Between Unlubricated Metals: A Theoretical Analysis of the Junction Model", Proceedings of the Royal Society, London, Series A, 228, 1955, pp. 191-204.

4. Rabinowicz, E., Friction and Wear of Materials, John Wiley, New York, 1965, pp. 151-154.

5. Bahadur, S., Ludema, K. C., "Viscoelastic Nature of the Sliding Friction of Polyethylene, Polypropylene and Copolymers", Wear, 18, n.2, 1971, pp. 109-128.

6. Pooley, C. M., Tabor, D., "Friction and Molecular Structure: The Behaviour of Some Thermoplastics", Proceedings of the Royal Society, London, Series A, 329, 1972, pp. 251-274.

7. Pooley, C. M., Tabor, D., "Transfer of PTFE and Related Polymers in a Sliding Experiment", Natural Physical Sci., 237, 1972, pp. 88-90.

8. Briscoe, B. J., Pooley, C. M., and Tabor, D., "Friction and Transfer of Some Polymers in Unlubricated Sliding", Advances in Polymer Friction and Wear, ed. Lieng-Huang Lee, 5A, New York, Plenum Press, 1974, pp. 191-204.

9. Tabor, D., "Friction, Adhesion, and Boundary Lubrication of Polymers", Advances in Polymer Friction and Wear, ed. Lieng-Huang Lee, 5A, New York, Plenum Press, 1974, pp. 5-30.

10. Tanaka, K., Uchiyama, Y., "Friction, Wear and Surface Melting of Crystalline Polymers", Advances in Polymer Friction and Wear, ed. Lieng-Huang Lee, 5B, New York, Plenum Press, 1974, pp. 499-532.

11. Bahadur, S., "Dependence of Polymer Sliding Friction on Normal Load and Contact Pressure", Wear, 29, n.3, 1974, pp. 323-336.

12. Briscoe, B. J., Parry, E., and Tabor, D., "Friction of Polymers Under Hydrostatic Pressure", Wear, 30, n. 1, 1974, pp. 127-134.

13. Briscoe, B. J., Tabor, D., "The Effect of Pressure on the Frictional Properties of Polymers", Wear, 34, n. 1, 1975, pp. 29-38.

14. Amuzu, J. K. A., Briscoe, B. J., and Tabor, D., "Shear Properties of Poly (N-Alkyl Methacrylates) in Concentrated Contacts", ASLE Trans., 20, n. 2, 1977, pp. 152-160.

15. Amuzu, J. K. A., Briscoe, B. J., and Tabor, D., "Friction and Shear Strength of Polymers", ASLE Trans., 20, n. 4, 1977. pp. 354-358.

16. Tabor, D., "Wear - A Critical Synoptic View", Wear of Materials 1977, ASME, New York, 1977, pp. 1-11.

17. Rabinowicz, E., "Dependence of Adhesive Wear Coefficient on the Surface Energy of Adhesion", Wear of Materials 1977, ASME, New York, 1977, pp. 36-46.

18. Rhee, S. H., Ludema, K. C., "Mechanisms of Formation of Polymeric Transfer Films", Wear of Materials 1977, ASME, New York, 1977, pp. 482-486.

19. Belyi, V. A., Sviridyonok, A. I., Smurugov, V. A., Nevzorov, V. V., "Adhesive Wear of Polymers", Wear of Materials 1977, ASME, New York, 1977, pp. 526-531.

20. Bikerman, J. J., "Thermodynamics, Adhesion, and Sliding Friction", Journal of Lubrication Technology, ASME Trans., 92, n. 2, 1970, pp. 243-247.

21. Bikerman, J. J., "The Nature of Polymer Friction", Advances in Polymer Friction and Wear, ed. Lieng-Huang Lee, 5A, New York, Plenum Press, 1974, pp. 149-163.

22. Ratner, S. B., Farberova, I. I., "Mechanical Testing of Plastics - Wear", Abrasion of Rubber, ed. James, D. I., MacLaren, London, 1967, pp. 297-312. (Translated from Soviet Plastics, n. 9, 1960, p. 51)

23. Ratner, S. B., Farberova, I. I., Radyukevich, O. V., and Lur'e, E. G., "Connection Between Wear Resistance of Plastics and Other Mechanical Properties", Abrasion of Rubber, ed. James, D. I., MacLaren, London, 1967, pp. 145-155. (Translated from Soviet Plastics, n. 7, 1964, (Plast. Massy 1963) p. 37.)

24. Rabinowicz, E., Friction and Wear of Materials, John Wiley, New York, 1965, pp. 168-169.

25. Ratner, S. B., "Comparison of the Abrasion of Rubbers and Plastics", Abrasion of Rubber, ed. James, D. I., MacLaren, London, 1967, pp. 23-35.

26. Lancaster, J. K., "Abrasive Wear of Polymers", Wear, 14, 1969, pp. 223-239.

27. Giltrow, J. P., "A Relationship Between Abrasive Wear and the Cohesive Energy of Materials", Wear, 15, 1970, pp. 71-78.

28. Rhee, S. K., "Wear Equation for Polymers Sliding Against Metal Surfaces", Wear, 16, 1970, pp. 431-445.

29. Warren, J. H., Eiss, N. S., Jr., "Depth of Penetration as a Predictor of the Wear of Polymers on Hard, Rough Surfaces", Wear of Materials 1977, ASME, New York, 1977, pp. 494-499.

30. Archard, J. F., "The Temperature of Rubbing Surfaces", Wear, 2, 1958, pp. 438-455.

31. Steijn, R. P., "The Effect of Time, Temperature, and Environment on the Sliding Behaviour of Polytetrafluoroethylene", ASLE Trans, 9, 1966, pp. 149-159.

32. Ratner, S. B., Lur'e, E. G., "Abrasion of Polymers as a Kinetic Thermoactivation Process", Abrasion of Rubber, ed. James, D. I., MacLaren, London, 1967, pp. 155-160. (Translated from Dokl. Akad. Nauk SSSR, 166, No. 4, 1966, pp. 909.)

33. Lancaster, J. K., "Relationships Between the Wear of Polymers and Their Mechanical Properties", Tribology Convention 1969, publ. by The Institution of Mechanical Eng., London, 1969, pp. 100-108.

34. Vinogradov, G. V., Bartenev, G. M., El'kin, A. I., Mikhaylov, V. K., "Effect of Temperature on Friction and Adhesion of Crystalline Polymers", Wear, 16, 1970, pp. 213-219.

35. Lancaster, J. K., "Estimation of the Limiting PV Relationships for Thermoplastic Bearing Materials", Tribology, 4, n. 2, 1971, pp. 82-86.

36. Lancaster, J. K., "Basic Mechanisms of Friction and Wear of Polymers", Plastics & Polymers, 41, 1973, pp. 297-306.

37. Price, H. L., Burks, H. D., "Friction and Friction-Generated Temperature at a Polymer-Metal Interface", Polymer Engineering and Science, 4, 1974, pp. 128-291.

APPENDICES

APPENDIX A

INSTRUMENTATION OF THE SYSTEM

1. Synchromous motor, Type CS
   0.5 HP, 1725 RPM, 115-230V
   Serial No: 305606-37
   Eastern Industries, Columbus, Indiana

2. Variable Speed Transmission, Model E2
   Torque 12 ft-lbs, Speed Range 0-400 RPM
   Zero-max, Minneapolis, Minnesota

3. X-Y Recorder, Model 7045A
   Serial No: 07045-60110
   Hewlett-Packard, San Diego, California

4. Oscilloscope, Type 561B
   Serial No: B081193
   Tektronix, Inc., Beaverton, Oregon

5. Carrier Amplifier, Type 3C66
   Serial No: 001534
   Tektronix, Inc., Beaverton, Oregon

6. Time Base, Type 2B67
   Serial No: 016903
   Tektronix, Inc., Beaverton, Oregon

7. Data Memory System, Model DMS 5003
   Zonic Technical Laboratories, Inc., Cincinnati, Ohio

8. Multichannel Fast Fourier Transform Processor
   Zonic Technical Laboratories, Inc., Cincinnati, Ohio

9. Microprocessor Graphics System, Model 4051
   Serial No: B082408
   Tektronix, Inc., Cincinnati, Ohio

10. Hard Copy Unit, 4631
    Serial No: B095093
    Tektronix, Inc., Cincinnati, Ohio

11. Talysurf Surface Analyzer, Model 4
    Gearbox, Serial No: 112/110-8129
    Electronic Unit, Serial No: 112/1000 F-3113
    Recorder, Serial No: 112/1005-2775
    Taylor-Hubson, Leichester, England

12. Timer Counter, Type 5300A
Serial No: 1212 A00839
Hewlett-Packard, San Diego, California

APPENDIX B

Cleaning Procedures for the Steel Disks

After the grinding process the disks were rinsed with tap water to remove the loose debris and the grinding oil. They were then cleaned with distilled water and dried with a soft cloth. Then they were dipped into clean solutions of hexane ($CH_3(CH_2)_4\ CH_3$), methanol (CH_3OH) and toluene ($C_6H_5CH_3$) for 2 minutes each. After these procedures they were put into an ultrasonic bath with toluene. They were then dried with a soft cloth and put into a dessicator.

The disks were cleaned once more before every experiment by dipping into toluene and drying with a soft cloth.

After the experiments the disks were boiled for 5 minutes in o-dichloro-benzene ($O\text{-}C_6H_4Cl_2$) to remove the polyethylene deposits. They were then dipped into toluene, dried with a soft cloth and put into the dessicator for reuse in subsequent experiments.

APPENDIX C

Calibration of the X-Y Plotter to Read Friction Coefficients

The wear machine was rotated 90 degrees on the axis of the pivot arm, so that the horizontal plane would become vertical. The loading mass on the platform was removed and a polymer pin was inserted into its place on the pivot arm. The pivot arm was then balanced with the use of the adjustable counter weight, so that there would be no load on the cantilever beam.

The output from the gages was connected to a carrier amplifier with a built-in bridge. The output from the amplifier was fed into the X-Y plotter. The zero adjustment of the X-Y plotter was made by the adjustment knob on the plotter.

A mass of 0.100 kg was placed on the platform and the multipliers of the amplifier and the plotter was adjusted in such a way that the plotter would mark a point 10.0 cm away from the origin on the Y-axis. The mass on the platform was then replaced with a 0.050 kg mass and the plotter was checked to see if it would mark a point 5.0 cm away from the origin on the Y-axis. The 0.050 kg mass was then removed and the plotter was checked to see if it would mark the origin. The procedure was repeated twice to make sure that the marks were exact. The Y-axis of the plots was then marked with a linear scale so that the 10 cm mark would read as 1 for the friction coefficient. This would mean that a force of 0.98 N was applied to the pivot arm, which had a load of 0.100 kg.

The wear machine was then rotated back to its original position and a test run was made to determine the scale on the X-axis. This scale was chosen to be 50 sec/cm which was then converted to number of passes.

APPENDIX D

Weighing Procedures

All of the pins were weighed by the Analytical Services, with with use of balances capable of detecting changes in the order of ±2 μg. The pins were carried in their marked vials and were handled with tweezers during the weighing procedures.

The first group of pins, which were 3 unused pins and the ones used in high speed experiments on medium roughness surfaces were weighed and the weight loss was recorded. The 3 unused pins were used to check the results and errors in the order of 20 μg were detected. This was found to be due to the calibration of the balances. It was decided that better results would be obtained if the pins were weighed against known standards of 3 mg, 5 mg, and 10 mg which were calibrated against each other. The rest of the weighing was done against these standards and the checks showed that the results were good to ±4μg.

The vita has been removed from the scanned document

INFLUENCE OF SURFACE ROUGHNESS AND SLIDING SPEED ON THE FRICTION AND WEAR OF LOW DENSITY POLYETHYLENE

by

Mehmet Mervan Bayraktaroğlu

(ABSTRACT)

The effect of surface roughness and sliding speed on the wear mode of low density polyethylene was studied with multipass experiments at the high sliding speeds by the use of a pin-on-disk wear machine.

Surface roughness was found to be the major parameter in determining the wear mode of the polymer at two different speeds of sliding. The wear mode was shown to be abrasive on the rough surfaces and adhesive on the smooth surfaces. The high wear rates occurring on the rough surfaces was related to the production of the large amounts of loose debris.

The effect of speed was found to be an increase in the temperature on the smooth surfaces. This temperature rise was used to explain the increasing wear rate and the decreasing coefficient of friction. No effect of speed was detected for sliding on the rough surfaces, where the frictional energy was dissipated by the formation of loose debris particles.